Durham E-Theses

The response of coarse and fine coal-mine discards under controlled load triaxial testing

Kennedy, George W.

How to cite:

Kennedy, George W. (1977) *The response of coarse and fine coal-mine discards under controlled load triaxial testing*, Durham theses, Durham University. Available at Durham E-Theses Online: http://etheses.dur.ac.uk/8986/

THE RESPONSE OF COARSE AND FINE

COAL-MINE DISCARDS UNDER CONTROLLED LOAD

TRIAXIAL TESTING

by

George W. Kennedy

being a Thesis submitted for the Degree of Master of Science in

the University of Durham.   September 1977

ABSTRACT

The aim of the project was to investigate the behaviour of coarse and fine colliery discards with respect to liquefaction potential, using controlled load triaxial testing. It was hoped to relate the behaviour in these tests to measured material properties such as strength, shape, chemistry and mineralogy.

The investigation of coarse discards contrasted the behaviour of a weak, seatearth-rich discard from Gedling Colliery with that of a strong shale-rich discard from Abernant Colliery. The former showed some liquefaction potential at low confining pressures, while the latter showed no liquefaction potential.

A seatearth and a shale from County Durham were used to demonstrate any possible links between these basic materials and the behaviours observed. However, both showed responses similar to the Gedling discard. Investigation of material properties indicated that the strength of material, its stability in water and its facility for pore pressure equalisation were the most important factors influencing response during controlled load testing. The strength and stability of the material are probably related to its organic carbon content. The Abernant discard had a high strength and stability in water and showed good potential for equalisation of pore pressures during testing, in contrast to the other three materials. Tests on mixtures of Abernant discard and the Durham seatearth showed a transition between the behaviours of the end materials for a mixture containing between 20 and 25 per cent seatearth.

Tests on fine discard from Peckfield Colliery showed significant differences in behaviour between samples from the lagoon and those

fabricated in the laboratory. The former showed strong dilatant behaviour, while the latter showed some potential for liquefaction. This is probably due to differences in soil structure (organisation of particles).

Tests on fine discard from Abernant showed a high potential for liquefaction. The most significant difference, possibly affecting liquefaction potential, between this discard and that from Peckfield was the uniformity of grading, the Abernant discard being considerably more uniform. The results for the Abernant fine discard showed no correlation with those for the coarse discard from the same colliery.

ACKNOWLEDGEMENTS

LIST OF CONTENTS

LIST OF TABLES

LIST OF FIGURES

CHAPTER 1

INTRODUCTION

1.1 Aims of Project.

The aim of this project was to investigate the susceptibility of coarse and fine colliery discard to liquefaction using the controlled load triaxial test, which is a suitable means of assessing this phenomenon.

The coarse discards chosen were from two separate areas, South Wales and Nottinghamshire. The former is an example of a shale-rich discard of high rank (rank 100) and the latter is an example of a high seatearth discard of low rank (rank 800 to 900). From the test results the different behaviours of these two types of discard could be contrasted.

To investigate further controlled-load behaviour in terms of specific rock types a typical shale and a typical seatearth from Esh Winning and Biggin South opencast sites in County Durham were also tested. For all the coarse materials tested variations in material properties together with chemical and mineralogical composition were used to try and explain the differences in behaviour that were recorded.

Tests were carried out on fine discards again with the object of comparing behaviours of different types of colliery tailings (slurries) and explaining them in terms of material properties. Developments were also made in the technique used for controlled load testing of fine grained materials.

In the investigation of fine grained discards it was also hoped to show the difference, if any, between the behaviour of samples taken from colliery lagoons and those made up (fabricated) in the laboratory.

1.2   The Concept of Liquefaction and Flow Slides

Concern about liquefaction and flow slides in colliery discards came about as a result of the Aberfan disaster of 1966, in which liquefaction was shown to be a major contributory factor.

Many different definitions of liquefaction have been used since Terzaghi and Peck (1948) described it as "the sudden decrease of shearing resistance of a quick sand from its normal value to almost zero without the aid of seepage pressures".

The definition used by Castro (1969), gives a comprehensive description of the phenomenon; "The phenomenon by which the soil suffers such a substantial reduction of its shear strength that the mass of soil actually flows, spreading out until the shear stresses acting within the mass become so small that they are compatible with its reduced shear strength".

Although liquefaction can occur in a dry situation in which air is the fluid, for example avalanches, it usually occurs in saturated or nearly saturated soils which have a metastable structure .   On collapse of such a metastable structure the load is transferred from the soil skeleton to the pore fluid, producing a flow slide, (Bishop et al.1969).

The results of liquefaction leading to flow slides can be rapid and disastrous.   Many flow slides have occurred in sand deposits as a result of earthquakes.   Liquefaction is generally produced by shock loading, such as that resulting from an earthquake, or movement of a previous failure plane.

1.3   Flowslides in Colliery Waste.

In the case of colliery spoil heaps, flowslides could potentially be caused by a number of different events such as tremors, or sudden shocks caused by mining subsidence, tipping of fresh spoil on a potentially

unstable slope, vibrations caused by plant used in tipping operations
and shocks resulting from slipping on old failure planes. The presence
of large quantities of water after periods of wet weather is often a
major contributory factor in this type of failure.

Some examples which illustrate a number of the above causes can
be cited. For example, in 1969 a 42m high, 20 year old tip suffered a
slip due to subsidence. Some time prior to the slip a crack 60m long
with a 200mm step had been noted in the tip. In 1967 a 14m high lagoon
bank failed one week after fresh spoil had been tipped over the old
bank. The failure followed a period of heavy rain. At Abercynon tip
in South Wales a flowslide occurred in 1939 in which a section 110m wide
flowed 430m in a few minutes, 180,000 tonnes of spoil being involved.
The tip was on a ground slope of 1 in 2.6 or steeper. The cause was
concluded to be water issuing from a fault plane beneath the tip. These
failures were documented by the National Coal Board (1970). At Aberfan
there had been a history of previous failures. In 1944 another tip in
the Aberfan complex suffered a collapse, which was probably caused by
spring water seeping into the tip. In 1963 there had been a major slide
in the tip which moved again in the 1966 disaster. All these slides
followed periods of heavy rain. The actual flowslide of 1966 was
triggered by a toe failure which reactivated a slip along the previous
failure surface. The results were accentuated by large volumes of water
being released from aquifers beneath the tip.

Flowslides are always a potential hazard in tips as has been pointed
out in the N.C.B.'s Technical Handbook (1970) "Flowsliding should always
be considered a probable secondary consequence when large quantities of
material are involved, when the material is very wet, and where the

natural ground in front of the tip in the probable direction of movement
slopes steeply away from the tip". The worst combination of the hazards
outlined above occurs in South Wales where there is high rainfall (up to
2000mm per annum) and the tips are often constructed on hillsides.
Although the problem requires special attention in South Wales, it cannot
be ignored in other areas. The problems of tips and their possible
solutions are outlined later in this chapter.

As well as flowslides involving tip material there have also been
examples of flowslides involving lagoon sediments. In North Derbyshire
in 1966 slurry from a lagoon flowed a distance of 100m following the
failure of a 8m high lagoon bank. Failure was due to artesian water
pressures in the bedrock caused by water seeping from the lagoons and
also groundwater seepage from higher ground. The lagoon bank was also
affected by subsidence due to old mine workings. A further danger in
the case of lagoon deposits is the possibility of drawdown leading to
possible failure of the lagoon bank. This could occur during the
excavation of lagoon deposits.

Further examples of failures involving tailings and tailings dams have
occurred outside this country. In 1972 a tailings dam near Buffalo
Creek, West Virginia failed after 94mm of rain in 72 hours. The dam was
15m high, had a base width of 120m, and was standing at the angle of
repose. The failure released 4.16×10^5 m^3 of water and killed 118
people making 4000 more homeless. Due to inadequate design of the dam
the failure mechanism was complex. It appeared to be a combination
of piping in the tailings, downstream slipping due to seepage pore pressures
and overtopping due to lack of overflow works (Bishop, 1973).

In Chile there are a large number of tailings dams built from mill
tailings produced in the extraction of copper. On March 28, 1965, there

was a serious earthquake (magnitude 7 to 7.25; 0.18g peak acceleration
at 120km) in Central Chile which led to the failure of a number of these
dams. A number of these failures have been described by Dorby and
Alvarez (1967). The most serious failure occurred at El Cobre, where
two dams failed during the earthquake. The failure caused 2 million
tonnes to flow, travelling 12km in a few minutes. The flow destroyed
part of the town of El Cobre and killed more than 200 people. Accounts
of the failures indicated that a slide of the frontal slope of the dam
was followed by the liquefaction and flow of the core. The core
material was generally very fine, between 45 and 60 per cent passing a
No. 200 sieve for the materials studied. It was also very wet and
uncompacted. These failures illustrate the importance of proper design
and construction of structures involving tailings,and especially in
seismic areas.

1.4 Review of some recent work.

Much of the current work is in the field of cyclic liquefaction
related to the occurrence of liquefaction in sand deposits during
earthquakes. However, in this work some theories, ideas and techniques
have been developed which are relevant to the current investigation.
Some of these are outlined in this section.

1.4.1 Critical Voids Ratio, E and F Lines and Flow Structures.

Casagrande has been involved in work on liquefaction from an early
stage (mid nineteen thirties) and has contributed a great deal to the
current ideas. Much of this work was summarized in his recent
publication (1976).

From as early as 1938 Casagrande observed that when a dense sand is
sheared it will dilate (increase in volume) and that a loose sand will
contract (decrease in volume). From this he developed the concept of

'critical void ratio', as the void ratio at which a sand would neither contract nor dilate, but shear at a constant volume. This void ratio was found to be dependent on the normal pressure and a plot of log normal pressure against void ratio was produced (Figure 1.1). The line on this plot was called the 'E Line'.

The response of sand subjected to a shear force will depend on its position relative to this line. For sand whose state lies above this line, point a, the natural tendency would be for the sand to densify, decreasing the void ratio, and to move vertically down to point b. However, if volume change is not possible the tendency is still to reduce in volume, but as this is not possible, the effective normal stress is decreased by the transfer of some of the load to the pore water, and the state moves to the right to point c. This produces a rise in the pore pressure and a reduction in the shear strength, i.e. the phenomenon of liquefaction is produced.

If a sand below the line was subjected to shear forces the effect would be the induction of negative pore pressures, and further load would be taken by the sand. Thus it was shown that a sand above the line would be liable to liquefaction and one below it would not. However, his work following the Fort Peck Dam slide of 1938 showed that a sand lying apparently below the line had liquefied(from field tests on the liquefied sand after the failure).

However, further work produced the concept of a flow structure. He concluded that when a sand liquefies and is flowing it has a structure completely different from that in the static condition forming a flow structure. In this structure the grains of sand are rotating relative to each other in such a way as to produce minimum frictional resistance.

This structure spreads by chain reaction and exists only during flow.
When the flow stops the grains revert to a static structure which is
slightly denser than the original structure.   This could explain the
observations concerning the Fort Peck Sand.   Thus, a change of structure,
reducing the susceptibility to liquefaction, could have taken place
e.g. from an unstable honeycomb structure to a stable single-grained
structure (Figure 1.2).

Although Casagrande had made these observations and postulations,
he was not able to demonstrate them in the laboratory.   This was finally
achieved by Castro (1969), who by using load control triaxial tests
instead of the usual strain control produced liquefaction and flow
structures in the laboratory.   The success of the load control method
was due to the fact that in order to maintain a flow structure the
driving force must be kept constant.   If a flow structure developed in
a strain-controlled test the driving force would be relaxed and the
structure could not be maintained.   In the case of load control there
would be no relaxation and the structure would be maintained.

From the results of Castro's and other subsequent tests, Casagrande
considered the relationship between void ratio and log effective minor
principal stress at failure.   He found from this plot that there was a
well defined line which he called the 'F Line' (the line for which
liquefaction with a flow structure developed).   Subsequently, he
produced flow structures in strain controlled and drained triaxial tests.
Again he plotted void ratio against log effective minor principal stress
during flow.   The resulting lines are shown in Figure 1.3, being termed
E_{sc} and E_u.

The actual position of the E_{sc} line is thought to be dependent on
the speed of loading, the F line being an extreme case.   As with the load
maintained the flow structure collapses almost instantaneously.

Casagrande defines three zones on the plot as follows:-

Zone A   the dilative zone below the F line in which no liquefaction will occur;

Zone B   between the F and E_u lines, either a dilative or contractive response may develop depending on the rate of strain, and on the proximity to the F line;

Zone C   above the E_u line - a contractive response to any strain will develop and liquefaction is the likely result of any rapid strain or shock.

Casagrande then concludes "The F line is of prime interest for engineering applications.   On the basis of my present knowledge and judgement, I consider the entire area above the F line to be a hazard with respect to actual liquefaction in foundations of dams and important structures in highly seismic zones.   Below the F line actual liquefaction is not possible, although small strains may develop".

The term "actual liquefaction" used here by Casagrande is defined by him as follows "the response of contractive (loose) sand which results in substantial increases in pore pressure and loss of strength that can cause a flow slide".

1.4.2   Liquefaction and Associated Results.

In his paper of 1973, Youd attempts to clarify the position regarding liquefaction and its resulting after effects.   Definitions used by Youd are as follows:

Liquefaction "The transformation of a granular material from a solid state into a liquefied state as a result of pore water pressures".

Solidification The opposite process to liquefaction.   Deformations in the solid state are described as plastic and elastic strains, whereas those in the liquefied state are called flow deformations.

Two types of flow resulting from liquefaction are defined:

(i)   Limited Flow -liquefaction in which flow deformation occurs, but which is subsequently arrested by solidification after movement without significant change of total stress.   This type of liquefaction has also been referred to as partial liquefaction by Castro (1969).   A phenomenon known as lateral spreading landslides can result from a number of limited flows occurring during repeated loading, such as in an earthquake.   Thus, although a single occurrence may only produce small displacements repeated flow can lead to large displacements.

(ii) Un-limited flow - the condition in which reductions in pore pressure due to dilation are not enough to arrest the flow.   In this case the flow deformation continues until the applied shear stresses are reduced to a level less than the viscous shear resistance of the liquefied material. Landslides produced in these cases are referred to as 'flow landslides'.

1.4.3   Sample Preparation and the Effects of Soil Structure.

Professor H.B. Seed of the University of California has,with a number of co-workers, carried out a great deal of work in the field of cyclic liquefaction.   In a paper published recently (April, 1977) with Mori and Chan, he discusses the effects of strain history and soil structure on a soil's susceptibility to liquefaction.

Using a large scale shaking table apparatus in order to eliminate the effects of boundary conditions, he compared the behaviour under large-scale cyclic loading of two different sand samples.   The first had been subject to a number of small vibrations not sufficient to cause failure. The second had had no previous loading history.   The two samples were tested in the same way, and it was found that the number of cycles to cause liquefaction in the pre-loaded sample was eight times that in the unloaded sample, even though the former had not suffered any significant change in relative density.

This shows that relative density alone cannot be used as an indication of liquefaction potential, and that previous strain history and soil structure are also significant. Casagrande's observations concerning the state of the Fort Peck Sand after liquefaction also show the effect of strain history.

A possible explanation of the change in susceptibility to liquefaction is that the soil undergoes a change in structure without a significant change in relative density. Seed has shown that a sand sample subjected to a number of stress cycles undergoes a settlement of 0.01 per cent in the first cycle but only 0.002 per cent in the fifteenth cycle, even though the relative density is not significantly altered. This confirms the observations of Mullis, Chan and Seed (1975) that the same sand can have the same relative density but different structure which will result in different liquefaction characteristics.

These observations raise the question of possible differences between soil structure in the field and those of prepared specimens in the laboratory. Seed has shown that undisturbed samples are less susceptible to liquefaction than samples prepared to the same density in the laboratory; the stress ratio to cause liquefaction being up 45 per cent higher for undisturbed samples. He has also shown that samples prepared by tamping in a moist condition are significantly stronger than those prepared by sedimentation. Another factor involved in liquefaction potential and soil structure considerations is the lateral earth pressure coefficient K_o. Seed puts forward five possible explanations for his observations:

1. Natural deposits have a somewhat more stable structure, perhaps due to the greater lateral movements associated with the deposition process, than those of the same sand deposited in the laboratory.

2. Natural deposits invariably acquire some increase in stability due to small local seismic events that occur in most environments - thereby producing a more resistant soil structure and an increase in K_o.

3. Natural deposits acquire some increase in stability as a result of the long periods of sustained stress to which they are subjected, thereby producing some type of "cementation" at particle contacts, in comparison with short term tests on laboratory samples at the same density.

4. Stratification which is invariably present to some degree in undisturbed samples, may influence the results of tests on these materials to some extent.

5. The vibrations inevitably associated with the extraction of samples from the ground are simply another form of seismic history, which sometimes tends to make "undisturbed" samples have a higher resistance to liquefaction than they would have _in situ_.

He concludes that there is a reasonable expectancy that the first two factors will improve the soil characteristics, and that there is no evidence to support the effect of long term pressures. Effects of vibration could well be offset by effects on density which are also evident.

Other workers have also shown differences in behaviour between undisturbed and laboratory prepared samples and also variations depending upon preparation techniques. Oda (1972) showed that in compressive tests the preferred orientation of natural deposits was stronger than the random orientation of laboratory samples. Ladd (1977) has shown that samples made up dry are weaker than those made up wet.

Seed finally puts forward the idea that the standard penetration resistance could be used to assess liquefaction potential. He points out that the liquefaction resistance increases with relative density and the penetration resistance also increases with relative density. Also the liquefaction resistance increases with the <u>in situ</u> value of K_o and the penetration resistance also increases with K_o. Finally, both liquefaction resistance and penetration resistance increase with increasing structural stability of the grains.

From this he makes a correction for the effect of overburden pressure and shows that there is a good case for using this as a criterion for assessing liquefaction characteristics.

1.5 Colliery Waste Disposal

Little attention was paid to the problems attending the disposal of colliery waste until they were highlighted by the Aberfan disaster of 21st October 1966. Until this time little attention was paid to the design or maintenance of tips, and it has only been as a result of the recommendations made following Aberfan, that anything has been done about this problem.

There are two types of discard produced in mining - coarse and fine. The coarse discard is partly the run.of mine material and belt and table pickings removed before washing. It is mainly composed however, of material above 0.5mm in size which is separated in the washery. Such material consists of the rocks associated with the coal seam. These fall into two categories - roof and floor materials (i.e. rocks above and below the seam). The roof materials are usually mudstones, shales, siltstones and minor amounts of sandstones, and the floor material seatearth, which is usually a special variety of the other four. Seatearths, however, contain fossil rootlets and are customarily slickensided. The particular characteristics of the coarse discard depend on the area and the seam.

Coarse discards were generally placed on the tip using wagons, tubs, aerial ropeways, Maclane tipplers, belt conveyors, lorries or dump trucks. Tips were either constructed in a single lift or in layers ranging in thickness from 1m to 10 or 20m, the material being loose tipped at the angle of repose, although subsequent slipping of wet discard may have reduced this angle. Tips constructed in fairly thick layers may contain perched water tables. Little attention was given to the design of the tip or the provision of drainage.

The fine discard is produced from the processing of the coal in coal preparation plants or froth flotation plants. Two types of fine discard are produced, slurry and tailings. The former is generally produced from a coal preparation plant and has a fairly high carbon content and is sometimes excavated from lagoons as a low grade fuel. The latter is the product of a froth flotation plant and may have a lower carbon content, which strictly speaking makes it of little value. The use of the two terms is often interchangeable, little attention being paid to their true meaning.

Both types of fine discard are produced in suspension with water and are either filter pressed or more commonly pumped into lagoons, where they are allowed to settle out. The supernatant water may then be removed from the lagoon surface or be allowed to evaporate. The actual state of the material within the lagoon depends very much on the drainage conditions within the banks and underlying rocks. As mentioned above, slurry has a potential as a fuel and is often excavated for sale. In these cases it only presents a short term storage problem, whereas the tailings present a long term problem.

In the past lagoons have been built into spoil heaps, using the coarse discard as the embankment material. As the lagoons have been extended, the banks were built up using the 'fir tree' or upstream method of construction (Figure 1.4).

The problems involved in this method of construction are the use of lagoon material as part of the support for the new bank, and the possible production of perched water tables. The banks were constructed in a similar fashion to the tips using single lifts. When a lagoon fell into disuse it was then over-tipped being incorporated into the structure. Thus many old tips contain old lagoons within them.

As an alternative to placement in lagoons, fine discard has also been spread over the surface of tips, mixed with coarse discard.

An indication of the size of the problem is given by the following figures. In 1970 the N.C.B. owned about 2000 tips of which 1100 were active. There were about 720 lagoons of which 200 were in use. There are probably about 3000 million tonnes of material in tips. Some 60 million tonnes of waste per annum is being produced although coal production is only 120 million tonnes. Of this waste about 55 million tonnes is coarse discard and 5 million tonnes fine discard.

As a result of the Aberfan disaster and subsequent research there has been a great change in the attitude to tips and their construction. Some of the major changes are outlined below.

1.6   Revised methods of Waste Disposal.

The most important change in attitude after Aberfan was to treat tips and lagoons as Civil Engineering earthworks, something which had not happened before.

From the observation of failures in the past, the serious affect of water is obvious. Hence the most important factors are to provide adequate drainage and to prevent large quantities of water from accumulating in the tip. As has been pointed out by McKechnie Thomson and Rodin (1972) the object of a tip is to store solids not water.

1.6.1 Spoil Heaps

One of the first actions was the phasing out of fresh tipping over high faces. Also all existing tips have been examined and remedial work such as regrading of slopes or provision of drainage has largely been carried out.

For the construction of new tips it was recommended that layered construction with a reasonable degree of compaction should be used. The layers should not exceed 5m in thickness. Dump trucks and scrapers are used in construction to provide the necessary compaction effort. As well as giving increased stability the extra compaction has reduced the risk of burning and decreased the permeability so reducing the possibility of seepage ~~pressures~~ acting through the tip.

For moisture contents greater than 10 to 14 per cent placement in layers of maximum thickness is the most common practice, although thick layer construction is limited to a height of 30m with a maximum outer slope of 1 in 2 ($26\frac{1}{2}^{o}$).On steeply sloping ground the maximum height is usually reduced to 15m.

Before building a tip adequate drainage facilities should be provided. Existing water courses should if possible be diverted round the site of the tip, or alternatively adequate culverts should be provided under the tip. Springs at a tip site should be dealt with by pipe drains and artesian pressures should be controlled by relief wells or inclined bored filter drains.

Decreased permeability due to better compaction leads to a greater degree of run off, and in order to prevent erosion adequate drainage should be provided. The recommendations given in the N.C.B. Technical Handbook (1970) are shown in Figure 1.5.

In general, this type of drainage facility has not proved entirely satisfactory and more conventional berms (terraces) with a fall towards a perimeter drain are favoured in other countries. The possible entrainment of water into the tip (drain behind the crest) was originally adopted to conform with West German practice, where a compacted outer bund retains a core of uncompacted coarse discard. In the latter case settlement of the central section necessitates the drainage provision shown in Figure 1.5. Here, again, the balance between seepage into the tip and erosion would now favour an outwardly inclined drainage facility.

1.6.2   Lagoons

For economic reasons maximum use of coarse discard is recommended in the construction of lagoon banks. New lagoons in Britain are not customarily more than 18m above the existing ground, nor are they constructed within a spoil heap except under special circumstances. Adequate provision is made for the draw-off of water from the lagoon. To aid drainage of the lagoon the bank should if possible allow maximum drainage, although post-Aberfan observations infer that lagoon embankments are commonly impermeable. Foundations would seem to be more permeable than embankments (for example, Cobb 1977). Drainage characteristics of lagoon sediments are improved if there is an even distribution of coarser grained material throughout the lagoon, and this can be achieved by moving the positions of the inlet and outlet around the lagoon.

At the end of the useful life of a lagoon it should be kept free of standing water. After an adequate period of time it can logically be over-tipped, so long as sufficient care is taken during this process. The properties of the lagoon deposits must be adequately investigated, to ensure that they have the required bearing capacity. The stability of the lagoon bank in these circumstances must also be checked, and over-tipping with more than 3m of spoil should not be undertaken unless a thorough investigation of the lagoon and the lagoon banks is carried out.

It is with this question in mind that the present work on the liquefaction potential of both coarse and fine discards has been carried out.
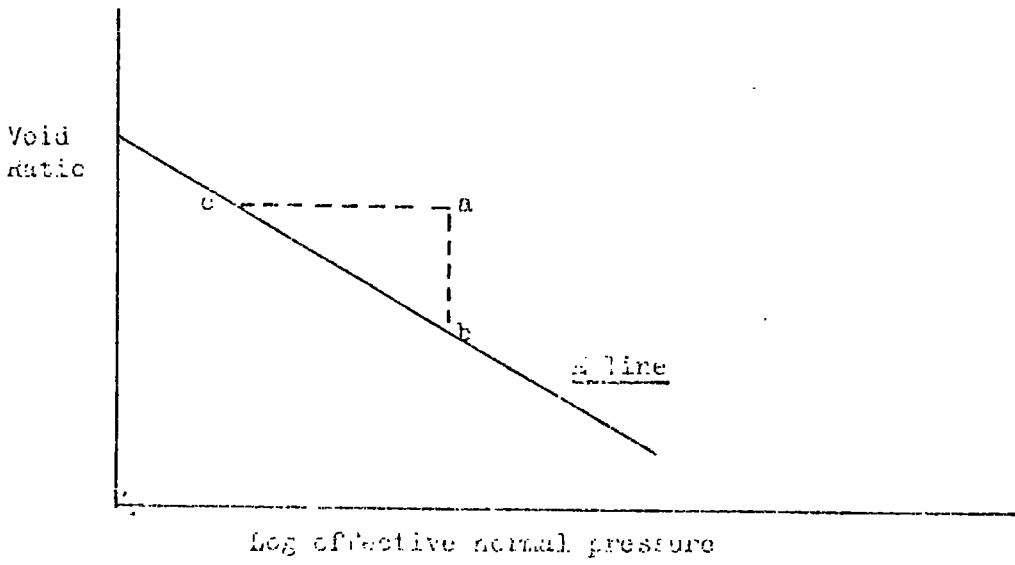
Figure 1.1 The 'n line' (After Casagrande, 1976)
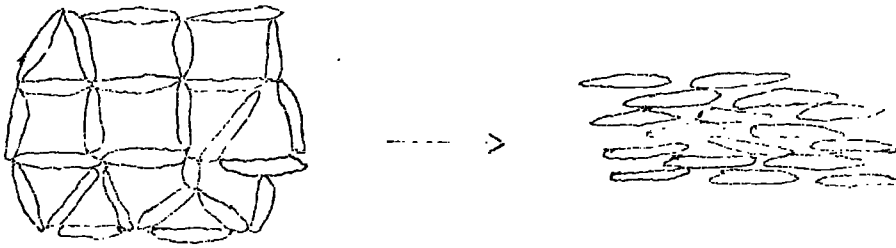
Figure 1.2 Possible Structural Change Resulting from a Liquefaction and ...
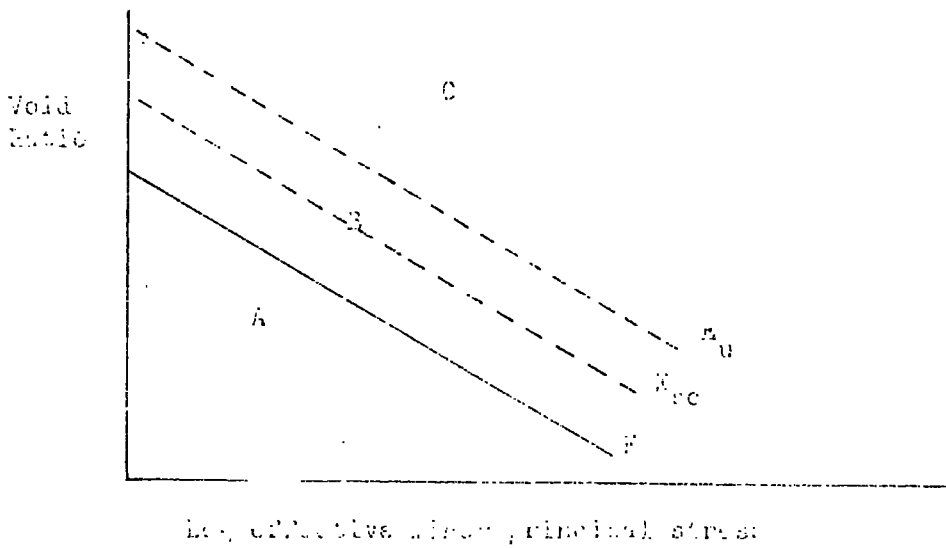
Figure 1.3 The 'F', 'Lsc' and 'Lu' Lines (After Casagrande, ...)
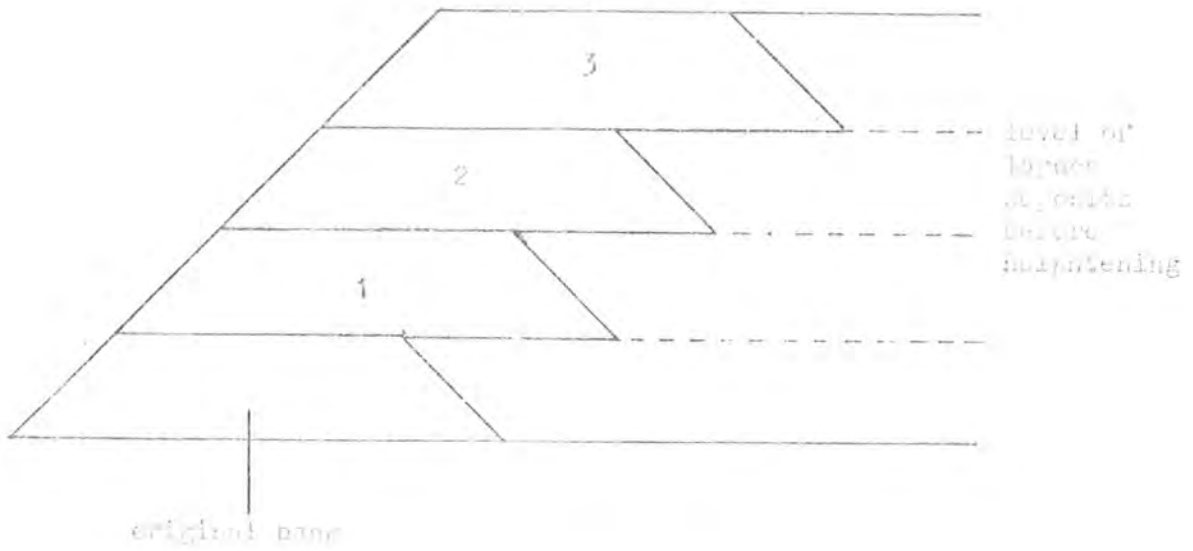
Figure 1.4   The 'Fir Tree' Method of Lagoon Bank Construction

Figure 1.5   Successive Stages of Spoil Heap Construction (adapted from BSI 6031, 1981)
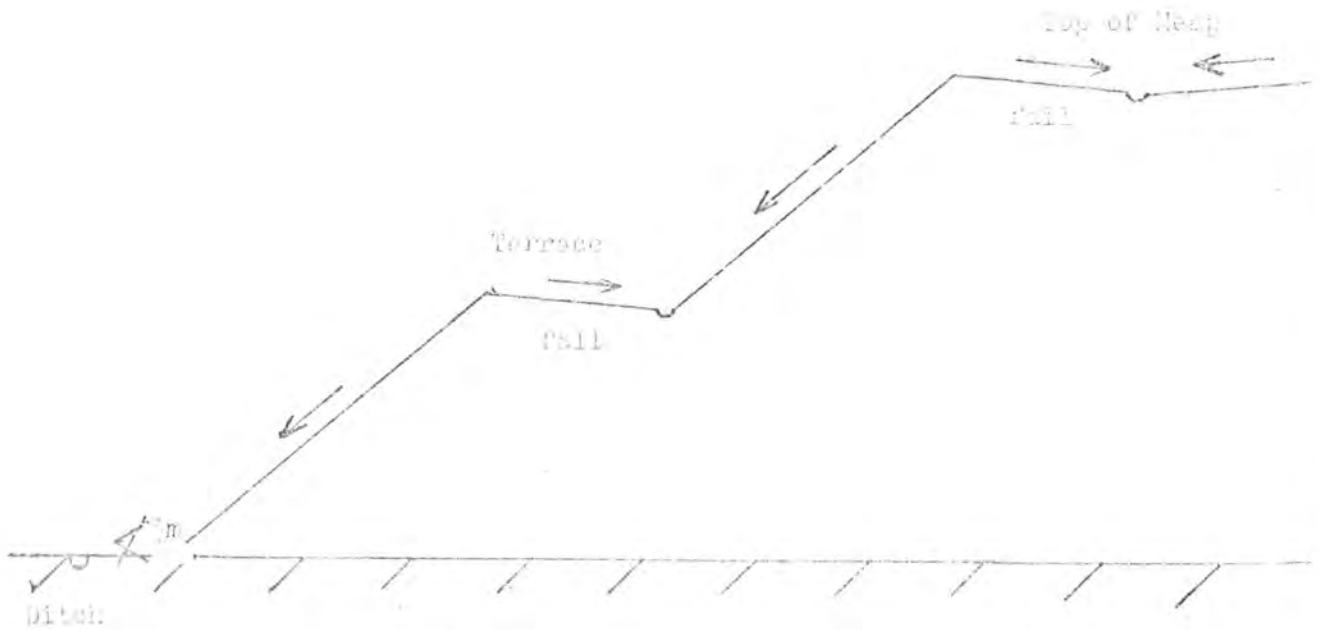
CHAPTER TWO

MATERIALS INVESTIGATED

2.1   Geographical Locations

Materials tested were from the following locations:-

Coarse Discard

Abernant Colliery, N.C.B., West Wales area.

Gedling Colliery, N.C.B. North Nottinghamshire area.

Comparative Materials

The shale was taken from above the Harvey seam at Esh Winning opencast

site, Co. Durham, and the seatearth from Biggin South opencast site,

Co. Durham.   Both sites are under the jurisdiction of the N.C.B. Open-

cast Executive.

Fine Discard (lagoon materials)

Peckfield Colliery, N.C.B. North Yorkshire Area.

Abernant Colliery, N.C.B. West Wales area.

The locations are shown on the map (Figure 2.1).

2.2.   General Description of Sites

2.2.1   Gedling

Gedling Colliery is situated 5km north east of Nottingham (Fig. 2.1)

in the bottom of a tributary valley of the River Trent.   There are two

tips at Gedling (West and East) built on the northern side of the valley

(See fig.2.2).   The tips are actually founded on the site of three small

valleys.   The bedrock at the site comprises Waterstones and Keuper Marl

of the Triassic system.

The two tips are quite extensive and have been built up over a number

of years.   The west tip has been constructed from several small heaps

originally deposited by aerial ropeway, Maclane tippler and railway
wagons.   The south western part of the tip contains a considerable
quantity of burnt material.   One of the valleys mentioned above was
dammed and used as a lagoon, being gradually extended by the raising
of the bund.   Since being abandoned this lagoon has been extensively
overtipped.   Further lagoons built on the northern side of the tip
have also been subsequently abandoned.   Extension of this tip is taking
place and this operation involves the raising of the height from 115m
to 125m AOD, the toe height being 65m AOD.

The east tip was originally constructed from material transported
by aerial ropeway and redeposited by scrapers.   It impounded a large
lagoon complex on its northern side, which has now been overtipped.
A pair of new lagoons are now being constructed above the old ones.
The height of this tip is being raised from 90m to 115m AOD, the toe height
being 55-60m AOD.   The valley in which construction is taking place
may have had springs emerging in its floor.

Both tips illustrate the pattern of overtipping and enclosure of
old lagoons.   They are both relatively high being in the range of
50 to 60m.   It is important to note that only 15 per cent of the
N.C.B.'s tips are over 50m high (McKechnie Thomson and Rodin, 1972).

2.2.2   Abernant

Abernant Colliery which lies within the N.C.B.'s West Wales Area is
situated about 18km north of Swansea near the town of Pontardawe.   It is in
the valley of the Upper Clydach River, a tributary of the River Tawe.   The
colliery and tip are adjacent to the A474 road from Pontardawe to Ammanford.

The tip lies to the south of the colliery and is built on a gently
sloping area on the eastern side of the valley, between the main road and

the river.   The tip ia about 20m high, the face on the river side having a

slope of between 1 in 3 and 1 in 4.   There is no face on the western side as

the natural ground slopes gently towards the river.   On the eastern side of the

tip there are six large slurry lagoons,all of which have supernatant water.

They are marked on the local Ordnance Survey Map (Sheet 160 1:50,000 First

Series) as ponds.   There are problems with the settling of the slurry and

floculant has to be spread on the lagoon surface to aid the process.   The

remainder of the tip is mainly coarse discard,although at least one old lagoon

is enclosed in the tip.   Tipping is currently taking place on the southern edge

of the site, where a number of drains have been provided in accordance with

current regulations.   A plan of the site is shown in Fig. 2.3.

2.2.3   Peckfield

Peckfield Colliery which lies within the N.C.B.'s North Yorkshire

Area is situated about 16km east of Leeds near the village of Micklefield.

It is close to the A1 and M62 and is adjacent to the Leeds to Hull

railway line (Fig. 2.4).

There are two spoil heaps at Peckfield.   One to the east of the

colliery area, now disused, and the second which is in current use lies

to the south of the colliery.   Both are built on flat ground and are

relatively low.   Number one heap has a height of 14m and number two heap

a height of 20m.   The area occupied by the tips is quite large, which

allows for quite gentle slopes.   The outer faces of both heaps have

been landscaped and No. 1 heap will eventually be completely landscaped.

Number one spoil heap contains a number of small disused slurry

lagoons, one of which is currently being excavated.   The samples used

in this investigation came from the beach area of No. 6 lagoon in number

one heap.   There is a large lagoon in current use in Number two heap, together

with some smaller lagoons.

2.3   Description of Materials

2.3.1   Gedling

The Gedling material tested was obtained from tippers at the spoil heap and thus is representative of the material being placed on the heap.   As obtained the material had a moisture content of about 16 per cent which reduced to about 11 per cent during storage in the laboratory.

The material from Gedling tip is a seatearth-rich spoil and hence is relatively weak (c.50% seatearth content).   It has quite a low organic carbon content of about 11 per cent.   The material is light grey in colour and some fragments are slickensided and fissured. Although particle corners are rounded the shape distribution (Fig.2.10) shows it to be quite 'platey'.   The grading curve shows it to have a high fines content (34 per cent) for a coarse discard, although this must be influenced to some extent by breakdown in water during sieving. The effect of water is demonstrated by the slaking test results (Table 2.2).   The associated coal has a rank of 800 to 900 (i.e. the measures are of low rank).

2.3.2   Abernant

The Abernant material was obtained as wet bulk samples from the tip with a moisture content of about 15 per cent.   It is a strong, shale-rich discard typical of those originating from the mining of Welsh anthracite.   It has a high organic carbon content of about 35 per cent and hence is black in colour.   It is quite angular and the shape distribution shows it to be 'platey'.   The grading curve is fairly typical of a coarse discard with a fines content of 15 per cent.   The Welsh anthracite has a rank of 100.

2.3.3   The Durham Seatearth

The Durham seatearth was obtained as large pieces of rock from below

the Harvey seam at Biggin South Opencast site.   It was broken down in

the laboratory and made up to the same nominal grading as Gedling.   As

a seatearth it was fairly weak and broke down quite easily.   The carbon

content was very low and the material was 'sandy' in colour.   It broke

down to quite angular grains and the shape distribution again shows it

to be 'platey'.

2.3.4   The Durham Shale

The Durham shale was also obtained as large pieces of rock from

the measures above the Harvey seam at Esh Winning opencast site.   It

was again broken down in the laboratory and made up to the same nominal

grading as Abernant.   As a shale it was stronger than the seatearth

but was weaker than the more carbonaceous Abernant shale.   It also

disintegrated extensively in water.   The carbon content was again very

low and the appearance was similar to that of the seatearth in terms of

colour, angularity and shape.

2.3.5   Peckfield Slurry

The material tested from Peckfield was obtained from the beach area

of No. 6 lagoon.   This has since been shown to be unrepresentative

of the main section of lagoon material at Peckfield, especially in

organic carbon content, but the material used served the purposes of

this investigation.   The material pumped to the lagoon at Peckfield is

from both Peckfield and Ledston Luck collieries, originating from the

Beeston and Flockton Thin seams, which have ranks of 702 to 802 and 702,

respectively.

The material tested had a typical fine discard appearance being black in colour and having quite a high moisture content. There was some degree of stratification in the sediment with occasional lighter coloured layers. The material is relatively coarse grained for a fine discard and is very non-uniform in grading as shown by the long 'tail' to the grading curve (Fig. 2.9).

2.3.6   Abernant Fine Discard

Due to the fact that the lagoon was submerged (with supernatant water overlying the sediment) only a bulk sample could be obtained. For this reason nothing can be said about the natural insitu state of this sediment. This material is also black in colour and similar in overall appearance to the Peckfield slurry. It is also relatively coarse grained for a fine discard, but in contrast to the Peckfield slurry is very uniformly graded. It is unusual in having a very low clay content.

2.4   Mineralogy and Chemistry

2.4.1   Methods of Analysis

The identification and semi-quantitative analytical mineralogical technique used in the present work was X-ray diffraction. Diffraction traces were run using a 2kw (3kw generator), Fe filtered Co tube at 50 kV and 30 mA. The scan speed used was 1° of 2θ per minute, the chart speed being 10mm per minute.

In order to obtain a semi-quantitative analysis 10 per cent boehmite was added to the samples which were subsequently made up as smear mounts. For colliery wastes, calibration charts have been in use in Durham for many years which enables an operator to obtain an estimate of the major minerals present. These calibration charts were made up using representative minerals such that the percentage of mineral present is plotted against

the ratio of the integrated peak area (measured with a planimeter) of the mineral, to the integrated 6.18 Å boehmite reflection. By comparing the requisite X-ray reflection ratio (e.g. 10Å illite) in the unknown with the standard charts an analysis is obtained which is customarily within $\pm$ 5 per cent of the total mineral count plus organic carbon (coal) content i.e. 100 per cent.

Major element oxides and sulphur were obtained by means of X-ray fluorescence (Philips PW 1212 automatic spectrograph), the counts for elements in the unknowns being compared with a wide range of previously wet analysed Coal Measures standards which bracket the percentage ranges of elements found in colliery wastes. X-ray fluorescence analyses are on an organic carbon, water and carbon dioxide free basis, i.e. the totals obtained exclude the latter.

2.4.2 Chemical apportionments in colliery wastes

The semi-quantitative X-ray analyses and the major element geo-chemistry are given in Tables 2.3 and 2.4. Diagnosis of colliery wastes in terms of mineral constituents is greatly facilitated by comparison of the diffraction (X.R.D.) and chemical (X.R.F.) results. Moreover it is advantageous to rationalise the chemical oxides by using Al_2O_3 as the common denominator (Table 2.5). This is because other silicates such as feldspars are only present as very minor constituents in argillaceous Coal Measures rocks. Alumina (Al_2O_3) is therefore the principal element oxide present in the clay minerals.

In the light of the present knowledge the element apportionment can first be discussed in general terms as follows:

a) total SiO_2 is apportional to quartz (free silica) and to silicon combined in the silicate minerals (combined silica) - dominantly clay minerals;

b) like combined silica, Al_2O_3, Na_2O and K_2O are attributed mainly to clay minerals;

c) both ferric and ferrous iron (reported here as Fe_2O_3), together with CaO and MgO are found in clay minerals other than kaolinite;

d) some ferrous iron may be combined with S to form pyrite in coaly materials, or as siderite ($FeCO_3$), particularly in non-marine shales;

e) some CaO, MgO, FeO may be combined as either calcite ($CaCO_3$), dolomite ($CaCO_3$ Mg CO_3), or as ankerite (a ferroan dolomite). In colliery wastes these carbonates are sometimes associated with the coal, i.e. found in the cleat (small-scale joints in coal).

f) TiO_2 is associated with clay minerals, either in the mineral lattice or as distinct rutile needles;

g) P_2O_5 is present as calcium phosphate, but some P_2O_5 and S may well be part of the organic component.

h) organic carbon in excess of about 5 per cent is usually present as coal.

2.4.3 Discussion of Results

From Tables 2.3 and 2.4 it is clear that in all samples clay minerals (illite and kaolinite) are dominant. We know that in the two rock types from the Durham coalfield the organic matter present is not coal. In the remainder of the samples, however, organic carbon is largely coal, attaining a very high value of 35 per cent in the Abernant coarse discard. In the two fine discards (Abernant and Peckfield), the organic carbon content is low for colliery lagoons - see Taylor and Cobb, (1977).

It is noteworthy that the lowest quartz contents are in the two fine discards. This can best be explained by the fact that the more resistant, and hence quartz-rich rocks, have been removed in the coal washing process. Quartz contents of shales and mudstones are commonly

between 15 and 30 per cent, which is true for all the remaining samples. With the removal of organic carbon (coal) from the coarse discards quartz will rise, particularly in the strong Abernant shale where it reaches a level of 20 per cent. The Durham seatearth is a quartz-rich variety and its X-ray analysis does not single it out as a clay-rich rock (i.e. a fireclay).

The most significant difference is that shown between the Durham rocks and the remainder - the high kaolinite content of the former - which confirms early work on colliery spoils (Taylor and Spears, 1970).

The combined silica/alumina ratios and the K_2O/alumina ratios confirm that the two Durham rocks are rich in kaolinite. A theoretical ratio for combined silica/alumina in kaolinite is about 1.18 and this is likely to be lower when the kaolinite component is slightly disordered, which is the case for the Durham rocks. It can also be seen from Table 2.5 that the K_2O/alumina ratio is considerably lower than in the other specimens. The siderite component in the Durham shale is highlighted by enhanced Fe_2O_3 (and higher Fe_2O_3/alumina ratio) in the chemical analyses).

The higher combined silica/alumina ratios of Gedling coarse discard, Abernant and Peckfield fine discards suggest that micaceous minerals (illite and mixed-layer clay) should be higher in these specimens. This is true also from the mineralogy, although the mixed-layer clay which is represented by a tail and the low 2 θ side of the 10Å peak has tended to increase the size of this reflection in the case of Peckfield and Abernant. In other words, the actual content of mica (illite) per se in the Gedling

sample is probably higher than in the Abernant or Peckfield materials.

Moreover, the K_2O/alumina ratio for the Abernant fine discard infers

that potassium may have been leached from the lattice. Here again,

South Wales micas may be somewhat different in their higher sodium

content (see Nagelschmidt and Hicks, 1943) and this is brought out

by the Na_2O/alumina ratio of Table 2.5.

One specimen that is difficult to confirm in terms of clay mineral

proportions is the coarse discard from Abernant. The total silica/alumina

ratio suggests that kaolinite should be the dominant clay mineral.

X-ray diffraction analyses show that this is not the case and it can

only be concluded that the 10 Å (micaceous) minerals in this material

are of poor crystallinity, to the extent that the ratio is no longer

a guide to clay mineral composition. Certainly the 10 Å peak is the

most ragged of all the samples, and this is a good indication of poor

crystallinity. It is pertinent to record that the combined SiO_2/

alumina ratio of the sodium-rich mica (brammallite) fraction which

Nagelschmidt and Hicks (1943) analysed is only 1.47, compared with 2.0

for more typical illites. This mica also came from the roof rocks of an

anthracite coal.

The higher MgO and CaO/alumina ratios of Gedling and Peckfield

confirm the presence of dolomite in these specimens and it is of interest

that sulphur figures for Abernant coarse discard and the Peckfield

slurry are not insignificant. No sulphates were identified in any of the

specimens and the amount of organic sulphur present is probably very

low. Consequently it is logical to recast the sulphur as pyrite (FeS_2)

in the coarse discard from Abernant and the Peckfield slurry. The amount

present on this basis is 3.74 per cent (Abernant) and 3.37 per cent

(Peckfield).   High backgrounds on the X-ray diffraction traces

precludes confirmation of pyrite, but the sensitivity of X.R.F. analysis

for indirect determination of minerals such as pyrite is illustrated by

these samples in which the coal content (and hence pyrite?) is high.

Table 2.1   Summary of Material Properties

Material	Maximum dry density Mg/m^3	Opt. Moisture Content %	Specific Gravity Mg/m^3	Carbon %	Liquid Limit %	Plastic Limit %	Plasticity Index %
Gedling	1.820	14.0	2.377	11.14	37	23	14
Abernant Coarse	1.600	15.0	2.191	35.33	23	19	4
Seatearth	-	-	2.591	2.51	=	-	-
Shale	-	-	2.652	5.99	-	-	-
Abernant Fine	1.725	15.1	2.536	10.71	17	16	1 (non-plastic)
Peckfield	1.655	15.8	2.382	18.35	26	24	2 (non-plastic)

85AB 15 SE			2.356				
80AB 20 SE			2.399				
75AB 25 SE			2.383				
50AB 50 SE			2.500				

Table 2.2   Results of Impact and Slaking Tests.

	Aggregate Impact Test		Slaking Test	
Material	Dry	Wet	No. 14	No. 7
Abernant	34%	44%	96.2%	95.6%
Shale	39%	52%	96.5%	66.1%
Gedling	50%	—	66.6%	—
Seatearth	47%	—	97.3%	—

Table 2.3   Chemistry from X.R.F.

	SiO_2	Al_2O_3	Fe_2O_3	MgO	CaO	Na_2O	K_2O	TiO_2	S	P_2O_5	C
Seatearth	59.24	31.45	3.02	0.54	0.24	0.16	1.67	1.40	0	0.01	2.51
Shale	48.51	29.85	9.60	1.54	0.41	0.21	2.61	1.17	0	0.11	5.99
Abernant Coarse	33.50	19.00	4.40	0.87	0.38	0.50	3.05	0.85	2.00	0.12	35.33
Gedling	52.25	22.10	5.78	1.69	1.26	0.51	3.92	1.00	0.30	0.05	11.14
Peckfield	44.50	23.60	5.15	1.58	1.55	0.36	4.35	0.90	1.80	0.08	16.13
Abernant Fine	46.19	29.91	3.85	1.28	1.10	0.82	4.40	1.04	0.55	0.14	10.71

Table 2.4   Semi-quantitative Clay Mineralogy

	Illite	Kaolinite	Quartz	Chlorite	Siderite	Dolomite/Ankerite
Seatearth	32	34	27	-	1	-
Shale	47	26	15	-	4	-
Abernant Coarse	44	6	13	-	-	-
Gedling	52	14	20	-	-	8
Peckfield	58	15	12	trace	-	7
Abernant Fine	58	8	5	-	-	

Table 2.5   Chemical Ratios (oxide/alumina)

	SiO_2	Fe_2O_3	MgO	CaO	Na_2O	K_2O	TiO_2
Seatearth	1.88	0.01	0.02	0.01	0.01	0.05	0.05
Shale	1.63	0.32	0.05	0.01	0.01	0.09	0.04
Abernant Coarse	1.76	0.23	0.05	0.02	0.03	0.16	0.06
Gedling	2.36	0.26	0.08	0.06	0.02	0.18	0.04
Peckfield	1.89	0.22	0.07	0.07	0.02	0.18	0.04
Abernant Fine	1.54	0.13	0.04	0.04	0.03	0.15	0.04
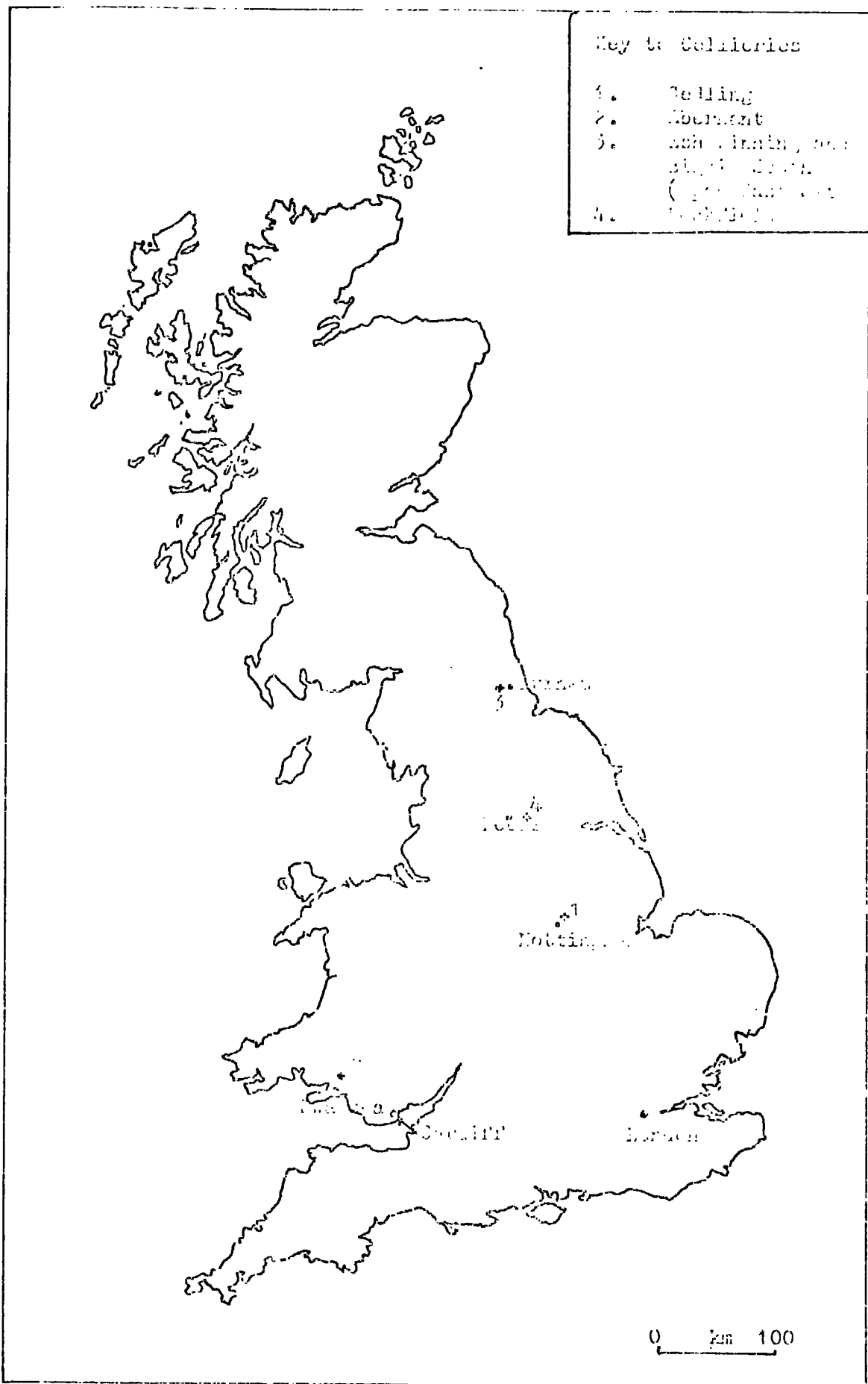
Figure 2.1 Location of Sites from which material was taken.
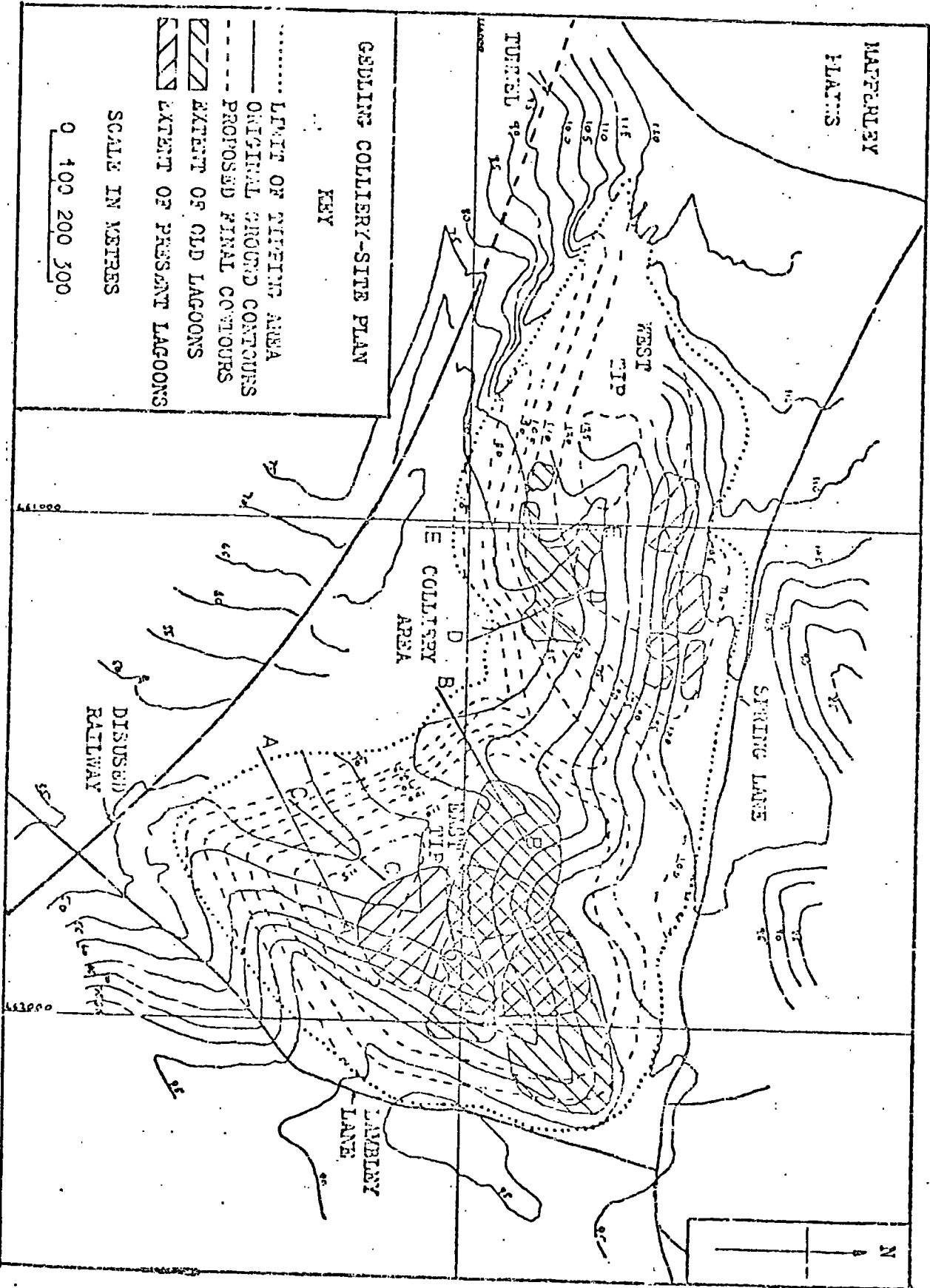
Figure 2.2   Site Plan of Gedling Colliery

SAMPLE

TIP 276

WASHERY WASTE

SLURRY
LAGOON 1 and 2.
173.04 W.L.

SLURRY
LAGOON 3 and 4.
172.80 W.L.

OLD
SLURRY
LAGOON

SLURRY
LAGOON 5

SLURRY
LAGOON 6
95.598 W.L.
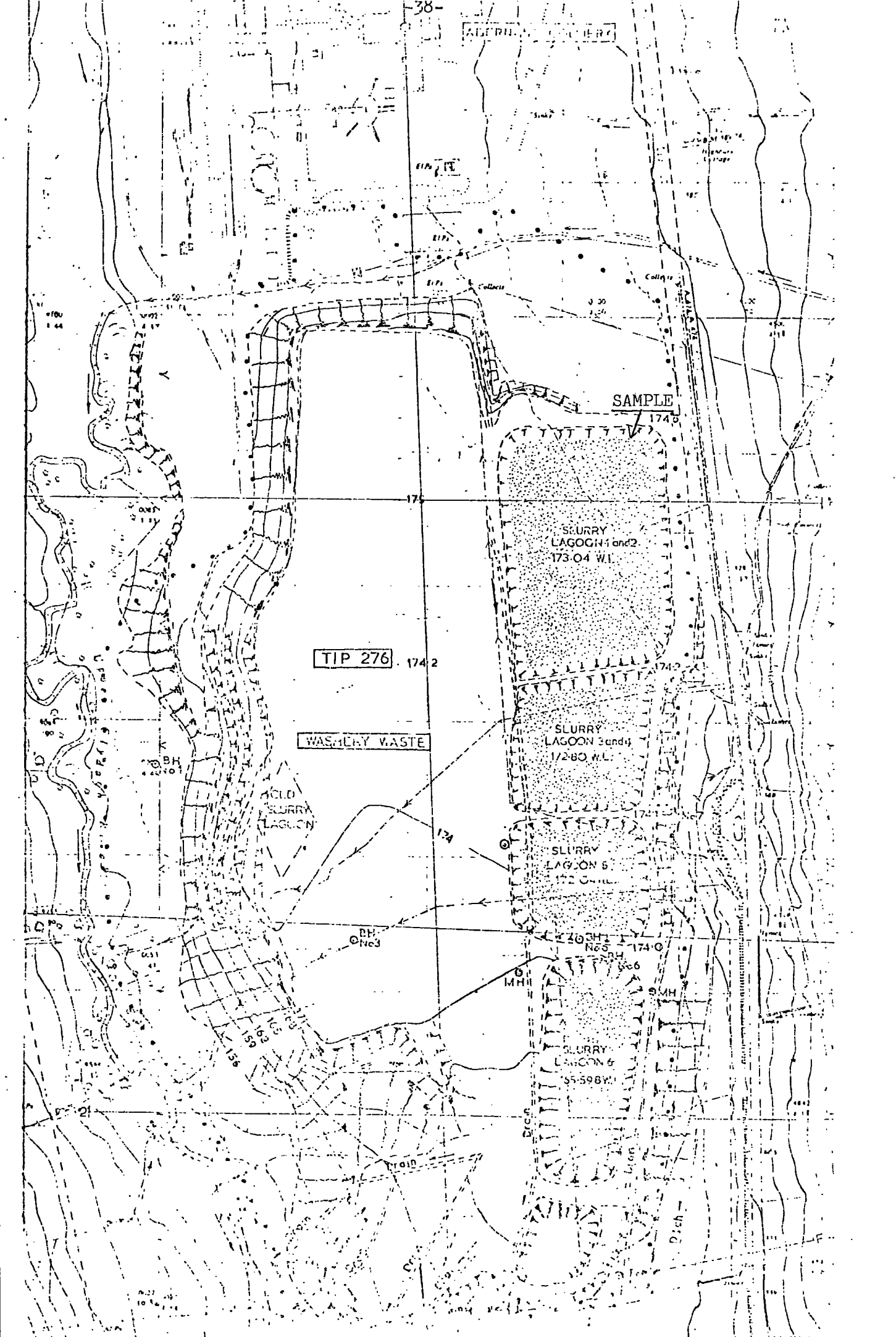
Fig. 2.3   Site Plan of Abernant Colliery
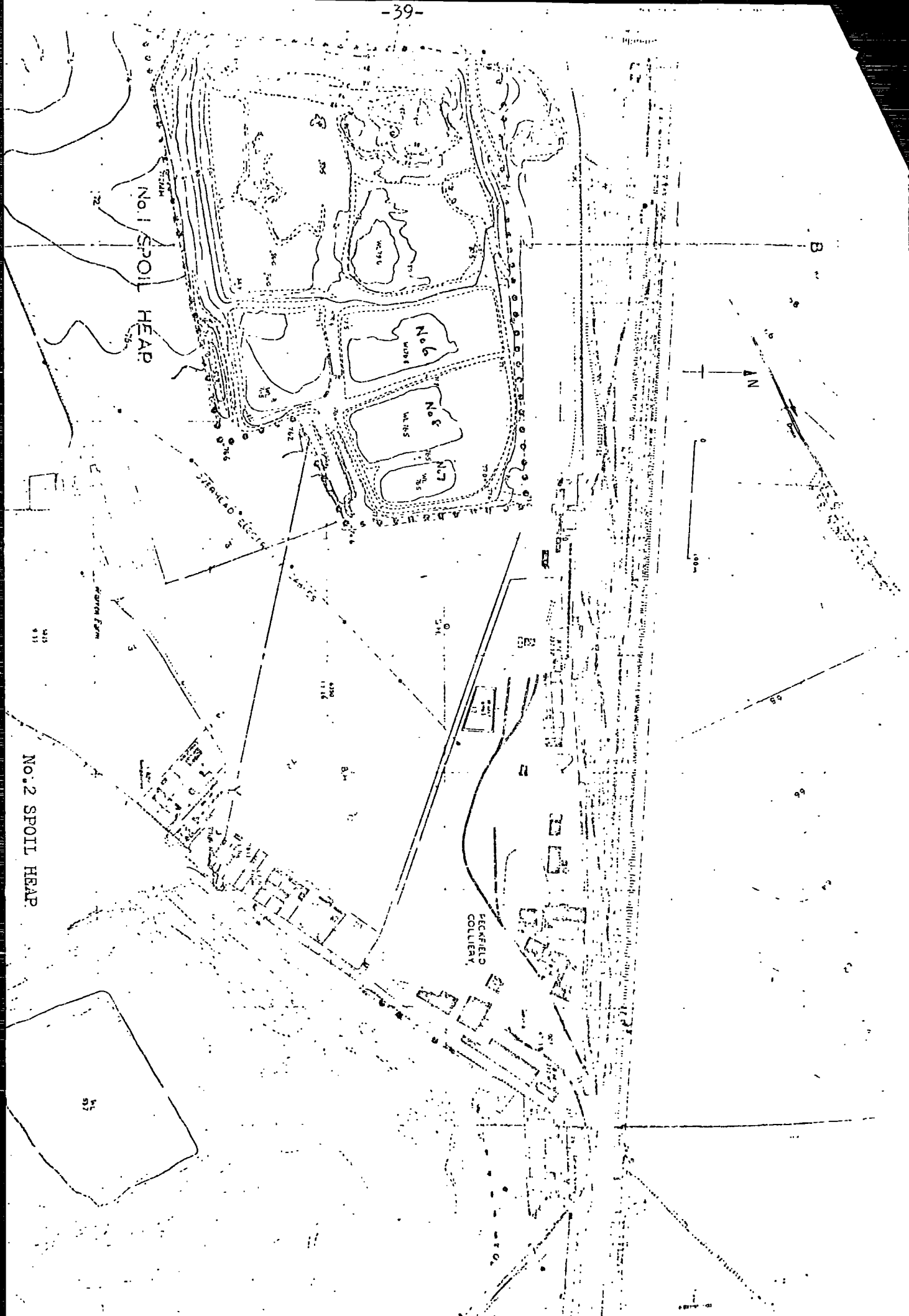
Figure 2.4   Site Plan of Peckfield Colliery

Grading Curves for ... ... Before and After Controlled Load testing.

Figure 2.7 Grading Curves for ... Material Before and After Controlled Load Testing.

Figure ... size distribution for ... stone piazza.

Figure 2.11 Size Distribution for Different Coarse Custard.

Figure 2.14 Gedling Coarse Discard.
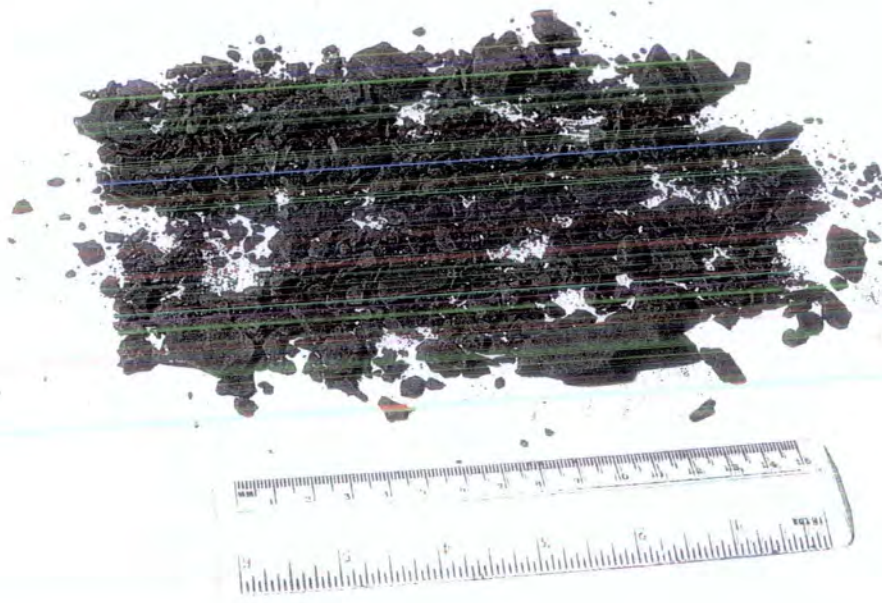
Figure 2.15   Abernant Coarse Discard
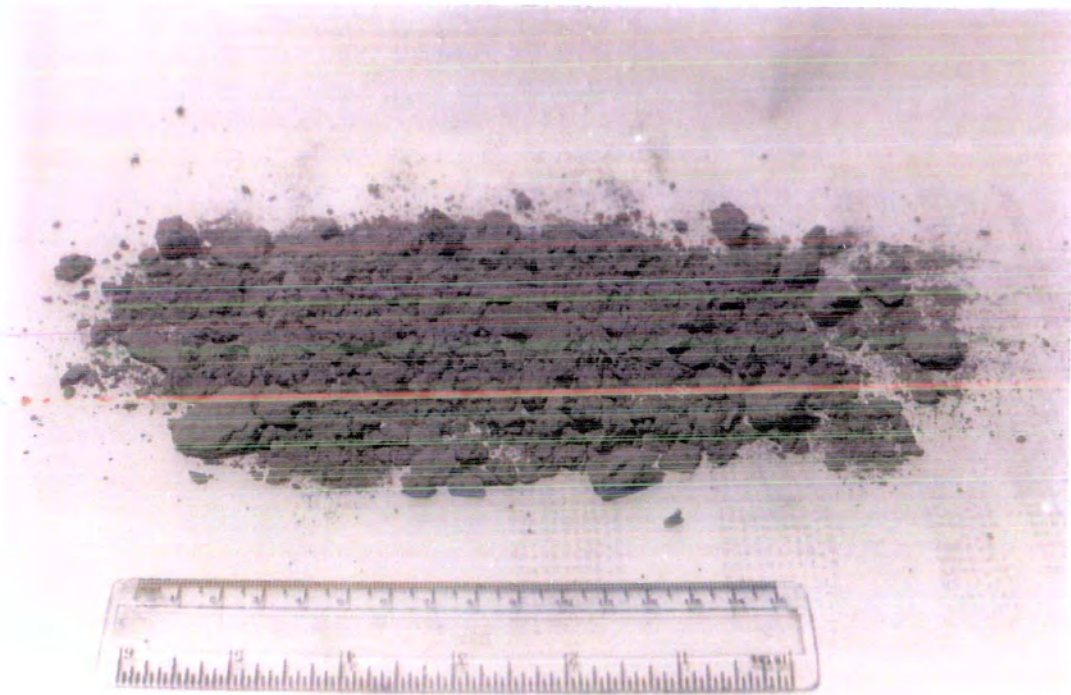
Figure 2.16   The Durham Seatearth
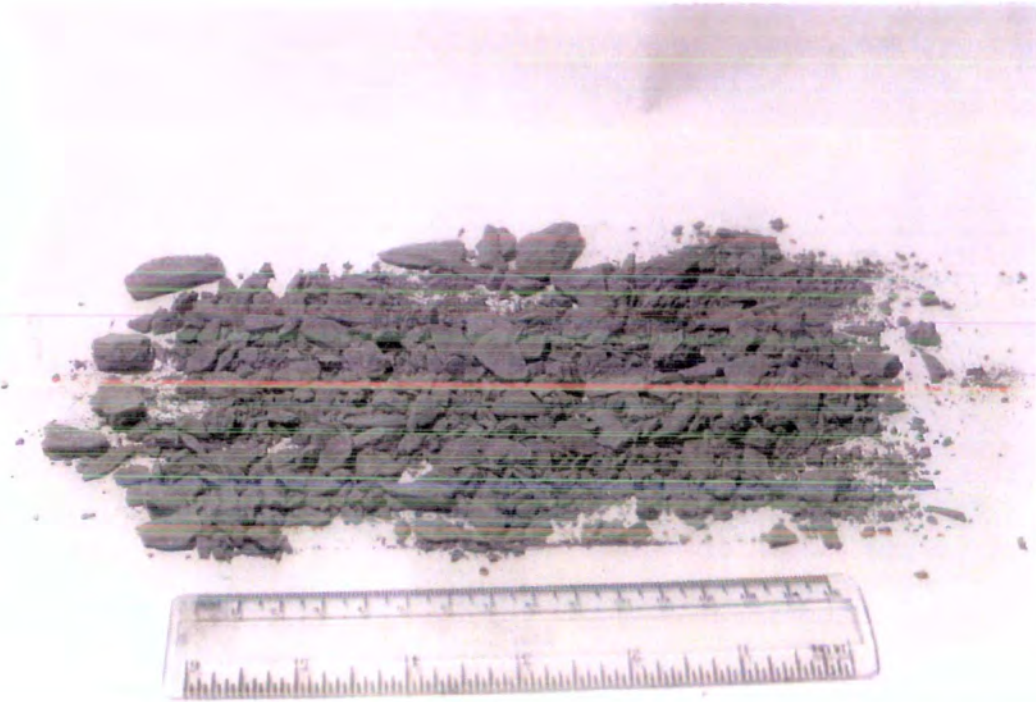
Figure 2.17   The Durham Shale
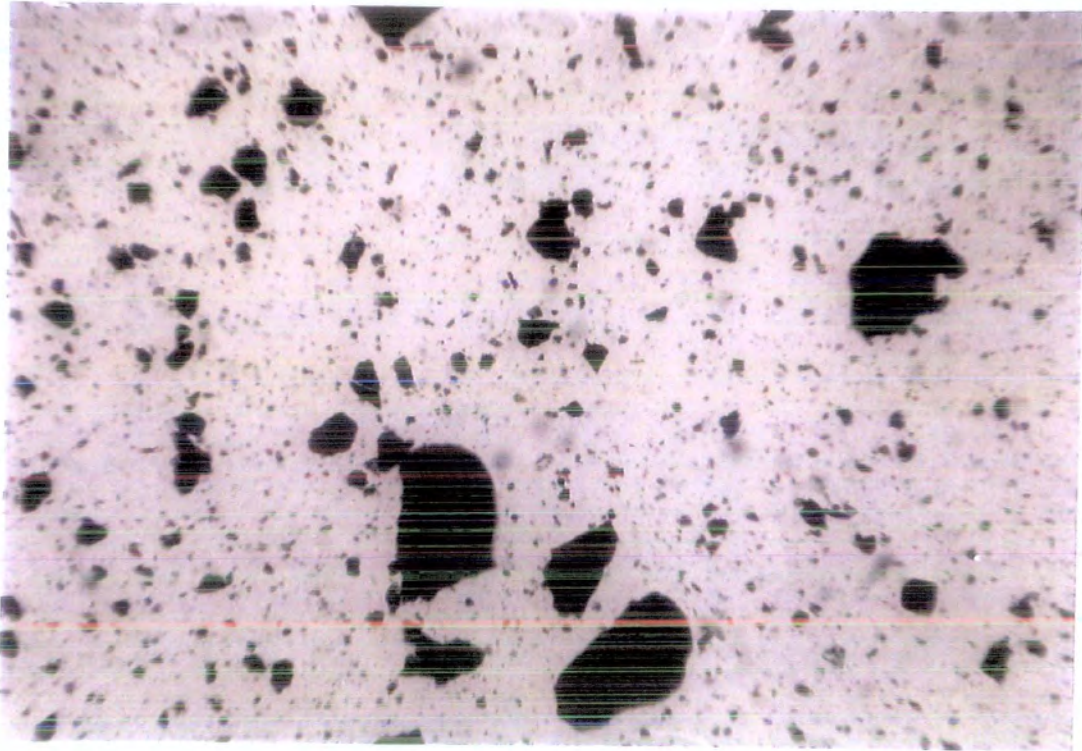
Figure 2.18   Peckfield Fine Discard

0   0.5
└──────┴──────┴──────┴──────┴──────┘
                    mm.
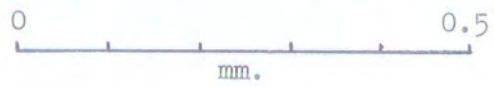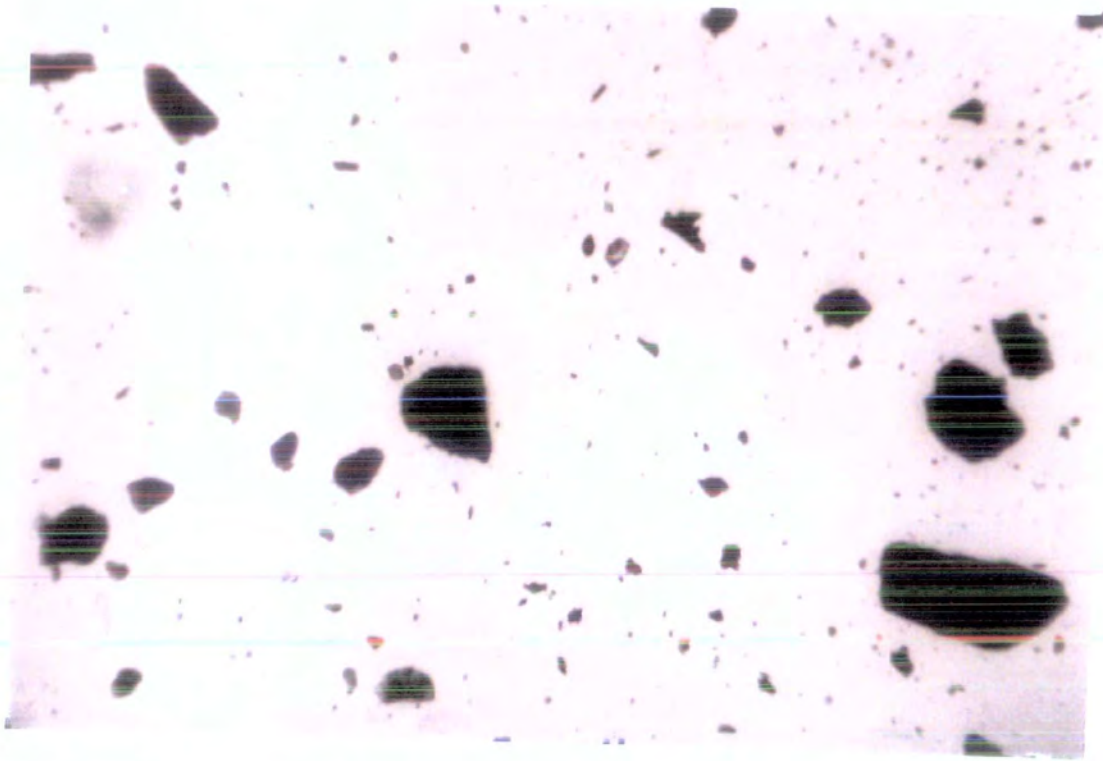
Figure 2.19   Abernant Fine Discard

CHAPTER THREE

APPARATUS USED

3.1   Introduction

In this Chapter the rigs used for the principal parts of the

investigation are described together with the associated equipment.

The two main rigs used were both developments of the standard

triaxial cell customarily used for strain controlled shear strength

tests.   The devices incorporated are for the application of a

controlled load as opposed to a controlled strain;   instrumentation

introduced is compatible with the possible rapid events which are a

feature of these tests.   This instrumentation was common to the two

rigs as was the pressurizing system.   Hence, the cells and loading

apparatus are first described individually and then the instrumentation

is considered.   Items mentioned in the text are referred to the

relevant Figures.

3.2   The Large Controlled Load Rig

3.2.1   The Cell

The cell used in the large rig is an adaptation of a standard

100mm triaxial cell as shown in Figure 3.1.   The standard cell was

modified by the addition of an extra base ring (L,Fig.3.3) between the

cell base and top (M,Fig.3.3) in order to accommodate an internal load

cell (C, Fig.3.3) instead of an ordinary piston loading device.   An

extended piston was added to the load cell in order to allow

sufficient travel for complete failure (extended strain) of the sample.

As a result of the above modifications the size of sample used in this

cell was approximately 180mm by 100mm as opposed to the normal 200mm by

100mm.

The cell was plumbed into a Bishop self-compensating pressure

control system (section 3.4), there being four lines connected to the

cell.   Three were fitted with blocks for pressure transducers, each

being fitted with two 'Klinger' taps to allow the transducer to be

isolated either from the sample or the pressure system.   One line

(line 8, Fig.3.2) was connected into the base of the cell from the

cell pressure pot, and this line was also connected to pressurized

water tanks (D, Fig.3.2) for filling the cell.   Two lines (lines 1

and 4, Fig. 3.2) were connected to the base of the sample (one (No.4)

without a transducer).   Both lines were connected to the back

pressure pots.   The first (No. 1) was connected directly.   The

second (No. 4) originated from the other side of the sample and had

two alternative paths to the back-pressure system.   It could either

be connected via the volume change apparatus (lines 6 and 7,Fig.3.2)

or by isolating the volume change, directly to the back-pressure

system (line 3, Fig.3.2).   Both paths originated from an extension

of the first base line (No. 1).   The second line was also fitted with

a junction taking a line direct to the board to allow the volume change

fluid to be moved during a test (line 5, Fig.3.2).   The fourth line

(line 2, Fig.3.2 and J, Fig. 3.3) was a junction from the back

pressure line (No. 1) through a small bore nylon tube to the top

platen, allowing saturation of samples from both top and bottom.

3.2.2   The Loading Beam.

As shown in the photograph (Fig. 3.1) the loading system was a

pivoted counter-balanced beam, with a hanger at each end.   It was

pivoted off-centre to magnify the loads applied, the magnification being

approximately a factor of five.   The beam was seated on a ball bearing

placed on top of the piston.   A scissors jack was also used in conjunction with the beam, as a support during saturation of the sample and a means of lowering the beam during consolidation.   The counter balance hanger allowed weights to be applied to counter the weight of the beam before loading, and to lift the beam from the cell during preparations for a test.

3.3   The Small Controlled Load Rig.

3.3.1   The Cell

In a similar manner to the large cell the small one was an adaptation of a standard triaxial cell designed to take an internal load cell (C, Fig.3.6), using a specially extended perspex section. A standard sample of 76mm by 38mm could be accommodated.

The plumbing was in principle the same as for the large rig, the main difference in this case being only one water line (line 1, Fig.3.5) to the base of the sample.   The volume change was taken from a junction in the latter line (line 5, Fig.3.5) with no by-pass being provided. The base pore pressure transducer (G, Fig. 3.5) was fitted to the second tap in the cell base, and this line (line 2, Fig.3.5) was originally used for the application of a vacuum as explained in the following Chapter.   A water bottle (L,Fig.3.5) for entraining water into the sample was fitted to an extension of the back-pressure line (line 4, Fig.3.5).

The top platen (D, Fig.3.6) was made of perspex, being in the form of a cylinder with a larger diameter disc attached.   The top line (line 3, Fig.3.5 and J,Fig.3.6) was side fed into the cylinder. A later modification involved the addition of a further larger diameter disc below the first, containing a central porous plug.   This was

designed to prevent the application of pressure to the sample while
fitting sheaths and 'O' rings, when a vacuum was no longer being used.

3.3.2   The Loading System

The loading system was similar to that of Castro (1969),
consisting of a yoke with a weight hanger beneath (A,Fig.3.6), the
whole being connected to a counter-balance hanger (E,Fig.3.6) by a
cable passing over a bicycle wheel (L,Fig.3.6).   A small hole in the
top beam of the yoke allowed it to be seated on a ball bearing placed
on top of the loading piston.   The principle of the counter-balance
is the same as for the large rig.

3.4   The Bishop Self-compensating Pressure Control System.

The pressurizing system used for both rigs was a Bishop mercury
pot system, illustrated in Figure 3.7 and described in detail in Bishop
and Henkel (1962).

The system consists of two separate sets of pots each consisting
of upper mobile pots on springs and fixed lower pots connected by
flexible small bore nylon tubing.   The nylon tubing is mercury filled
with a mercury/water interface in each pot.

The lower pots are connected to the cell via the junction board,
which allows the system to be isolated.   A hand pump (B, Figs 3.2 and
3.5) for the repumping of mercury and a gauge (C, Figs 3.2 and 3.5) for
setting and reading pressures are incorporated.   Pressure is applied
to the cell by the head difference between the upper and lower pots.
When water moves in or out of a sample during saturation or consolidation
it causes the mercury level to change.   This is compensated for by the
springs which, having the correct stiffness, maintain the original head.

The back pressure pots, connected to be cell base, have two upper
and lower pots, to provide a larger quantity of mercury, to allow for

the large quantities of water forced into a sample during saturation.

The cell pressure pots just have a single upper and lower pot.   These

are connected in series with the back pressure pots.   This allows the

same pressure to be applied both to the cell and the sample, or for

slight differentials to be set by raising the cell pot above its

datum level.   Extra pressure is applied to the cell for consolidation

purposes by raising the single pot.   A modification of the system

incorporates extra pots at a fixed height, the head of which can be

added to the variable head of the basic pots.   The pressure range is

$0-600$ kN/m^2 for back pressure and $0-1200$ kN/m^2 for cell pressure.

3.5   Volume Change Apparatus

Both rigs were fitted with a volume change apparatus for measurement

of volume changes during consolidation.   The principle of operation is

the same in both cases although there are variations in detail due to the

different order of volume changes obtained.

As shown in the photographs (Figs 3.1 and 3.4) the apparatus

consists of a tube (J,Figs 3.2 and 3.5) and a reservoir (I, Figs 3.2

and 3.5) containing dyed petroleum spirit.   When a sample consolidates

it dissipates the excess pore pressure built up by the application of

extra pressure by forcing the water out of the sample, this water causes

the dye to be moved up the tube into the reservoir.   On the small rig

the amount of volume change is read directly in the calibrated burette

(J, Fig.3.5).   However, due to the much larger volume changes for the

large sample a larger diameter tube (J, Fig.3.2) is needed on the large

rig.   The distance moved by the dye/water interface up this tube is

measured by the rules fixed to the board, and the volume calculated from

the known dimensions of the tube. The tube used was of 19mm internal
diameter. Two tubes are provided on both boards to give extra
capacity for large volume changes. During volume change the systems
are back-pressurized from the pots, the water being forced back into
the pots.

3.6   Instrumentation

Because of the rapid changes during tests in which liquefaction
occurs, a recording system with fast reaction time was required for
monitoring data. Hence transducers were used in connection with an
ultra-violet recorder.

3.6.1   The U.V. Recorder

The U.V. recorder used for most of the tests was an SE3006, 12
channel recorder with a paper speed range from 5mm/min to 125mm/sec,
although an SE 6008, 12 channel recorder was used for some of the
earliest tests.

Four channels were used in the tests, one each for load, strain,
cell and pore pressures. The principle of operation is that the
voltage from the transducer is fed to a galvanometer on which is
suspended a mirror. This mirror reflects UV light on to the photo-
sensitive paper, producing a trace of the variation of the exciting
voltage.

The same galvanometers were used throughout the investigation,
since although galvanometers of the same type have the same nominal
sensitivity, there can be significant variations between individual
galvanometers. The same four galvanometers were used in the same
four positions when using both rigs. Two types of galvanometer were
used; SE labs type B100 of nominal sensitivity; 0.20 mV/cm for the

load and strain and Southern Instruments Type SM1V of nominal

sensitivity 0.132 mV/cm for the cell and pore pressures. Both types

of galvanometer have a natural frequancy of 100 Hz.

As well as producing a trace, the UV recorder also produces a

grid and timer bars (at intervals of either 1 minute or 1 second

depending upon setting), both of which are of great importance in

interpreting and calculating results from the traces.

3.6.2   Amplification

Before the signals could be fed into the galvanometer they had to

be either amplified or attenuated so as to give a voltage and voltage

variation appropriate to the range and sensitivity of the galvanometer.

Since different ranges of pressures were being used, and hence

different loads expected, variable amplifiers were used for these

signals, so that the full-scale deflection of the trace was produced

by the kind of variation produced in that particular test. In this

manner it was always possible to achieve maximum sensitivity and

accuracy from the trace. The amplifiers used were Fylde type 251GA

Mini-Amps supplied in a set of six amplifiers. Each had a variable

sensitivity and shift of zero, which were preset to give maximum range

and the correct order of voltage for the galvanometers at the

particular settings used. These settings were not altered throughout

the investigation. Each amplifier had 6 different settings, although

2 of these settings proved sufficient for the range of values experienced

in the tests: Calibration for each transducer was carried out at 3

settings to cover any change of range. The calibrations are shown in

Appendix 1.

For the strain, the same values of strain were expected for each

test on a particular rig, and hence no variation in range was required. It was found that the signal from the strain transducer required attenuating, and this was achieved by use of an in line resistance of the correct value in the output line.   This was placed in the junction box used.   Initially separate resistances were used for the two rigs, but it was found that on the small rig much larger percentage strains occurred, so that the resistance for the large rig was sufficient to give full-scale deflection (f.s.d.) in both cases.   The resistance used was 150 k.Ω as this gave an f.s.d. for a deflection of about 50mm, which was the range required.

3.6.3   Power supply

The power supply required for all the transducers was 10V d.c., as was that for the load cells.   The LVDT had a nominal supply voltage of 12V, but 10V proved sufficient for satisfactory operation.   A common power supply of 10V was used for all the instruments.   The power supply type was a Farnell Stabilised Power Supply Type L30B with a range of 0-30V and capable of withstanding a mains variation of $\pm$ 10%.

3.6.4   Large Rig Load Cell (C, Fig. 3.3)

This load cell was an internal triaxial load cell from Transducers (CEL)Ltd., Reading, serial no. 4438, with a load range of 0-2000 kg and an output of 0-25 mV at an exciting voltage of 10V.

The cell was calibrated onto a Digital Voltmeter (D.V.M.) and direct on to the U.V. at the appropriate amplifications.   These amplifications were necessarily high due to the large range of the cell compared to the loads used.   This had the disadvantage of producing 'noisy' load traces from this rig, due to background mains   which could not be eliminated.   The calibration was carried out against the

proving ring on a standard triaxial machine, readings being taken both ascending and descending the load range. The calibration graphs are shown in Appendix 1. A certain amount of non-linearity is present at low loads. However, as the cell is not compensated against cell pressure a load already exists on the cell prior to loading in a test, which results in subsequent readings being in the linear range.

3.6.5 Small Rig Load Cell (C, Fig.3.6)

The Load Cell used in the small rig is also an internal triaxial cell, designed at Imperial College and supplied by Wykeham Farence Ltd. It is a high sensitivity load cell with a range of output of 120mV with a power supply of 10V and a load range of 0-500 kg.

This cell was also calibrated against a proving ring on to a D.V.M. and direct on to the U.V. The calibration graph is produced in Appendix 1. It has good linearity except at very small loads and the return curve shows some degree of hysterisis at higher loads. The cell is nominally compensated for cell pressure, but observation has shown that there is some effect due to varying cell pressure. Hence, like the Large Rig its test operation is probably within the linear range.

3.6.6 Pressure Transducers (F,G & H, Figs 3.2 & 3.5)

The pressure transducers used on both rigs were of type P721-0002 manufactured by Electromechanisms Ltd. They had a pressure range of 0-100 p.s.i (690 kN/m^2) and an output range of 0-25 mV for an exciting voltage of 10 V.d.c.

Three transducers were used on each rig, one for cell pressure, one for top pore pressure and one for bottom pore pressure, although only one pore pressure transducer (the bottom one) was monitored during tests.

Each transducer used was calibrated on to a D.V.M. and direct on to the U.V. recorder. They were calibrated in position on the rig, by applying pressure using the hand pump on the board (B, Figs.3.2 and 3.5). Each was calibrated at three different amplifications giving three pressures ranges. All calibrations were carried out whilst ascending and descending the pressure range. The calibration curves are again shown in Appendix 1. All show good linearity over the whole range. When used in tests the transducers were not monitored from zero, but from the final saturation pressure that was applicable.

3.6.7 The Strain Transducer (B, Figs 3.3 & 3.6)

Linear strain was recorded using a d.c. linear variable differential transformer (LVDT) made by Sensonics. The same LVDT (serial no.1024) was used for both rigs. The LVDT had a maximum exciting voltage of 12V, but as mentioned earlier worked satisfactorily at 10V. The output range was +3V to -3V over the linear operating range of $\pm$ 25mm. This range started from the lower limit of the travel.

The LVDT was calibrated against a dial gauge on a standard triaxial machine, both on to a DVM and the UV recorder, and was found to have good linearity over the specified range. The calibration graph is shown in Appendix 1.

On both rigs the LVDT was attached to the top of the piston, measuring displacement relative to the top of the triaxial cell (see Figs 3.1, 3.3., 3.4 and 3.6).

3.7 The Controlled Strain Rig

A number of consolidated undrained triaxial tests with pore pressure measurement were performed on coarse discards. These tests were performed using a standard strain control triaxial machine manufactured by

Wykeham Farance Ltd.

The cell used was a standard 4" (100mm) triaxial cell which was plumbed to the same system as the Large Controlled Load Rig (Fig.3.2), except that no top line was used.   Due to the much slower rates of change involved, more conventional monitoring techniques could be used. Pressure transducers were used on the pressure lines, being used for the B-test.   During the tests, cell pressure was not found to vary very greatly, being checked on the gauge on the board.   The pore pressure was monitored from the transducer using a DVM.   The load was measured using a proving ring and linear strain was measured using a conventional dial gauge.
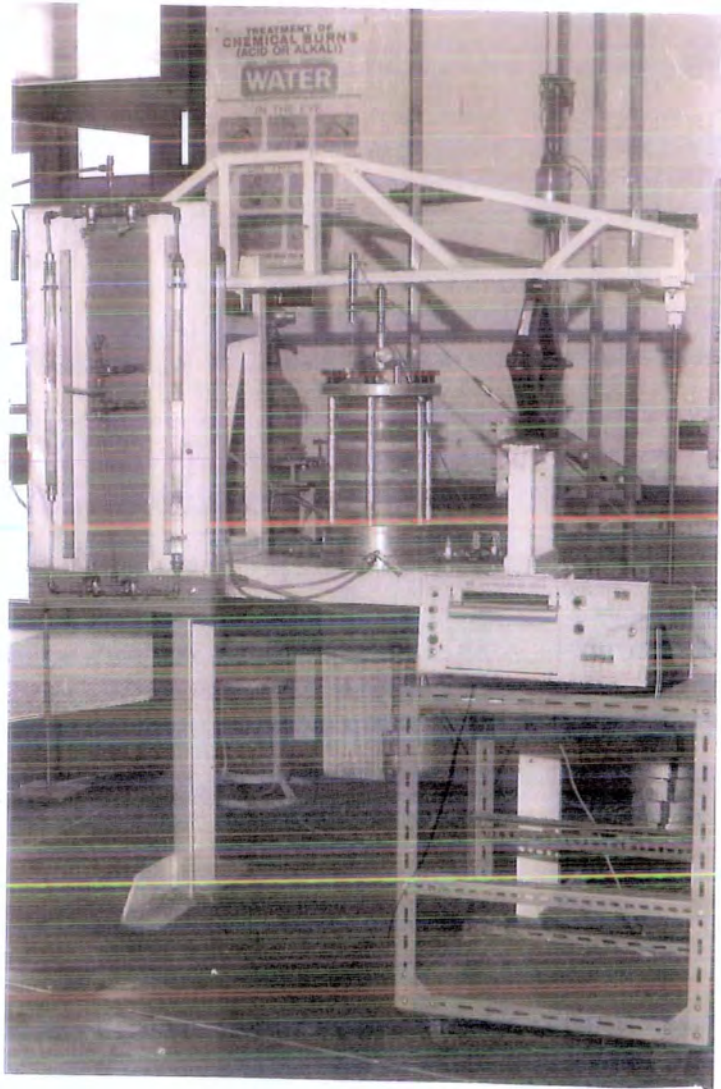
Figure 3.1   The Large Controlled Load Rig

Pressure Source

✕ ——— Taps

A   Loading Ram
B   L. ....
C   Load Cell
D   ....
E   ....
F   Calibrated ... Transducer
G   ... Pressure Transducer
H   ... Pressure Transducer
I   ....
J   Top Plate
K   Sample
L   ... Base Ring
M   Cell ...
N   Bottom Piston
O   ....
Q   Back Pressure

Line 1 – Load Transducer (Direct)
Line 2 – Air Suspension
Line 4 – Back Pressure (Indirect)
Line 8 – Cell Pressure

→ Electrical Outputs to Junction Box for U.V. Recorder

Line 2
Line 1

Line 0
Line 4

✕ Bag

Figure 3.3   Arrangement of Cell for ... Controlled Load Rig.
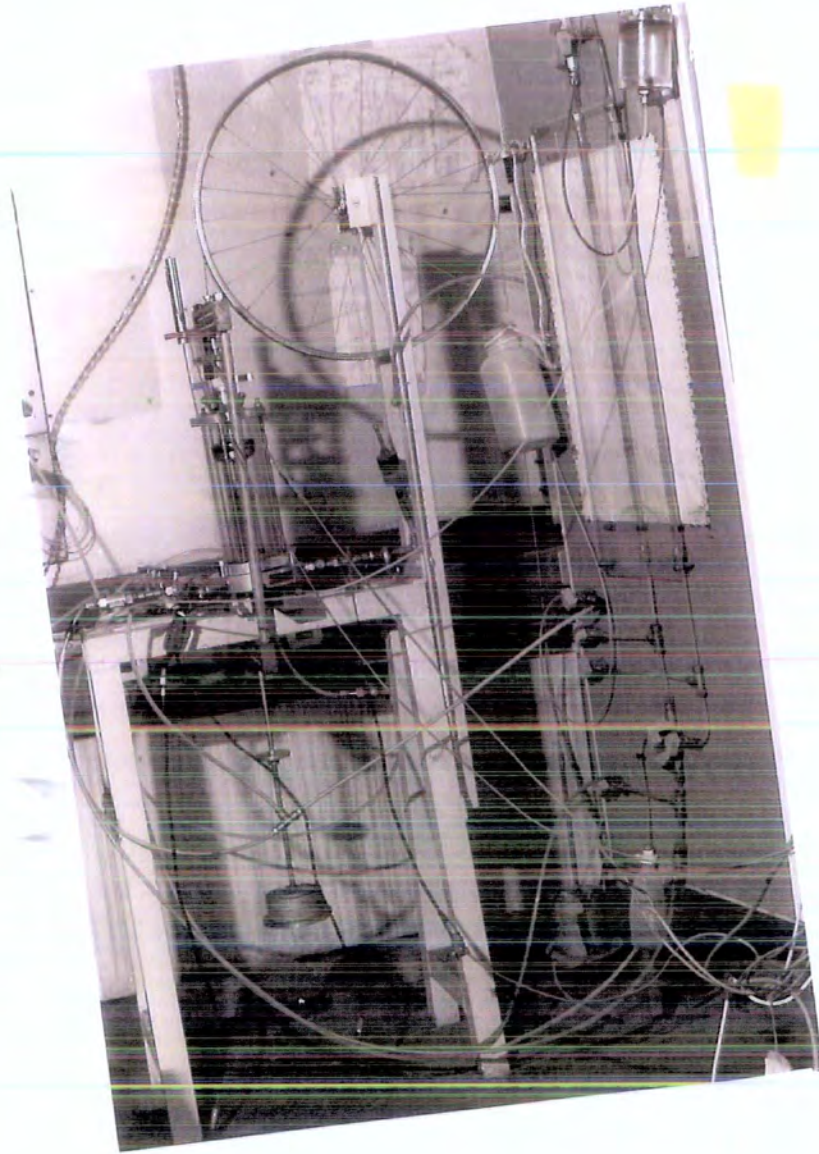
Figure 3.4   The Small Controlled Load Rig

Pressure Board

Taps

to vacuum

Figure 4.5 Diagram of Cell Connections etc.

Loading Yoke
L.V.D.T.
Load Cell
Top Piston
Counter Balance Mass
Cell Pressure Transducer
Pore Pressure Transducer
Top Pore Pressure Transducer
Porous Discs
Top Line
Sample
Bicycle Wheel
Cell Top
Bottom Platen
Air Valve
Ball Bearings
Underslung Load Hanger
Piston Lock

Line 1 - Back Pressure
Line 2 - Vacuum Line
Line 3 - Top Saturation
Line 7 - Cell Pressure
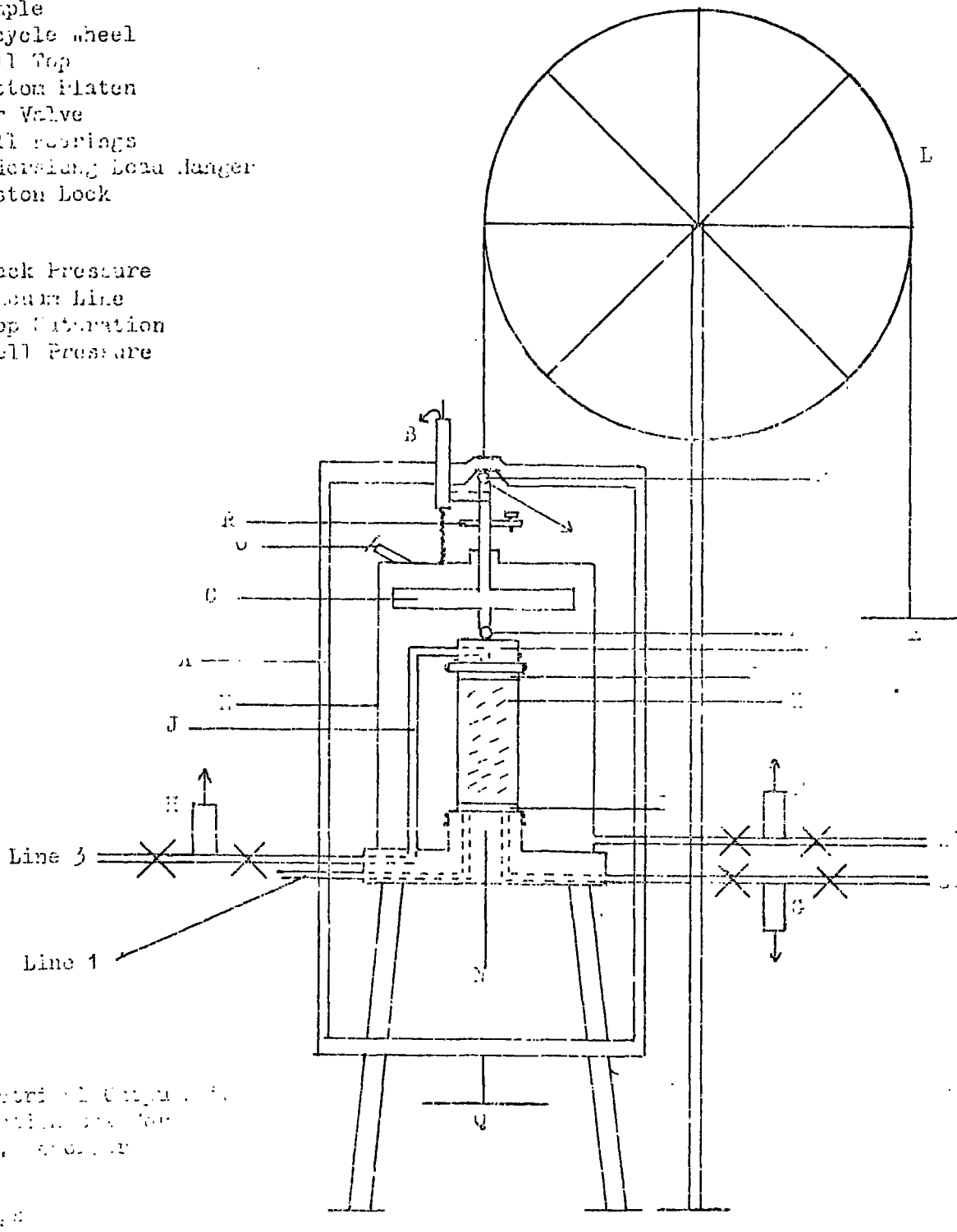
Figure 5.6 Arrangement of the Small Controlled Load Rig.
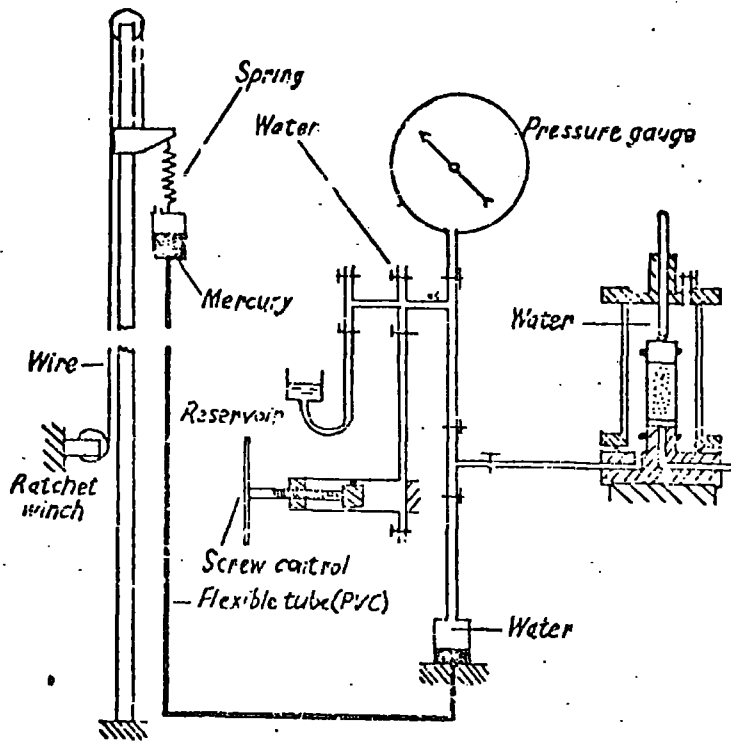
(a) The basic layout of self-compensating mercury control
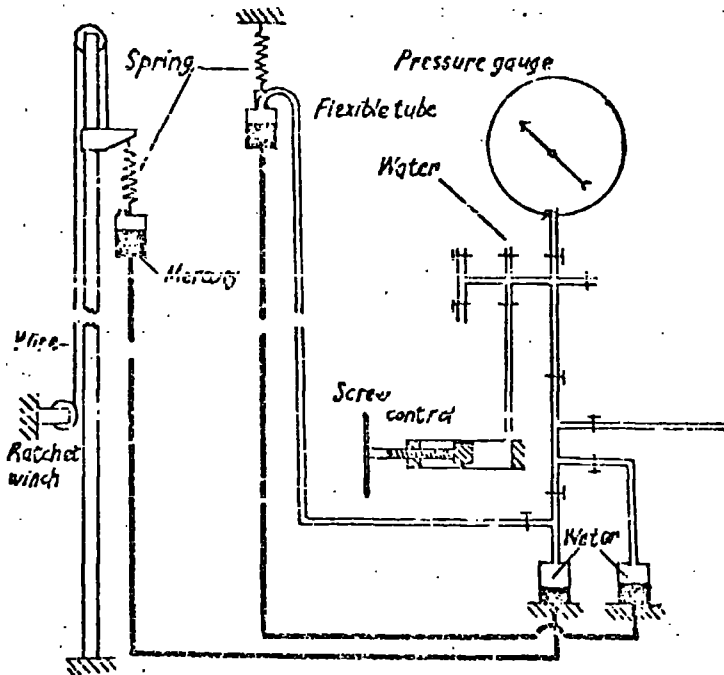
(b) The layout of the self-compensating mercury control with extended pressure range

Figure 3.7 The Bishop self-compensating pressure control system.

CHAPTER FOUR

EXPERIMENTAL METHOD

4.1   Soils Classification Tests

For the purposes of classification and comparison, all materials were subjected to the following standard soils tests:

(i)   particle size analysis (a) sieving

(b) pipette analysis

(ii)   liquid and plastic limits

(iii) compaction test

(iv)   specific gravity.

The methods used for these tests were the standard ones given in British Standard 1377 (1975).   Certain extra tests were carried out on the coarse materials and are briefly described here.

4.1.1   Shape analysis

In order to be able to draw comparisons between the shape of the particles and the possible effects of shape on liquefaction   potential, measurements were taken of the three dimensions of particles passing a 19mm sieve and retained on a 13mm sieve using vernier calipers.
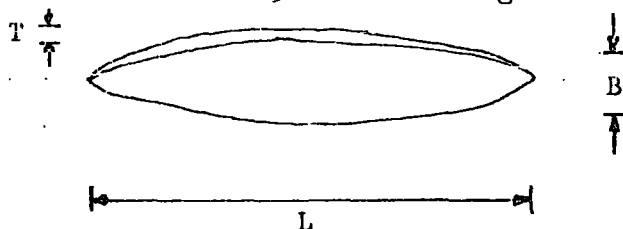
Approximately average values were taken in all cases.   The results were plotted as B/L against T/L and are produced in Chapter 2 (Figs 2.10 to 2.13).

4.1.2   Slaking Test

The effect of water on the coarse materials studied was explored by means of a simple slaking test.Material passing a 6.35mm sieve and retained on a 4.76mm sieve was carefully brushed to remove fine material from the

surface and then weighed out accurately. The material was placed on a

B.S. No. 14 sieve which was left standing in distilled water for about

30 minutes. The sieve was then placed in the oven until dry. The

weight retained on the No.14 sieve was then accurately measured and the

degree of breakdown expressed as the weight retained over the original

weight. For the Abernant material and Durham Shale the same method

was used with a No. 7 sieve. The technique used was essentially similar

to that of Taylor and Spears (1970).

4.1.3   Aggregate Impact Test

The strength of the coarse materials was measured indirectly by means

of the aggregate impact test, as described in British Standard 812 (1967,

section 34). These results are also given in Chapter 2.

A modification to this test (a saturated impact test, Shergold and

Hosking(1963) was carried out to find the effect of water saturation on

strength. Material of the usual size was weighed out, and soaked in

water for 30 minutes, followed by testing in the usual way. The results

were expressed in the conventional fashion, although the accuracy was

much less because material was lost through splashing out of the

container.

4.1.4   Organic Carbon Determination

The organic carbon content of the materials used was determined

using a simple oxidation method (Keeling, 1962). About 0.3 gm of

oven dried ground material (passing No. 36 sieve) was placed in a small

test tube which had been accurately pre-weighed. The tube was then

re-weighed with the sample and placed in a Furnace set at a temperature

of $350^{\circ}C$ for 48 hours. After removal the tube was allowed to cool in a

desiccator and then re-weighed. The percentage of organic carbon was

expressed as the weight loss divided by the original weight.

4.2   The Large Controlled Load Rig Method

Before every test was carried out or the sample set up, the rig
had to be prepared.   The main operation carried out was the de-airing
of the water lines.   This was done by pumping water through the lines
by means of the hand pump (B, Fig.3.2).   Also, the dye in the volume
change tubes was moved back down the tubes (J, Fig.3.2) so that there
was sufficient volume in the tubes to accommodate the expected volume
change.

4.2.2   Sample Preparation

All tests were carried out on samples screened through a B.S.19mm
sieve.   The sample was prepared to a nominal size of 180mm by 100mm.
Assuming this approximate size the weight of material needed for the
particular dry density required was calculated.   In general, the aim
was to produce a sample as loose as possible which would still stand up
during preparation, and which would have reasonable uniformity.   This
was found to be in the order of 75-85 per cent, B.S. Standard Compaction
density (British Standard,1377, 1975).

If the sample had been obtained from the colliery in a wet condition,
and had been kept wet,it was made up in this state, the moisture content
being estimated from previous measurements for the calculation of density.

However, some samples were obtained in a dry condition and a different
method had to be employed for the initial preparation.   The sample was
weighed out, and then 10 per cent by weight of water was added and
thoroughly mixed into the sample by hand.   After this stage the methods
of preparation did not differ.

The sample was prepared in a 100mm internal diameter steel tube, with
a screw thread at one end for placement on the hydraulic jack.   A metal

platen was placed in the bottom of the tube, and the sample was then carefully placed in the tube. A second metal platen was then placed on top of the sample. The tube was then placed on the Denison compression machine; a heavy cylindrical piece of steel was then placed on top of the upper platen. On the cylinder there was a band of tape which had been positioned so that when it was in line with the top rim of the tube, the separation of the platens would be 180mm. The ram of the machine was then lowered onto the cylinder, and allowed to compress the sample until the tape band and the tube rim were in line. The ram was then raised and the cylinder removed from the tube.

The tube was removed and screwed onto the hydraulic jack. The sample was then jacked until the top platen could be removed, leaving the top surface of the sample just below the rim of the tube. A triaxial specimen mould of 105mm internal diameter and 230mm length, with rubber membrane was placed over the sample, and jacking was then continued until the top of the sample was close to the rim of the mould. While still sucking, four strips of filter paper approximately 25mm wide and 200mm long were slipped down between the membrane and the sample, at approximately 90° intervals around the sample. The top ends of the papers were folded over onto the top of the sample. These strips acted as drains to aid in saturation.

Ideally they should be placed wet on the outside of the sample without the presence of the mould. However, due to the granular and loose nature of the samples used it was not possible to leave them standing without the mould. A circular piece of filter paper which had been soaked in water was then placed on top of the sample, making contact with the folded tops of the side drains. The top platen was then replaced and the mould removed from the jack and carefully inverted.

The second platen was then removed, and the protruding ends of the side drains folded over this end of the sample. A second soaked circular filter paper was placed on this end and the platen replaced. The mould was then carefully removed from the jack. As a check on the initial weight of material, the mould was weighed at this stage, the total weight of mould, membrane, platens and filters having been taken previously.

4.2.3 Mounting of Sample

Once the sample had been prepared it had to be transferred from the mould to the cell. In order to aid saturation and to prevent fine material blocking the sample lines, top and bottom porous discs (I,Fig.3.3) were used. These discs had been boiled for about 20 minutes to remove any air from the voids.

One of the platens was removed from the sample and a porous disc placed over the end of the mould. The sample was then allowed to slide gently down the mould until it was resting on the porous disc. The mould was then placed on the sample base in the cell (N, Fig.3.3) and the bottom of the membrane carefully taken from the mould over the sides of the base. The top of the membrane was also removed from the mould, which was gently slid off the sample. A second membrane was placed in the mould in the same way as the first, and while sucking, the mould was carefully slid over the sample, the membrane being removed in the same way as for the first membrane. Two membranes were used in order to prevent leaks caused by sharp edges puncturing the inner membrane. Two 'O' rings (E, Fig. 3.3) were placed around the bottom of the membranes by stretching them over the mould and sliding it back over

the sample and removing the rings at the bottom. The tops of the membranes were gently folded over the top of the sample and the second metal platen removed. The second porous disc was placed on the top of the sample followed by the top platen (D, Fig.3.3) the side of which had been greased in order to achieve a good seal between it and the membranes. The membranes were lifted back over the disc and platen and the top two 'O' rings (E, Fig. 3.3) which had been placed over the top line (J, Fig. 3.3.) were stretched over the top platen. The tops of the membranes were folded down in such a way as not to be protruding over the top of the platen or giving extra thicknesses on the sample. This ensured that there was no obstruction to visibility at the top of the sample during testing.

Once this was completed the sample dimensions were taken. Four heights were measured using a steel rule and nine diameters using vernier calipers accurate to 0.02mm. A ball bearing was placed in the hollow in the centre of the top platen and the cell top (M, Fig.3.3) fastened down after the additional base ring (L, Fig.3.3) had been placed and carefully tightened down. In doing this it had to be ensured that the load cell (C, Fig. 3.3) was seated on the sample. This was achieved by gently lowering the load cell until it just rested on the ball bearing and then placing the cell top gently while keeping the load cell in contact. The piston of the load cell was then locked, and the cell top tightened down. The jack was put in position and the beam (A,Fig.3.3) lowered by removal of the counter balance weights; extra weights were added to the loading end to ensure that the piston was not able to be lifted by the cell pressure. The jack was screwed down until the beam just rested on the ball bearing on top of the piston. The cell was then filled from the

water tanks (D, Fig. 3.2), the cell tap and air bleed (O, Fig.3.3) being

closed when full - the air bleed being closed slightly after the tap,

to ensure that no pressure was applied to the sample at this stage.

4.2.4   Saturation

Once the sample had been mounted, saturation could begin.   The

back pressure pots were raised to give a pressure of 70 kN/m^2, with the

sample isolated from the board.   The cell pressure pot was then raised

a small distance to give a small excess pressure of between 5 and 10

kN/m^2, this was to ensure that the sample was held in a vertical position

during saturation and to ensure that there was no danger of volume

increase in the sample due to excess back pressure.

All the taps to the sample were then opened followed by the taps

on the board.   The pressure on the gauge (C, Fig.3.2) returned to zero

at this stage, gradually building up as water was forced into the sample.

It was generally found that mercury had to be pumped back into the upper

pots at least once before this first pressure was fully effective on

the sample.   Further increments of 70 kN/m^2 were added to the back

pressure at about 30 minute intervals up to 350 kN/m^2.   The increments

and time delay had been shown to be sufficient for pressure to equalise

throughout a sample of this size.   The sample was left to saturate at

350 kN/m^2 overnight, although with some later samples being consolidated

at only 50 kN/m^2, an extra increment to 420 kN/m^2 was added to aid

saturation.

4.2.5   The B-Test

Before the sample could be tested it had to be fully saturated.

In order to find the degree of saturation a B-Test was carried out.   This

measures the pore pressure B parameter defined as:

$$B = \frac{\text{pore pressure change}}{\text{total stress change}} = \frac{\Delta u}{\Delta \sigma}$$

Water has a high compressibility and hence in a saturated soil all
the voids should be full of water and the B value should be close to
1.0, i.e. a change in confining pressure should produce an equal change
in pore pressure.

To perform the B-test the sample was isolated from the back pressure
system, the pore pressure transducer (G, Figs 3.2 and 3.3) being left
open to the sample, and readings taken on a D.V.M. of cell and pore
pressures. The cell pressure was then raised slightly and the changes
in cell and pore pressure readings measured, and hence the B-value
calculated.

When testing specimens from Gedling Colliery it was found that
after overnight saturation B-values only reached 0.90- 0.92, and subsequent
B-tests produced lower values. It was also found that even after
prolonged saturation for 3-4 days there was still no increase in B-value,
and hence these samples were tested when B-values of this order were
obtained. Possible explanations of this phenomenon are discussed in
Chapter 8.

4.2.6 Instrument preparation

Once the sample was saturated it could be consolidated. Prior to
consolidation the instrumentation was prepared for the test. The
transducers(F & G, Figs 3.2 and 3.3) load cell (C, Fig.3.3) and LVDT
(B, Fig. 3.3) were plugged into the junction box, the required ampli-
fications selected and the U.V. recorder and power supply turned on.
When the U.V. had warmed up and the trace spots were visible the galvano-
meters were adjusted to bring the spots to their required position. The
load and strain traces were placed near to the edge of the paper to allow
them full deflection. The pressure traces were placed near to the centre
of the paper to allow them to move in either direction depending upon

test behaviour. For calculation of the actual pressures the two pressure traces were made to coincide at a common pressure. This was achieved by isolating the sample completely, and opening the transducers to the board. The back pressure was then registered on the gauge (C, Fig.3.2) and the pots shut off. The cell pressure line was then connected to the gauge so that the same pressure was on both lines. The two spots were then made to coincide. One of the lines to the gauge was shut off, the pots connected, and the taps to the sample re-opened. The U.V. was kept on after this as a check on events during consolidation.

4.2.7 Consolidation

To consolidate the sample the sample lines were all shut off, with the pore pressure transducer (G, Figs 3.2 & 3.3) left open to the sample. The sample taps on the board were shut and the cell pressure pot raised to give the required pressure above the back pressure. This pressure was then applied to the sample. Once the pressure had equalized as shown on the gauge (C, Fig.3.2) and the pressure spots on the U.V., the volume change could take place. The volume change tube was opened to the back-pressure and the direct path from the second sample line closed (Line 3, Fig.3.2). An initial reading on the tube was taken and the sample line (Line 4, Fig. 3.2) opened at a fixed time. Readings on the tube (J, Fig.3.2) were taken at times appropriate for a root time plot used for consolidation curves, readings being taken until the volume change stopped, showing the complete dissipation of excess pore pressure. The time taken depended greatly on the material and consolidation pressure used, varying from a few minutes to over two hours. In the case of large volume changes the second tube had to be used, the

consolidation being stopped to effect the change over.   Also, when large

volume changes occurred the amount of mercury in the pot was often not

sufficient to apply the full pressure and consolidation had to be stopped

to repump the mercury.   Throughout the consolidation the seating of the

load cell on the sample had to be maintained, otherwise the sample

might consolidate out of the vertical and the test could not be run.

To do this the jack was gently screwed down as the sample moved, while

the load spot on the U.V. was watched to ensure that no load was applied

to the sample.   When consolidation had finished the sample line (Line 4,

Fig. 3.2) was closed and the volume change shut off (Lines 6 & 7, Fig.3.2)

and the spot positions checked.   The sample was then ready for testing.

4.2.8   Testing

Before testing the jack had to be removed.   The weights on the

loading hanger were removed, and 7kg placed on the counter balance hanger,

in which state the beam applied no load to the piston and maintained its

position.   The jack was removed and the piston unlocked, the screw of the

locking device being completely removed to ensure that it did not stick

at the join in the piston.

The U.V. paper was then started at a slow speed (5mm/sec or 125mm/min)

and weights added to the load hanger continuously, ensuring that there

was no swinging of the hanger.When failure appeared imminent from the

behaviour of the traces, the paper speed was increased to either 12.5mm/sec

or 50mm/sec depending upon the rapidity of events and the size of load

increments was decreased.   The particular load increments used depended

on the expected size of failure load.   The paper speeds were selected

so as to provide reasonable detail combined with economic use of paper.

After failure had occurred the U.V. recorder was switched off and

the instruments unplugged.   The pressure on the cell was reduced by

lowering the pots, and the cell emptied by allowing the water to syphon

back to the tanks (D, Fig.3.2). The loads were taken from the hanger

and the beam allowed to lift from the piston. The cell was removed

and the sample carefully removed, placed in a tray and weighed prior to

placing in the oven to dry overnight. It was then re-weighed to

obtain a dry weight of sample for use in density calculations.

4.3 Controlled-Strain Tests.

The methods used for the consolidated undrained tests with pore

pressure measurement were identical to those used for the controlled

load test except for the loading stage and the maintenance of seating during

saturation and consolidation. This latter was achieved by winding the

machine up until the small section protruding from the proving ring

was in contact with the top of the piston.

Loading was achieved using the automatic driving mechanism of the

machine at a rate of 0.3mm/min. Readings were taken as described at

selected values of strain representing $\frac{1}{2}$ per cent strain up to 6 per

cent and then 1 per cent up to 25 per cent strain.

4.4 The Small Controlled Load Rig Method

The principles behind the method used on the small rig were very

similar to those for the large rig, there being certain differences in

detail. As a result of problems encountered during the investigation,

certain alterations were made to the method and are discussed here.

The method originally used was based on that of Castro (1969) and

incorporated the use of a vacuum applied to the inside of the sample to

hold it up during mounting and measuring. However, during some tests on

loose Leighton Buzzard Sand, the samples were found to show very strong

dilative tendencies when a liquefaction was expected. It was suspected

that this might be due to densification caused by the application of the

vacuum. It was therefore decided to attempt setting up the sample without

the use of the vacuum.

A second function of the vacuum was to de-air the sample, and without a vacuum some alternative method had to be tried. This involved passing water from the water bottle (L, Fig.3.5) through the bottom of the sample using its own head. The air bleed on the top line (Line 3, Fig.3.5) was removed until water started coming out when it was replaced and the water turned off. This method was found to work satisfactorily. It was also found that when the Leighton Buzzard Sand was set up without vacuum it could be liquefied.

It was therefore decided to abandon the vacuum and use the alternative technique outlined above. The main problem when not using a vacuum was in measuring of diameters of soft or very loose samples, as the vernier calipers tended to squeeze the sample. However, for carefully made up samples there is little variation in mean sample diameter from sample to sample and so estimated values are generally good enough in these cases. In the case of in situ samples the uniformity of diameter is not as good, and some alternative measuring system which does not apply pressure needs to be devised.

4.4.1   Sample Preparation.

Three different methods of sample preparation were used for three different possible cases:

   (a)   In situ samples

   (b)   Made up dense samples

   (c)   Made up loose samples.

4.4.1.1   In Situ samples

In situ samples were taken from U100's which had been taken from the site in question. In order to obtain 38mm diameter samples from a 100mm diameter tube, three 38mm diameter tubes were screwed in a special jig to the top of the U100 on the hydraulic jack. The material was then jacked

out, filling the three tubes. The material was jacked from the 38mm diameter tubes into a mould of 76mm length similar to the one used in preparation of the large samples. In order to make a check on the sample moisture content the remaining content of the tube was weighed in a tin and placed in the oven to dry. Also the sample was weighed in the mould and sheath to obtain its original weight. Once in the mould, the sample was ready for mounting.

4.4.1.2 Made up Dense Samples

For made up dense samples a method similar to the one used for the large rig was used. The calculated weight was weighed out and thoroughly mixed with water. The material was placed in a thick-walled metal tube of 36mm internal diameter, fitted with two end stops which when fully in position gave a separation of 76mm. The lower stop was placed in the bottom of the tube and held out from the tube by means of a nut. When full the top stop was put in place and the nut removed from the lower one. The tube was placed in the Denison compression machine and compressed until the stops were fully in the tube. The sample was jacked from the tube into the same mould as that used for the in situ samples and was weighed in a similar way.

4.4.1.3 Made up Loose Samples

Loose made up samples were made up in a position on the rig. The correct quantity for the required dry density was weighed out and thoroughly mixed with water (usually at 10% moisture content).

One membrane was placed over the base platen (N, Fig.3.6) and secured by 2 'O' rings. The bottom porous disc (I, Fig.3.6) (pre-boiled) was placed inside the membrane on the bottom platen.

A longitudinally split mould in two sections held together by tape was placed over the membrane. The two 'O' rings for the top platen were stretched over the top section of the split mould. The material was placed in the mould in ten layers, each layer being tamped ten times with a metal rod. When the sample was complete the top was carefully flattened off.

In samples prior to modification of the method the top porous disc was placed and the top platen (D, Fig.3.6) placed on top of it. The platen was gently pressed down while the top of the membrane was carefully brought onto the platen. The vacuum was gradually applied using a screw tap (M, Fig.3.5) in the vacuum line (Line 2, Fig.3.5) While still gently pressing on the platen the top 'O' rings were gently brought onto it. The split mould was then untaped and removed.

In samples made up after the modification to the method, the wider top platen (D, Fig.3.6) with a porous plug was used, and so no top porous disc was needed. The wider platen was used as it was felt that pressing on the sample with the narrower platen (which did not rest on the mould) might be a further source of densification. The membrane and 'O' rings were taken onto the top platen in a similar fashion to previously, except that more care was needed as the sample was not held rigid by the vacuum.

4.4.2   Mounting the Sample

The in situ and denser made up samples were mounted in a similar fashion to the samples on the large rig.

The lower porous disc (I, Fig. 3.6) was placed on the end of the sample, which was placed on the bottom platen (N, Fig. 3.6.). The bottom of the membrane was carefully taken onto the bottom platen and the top of the membrane was removed from the mould, which was carefully taken from the sample. A second membrane was placed in the mould and

carefully taken over the sample.   Two sheaths were used on these samples as a precautionary measure, but not on the loose samples made up in position as there was no opportunity for putting one on without potential damage to the sample.   The bottom 'O' rings were then put on.   The split mould was next placed over the sample with the top 'O' rings on the top section.   From this point the methods used were the same as described in Section 4.4.1.3.

For some later samples a single section split mould was used in conjunction with samples of slightly reduced diameter (36mm), which were produced for the made up samples and could also be produced using 36mm diameter sampling tubes for in situ samples.   This was done to prevent possible damage to the sample caused by relative movement between the two sections of the double split mould.

After the samples had been mounted the dimensions were taken in the same way as for the large samples.   The cell top (M, Fig.3.6) was positioned and tightened down ensuring that the load cell (C, Fig.3.6) was seated on the ball bearing on the top platen (D, Fig.3.6).   The cell was filled nearly to the top and a thick oil was then fed into the top of the cell to form an oil seal between the piston and its bush, as this had been found to leak considerably when first used, leading to pressure loss. When sufficient oil was in place, the cell was filled right up and the water line (Line 7, Fig.3.5) and air bleed shut (O, Fig.3.6).

The piston was locked and the LVDT (B, Fig. 3.6) put in position. The loading yoke (A, Fig. 3.6) was seated on the ball bearing on the top of the piston and screwed down until the bottom of the yoke was locked rigidly on the bottom of the supporting structure.   This ensured that the

piston was not able to lift due to effects of cell pressure.

When in this state water was either sucked through by the vacuum or passed through under its own head depending upon the method used. When de-aired the sample was ready for saturation.

4.4.3 Saturation

In the case of samples set up without the vacuum the saturation process was the same as for the big rig except that pressure increments of 100 kN/m^2 were used as it was thought that the smaller sample could equalize satisfactorily under this larger increment. Saturation was generally quicker and a sample set up in the morning would be saturated by the afternoon. Samples set up in the afternoon were left overnight. Final saturation pressures were either 300 kN/m^2 or 400 kN/m^2.

When the vacuum was being used this had to be released before saturation could begin. This was done in two stages. The screw tap (M, Fig.3.5) in the vacuum line (Line 2, Fig.3.5) was partially opened, allowing half the vacuum to dissipate. A cell pressure of half the vacuum was then applied. The full vacuum was then released and a second increment of cell pressure applied up to the vacuum value. This ensured that the equilibrium of the sample was maintained. After allowing a short time for the pressure to become fully effective, the sample was isolated and the first increment of saturation pressure applied in the normal way.

4.4.4 Consolidation

Saturation was checked by a B-Test identical to the one used for the large rig. The preparation was identical except that it was not possible to apply the back pressure direct to the pore pressure transducer (G, Fig.3.5). The pressure was applied to the sample and the pore pressure spot positioned. The sample was then isolated and the same pressure applied to the cell pressure transducer (F, Fig.3.5) in the same manner

as on the large rig and the spot moved to the same position as the pore pressure spot.

The consolidation could then be carried out in the same way as on the big rig, except that due to the much smaller volume change no values were taken for consolidation curves. Consolidation was complete when the reading did not change over a period of 5 minutes. The duration of volume change was generally only a few minutes, and the movement of the sample small enough for there to be no danger of loss of seating.

4.4.5   Testing

The testing procedure was very similar to that used on the large rig, the U.V. recorder was used in an identical way. Initially any remaining weights in the counter balance (E, Fig.3.6) were removed and the piston unlocked. Large increments were applied to the hanger until there was movement of the load trace,(i.e. weights to counter the cell pressure). After this smaller weight increments were added continuously, the increments being reduced when failure seemed imminent. For samples showing strong dilative tendencies there was often not enough room on the hanger and the extra load had to be applied by pressing on the top of the yoke.

Once the test was complete the pressure was released and the cell drained, care being taken not to allow any of the oil to pass into the water lines. The sample was finally removed for weighing.

CHAPTER FIVE

CALCULATION OF RESULTS

5.1   Presentation of Controlled Load Test Results

It was decided that a convenient way of presenting the results of the controlled load tests was to plot the requisite effective stress paths.

The Stress Path method is described in detail by Lambe (1967) and the basis of the technique is outlined here.

5.1.1   Failure Envelopes

The most common way of showing the state of stress in a triaxial test is by plotting Mohr's Stress circles on plots of shear stress against principal effective stress.

For a series of triaxial tests the state of stress at failure can be plotted as a series of Mohr's circles (Fig. 5.1).
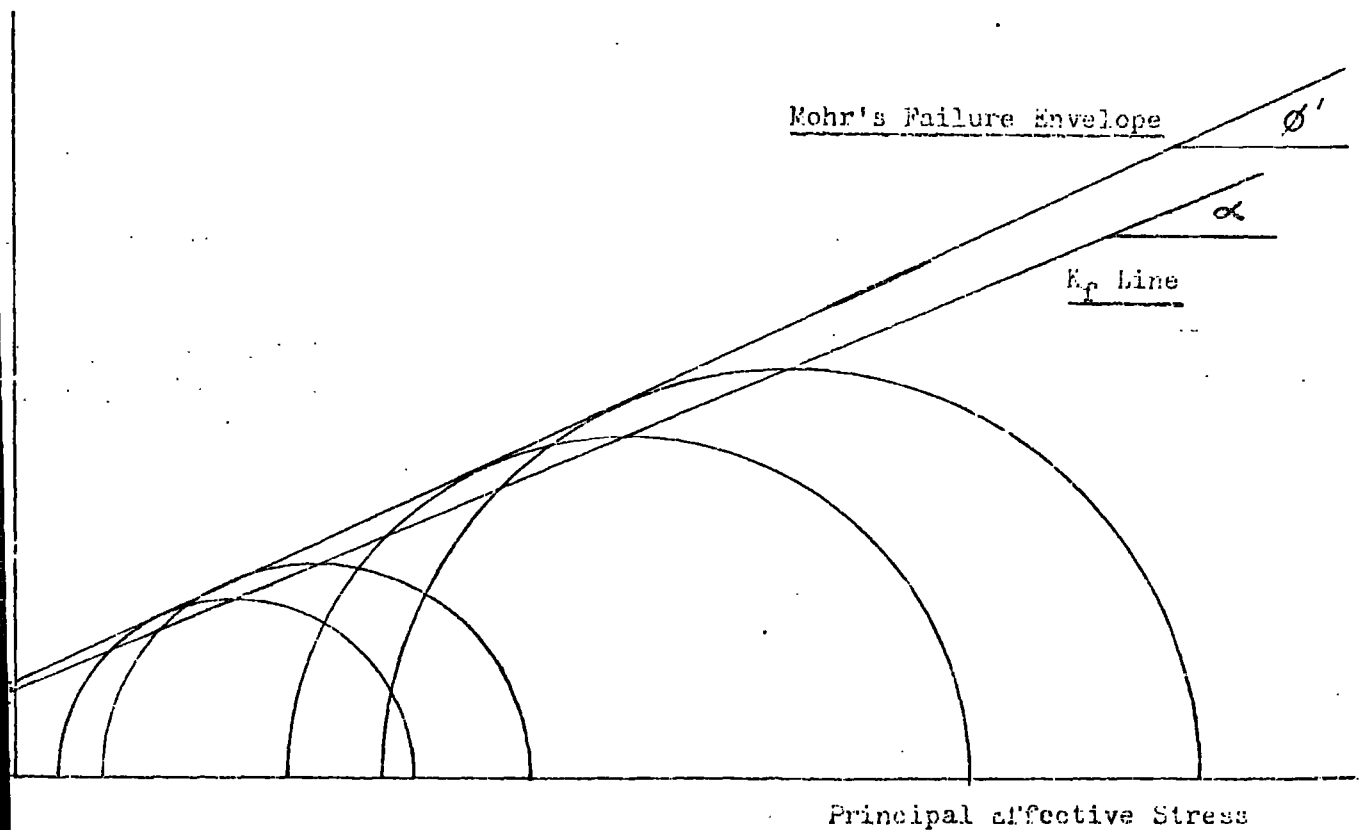
Figure 5.1   Mohr Failure Envelope and K_f Line

From these circles two failure envelopes can be drawn. The first is tangential to the circles and is the Mohr failure envelope, its intercept with the τ axis is the cohesion and its slope the angle of shearing resistance of the material $\emptyset'$; so that :

$$\tau = c' + \sigma \tan \emptyset'$$

The second envelope passes through the top points and is designated the K_f line. This has a slope $\propto$, related to $\emptyset'$ as:

$$\tan \propto = \sin \emptyset' \text{ and } c' = \frac{a}{\cos \emptyset'}$$

Both of these envelopes can be curved implying a reduction in friction angle at high values of normal pressure.

5.1.2 Stress Paths

A stress path is a plot of the successive states of stress existing in a sample during a test, as represented by the top point of the Mohr's circle (Fig. 5.2)
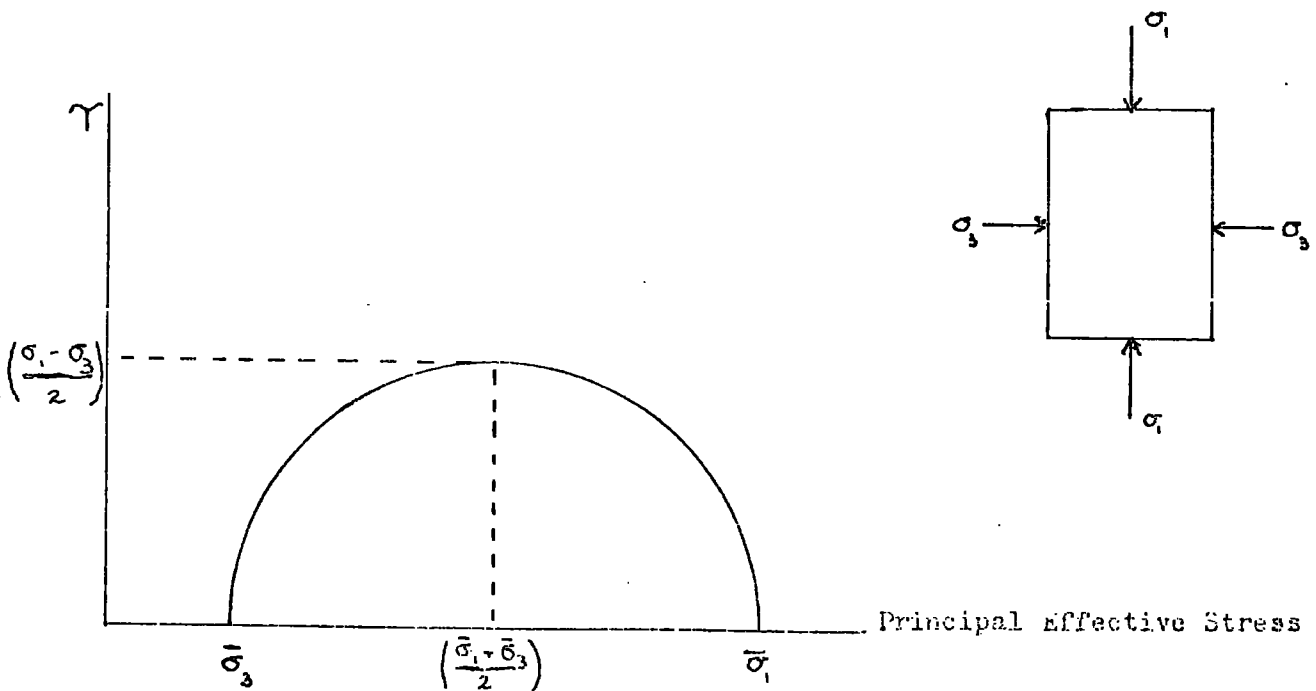
Figure 5.2   Definition of p and q

The coordinates of this point are as shown above.

$$p = \frac{\bar{\sigma}_1 + \bar{\sigma}_3}{2} \quad , \quad q = \frac{\sigma_1 - \sigma_3}{2}$$

q is half the deviator stress.

This plot is obviously much clearer than plotting a large number of circles for each test.   It is also possible to plot total stress paths and paths of (total stress) - (static pore pressure).

These stress paths will all tend to the K_f line at failure.

The stress paths for normally and over-consolidated clays are shown in Figure 5.3 to illustrate some important points:

——————— Effective Stress Path (ESP)

—·—·—·—·—·— Total Stress Path (TSP)

— — — — — — Total minus Static Pore Pressure Stress Path $(T - u_s)$SP

(a) Normally Consolidated.   (b) Over Consolidated
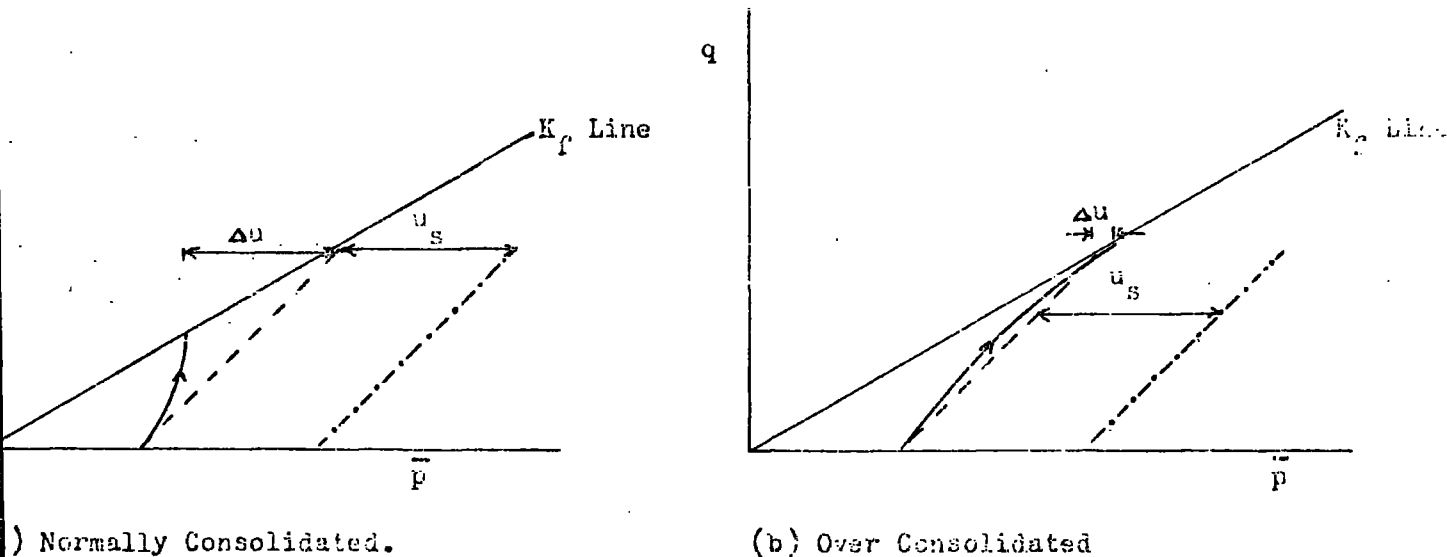
Figure 5.3   Typical Stress Paths for Clays

Points to note are:

1. q is both total and effective.

2. A negative value of q indicates horizontal stress greater than vertical stress.

3. T.S.P. to the right of E.S.P. indicates positive pore pressure.

4. T.S.P. to the left of E.S.P. indicates negative pore pressure.

5. $(T - U_s)$ SP to the left of E.S.P. indicates negative excess pore pressure.

Finey (1973) showed the classic stress paths for controlled load tests and these are reproduced in Figure 5.4.

a - Liquefaction
b - Partial Liquefaction
c - Dilation
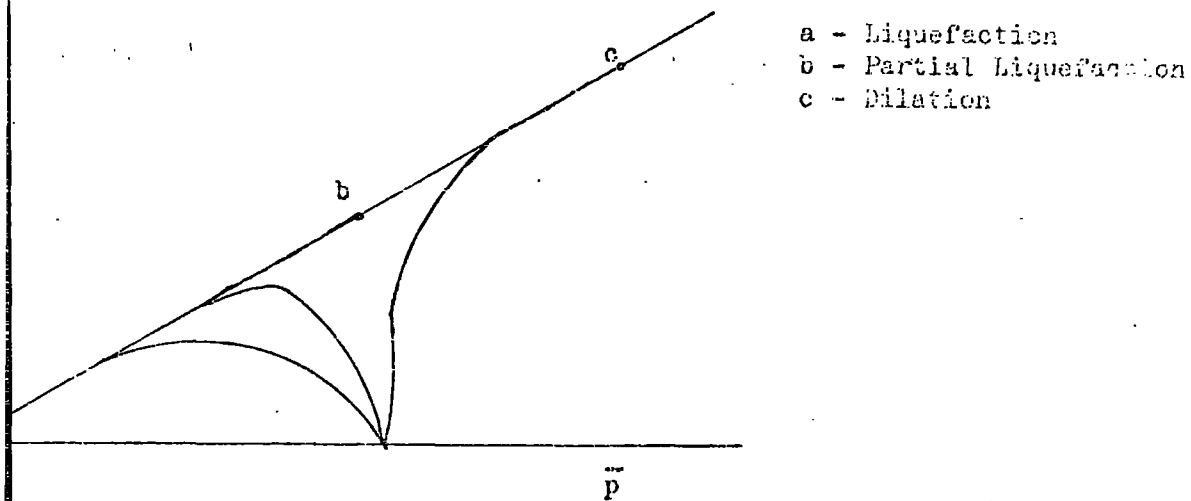
Figure 5.4 Controlled-Load Stress Paths.

a shows large build up in pore pressure and a large loss in stress;

b shows a build up in pore pressure and some loss in strength, followed by a fall in pore pressure and a gain in strength

c shows a fall in pore pressure and a large gain in strength. This illustrates that a dilatant failure will move up the K_f line.

5.2   Calculation of Results

The results were calculated using a programme written for a Hewlett
Packard programmable calculator.   The programme was written to convert
the measurements taken from the Ultra Violet Trace into a direct read out
of $\bar{p}$, q and percentage strain.

The initial part of the programme read in the sample measurements and
calculated the initial sample volume.   The next section calculated the
actual volume and height of the sample during the test using the volume
change.   This was done assuming the strain to be equal in all three
directions using the relationship:

$$L_f = L_i \left(1 - \frac{\delta V_c}{3V_o}\right)$$

where L_f =   final length
L_i =   initial length
δV_c =   volume change
V_o =   original volume.

The next section read in the constants needed to convert the measurements
from the trace in millimetres into actual loads and pressures.   The two
pressures had been zeroed to the same point at a known pressure and this
pressure was read in and the measurements given relative to this pressure.

Having calculated the values of pressure the main calculation was
performed.   Constant volume was assumed for the test, and the deformation
assumed to be as a right cylinder, producing a uniform area throughout the
sample.   The vertical deformation was subtracted from the test length and
divided into the test volume to give the area.   The load was then divided
by this area to give the applied stress.   This was added to the cell
pressure to give σ_1.   This produced the total values of σ_1 and σ_3.   The
pore pressure was then subtracted from these to give the effective pressures
from which the values of $\bar{p}$ and q were calculated and printed out.

The percentage strain was also calculated and printed out. From these the stress paths were plotted and also plots of q against percentage strain (stress-strain curves).

Although the assumption concerning the deformation during the test is obviously not accurately true, any accurate estimation of the true deformation would be very difficult. This method does give a good idea of the changes in the state of stress within the sample, and is probably as accurate as any alternative method.

5.3 Rubber Membrane Correction

In the case of 38mm diameter samples, the strength of the rubber membrane can have a significant effect on the measured value of load, and so a correction has to be introduced. In the case of the 100mm diameter sample the effect is very much less significant and no correction was used.

A standard test, described in British Standard 1377 (1975) was performed to find the correction, which must be applied to the value of q; to allow for the compressive strength of the membrane(s). The compression modulus could not be measured directly but was assumed to be equal to the extension modulus.

The test involved loading a strip of membrane, 25mm wide, supported between two glass rods. The contact faces between the rods and the membrane were dusted with French chalk to reduce friction. The extension was measured for increasing loads, giving the extension modulus as

$$M = \frac{\text{Force per millimetre}}{\text{strain}}$$

The correction factor was

$$\frac{4M\varepsilon \, (1 - \varepsilon)}{D}$$

where D = initial sample diameter (mm)

ε = axial strain at maximum principal stress difference.

Values were calculated and the correction applied to the results of the controlled-load tests. For 20 per cent strain it was found that a

correction of approximately 4 kN/m^2 was required for 2 sheaths and 0.8 kN/m^2 for one sheath.

5.4   Coefficient of Consolidation

As a further indication of differences in the properties of the coarse materials, the value of the consolidation constant c_v during the consolidation stage was calculated from curves plotted using the volume change readings (Figs. 6.15-6.17).

The value of c_v was calculated according to a formula given by Ackroyd (1957) for triaxial consolidation of a sample including radial drains and having only one line open to the volume change.

From this:

$$c_v = \frac{0.524 \, \bar{R}^2}{t_{90}} \times 60 \times 24 \times 365 \ m^2/year$$

where $\bar{R}$ is the mean radius of the sample during the test in metres and t_{90} is defined as shown in Fig. 5.5.
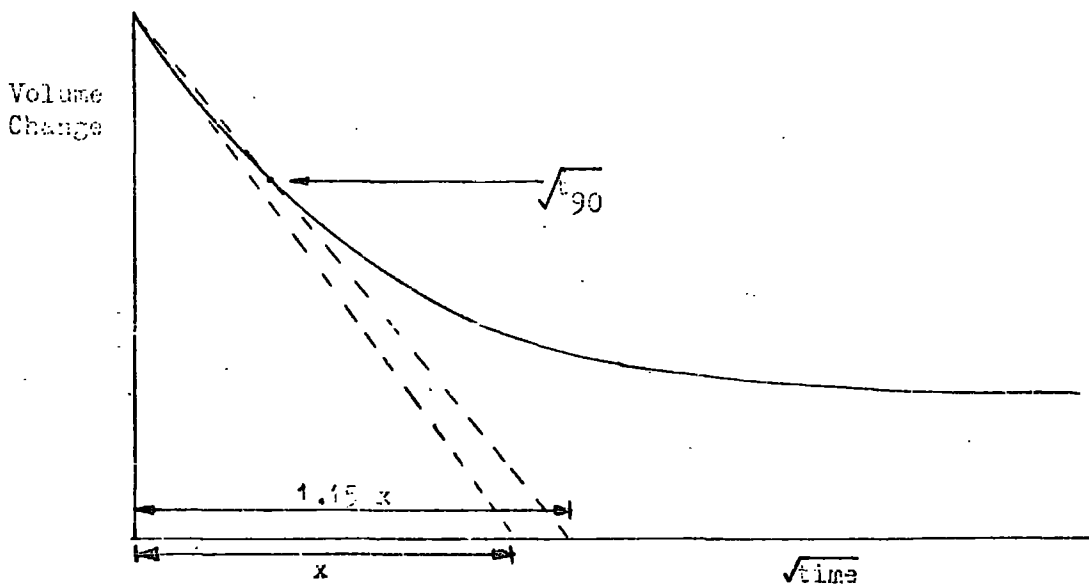
Figure 5.5   Definition of t_{90}

The values of c_v were calculated using a programme on the Hewlett Packard calculator.

CHAPTER SIX

RESULTS FOR COARSE DISCARDS

The results for the controlled strain and controlled stress triaxial tests are presented here as stress paths and stress-strain curves. Also plotted are the consolidation curves for the various materials.

The numbers in brackets after Test numbers on Figures 6.2, 6.4, 6.11, 6.15, 6.16, 6.17 represent the . consolidation pressures used.
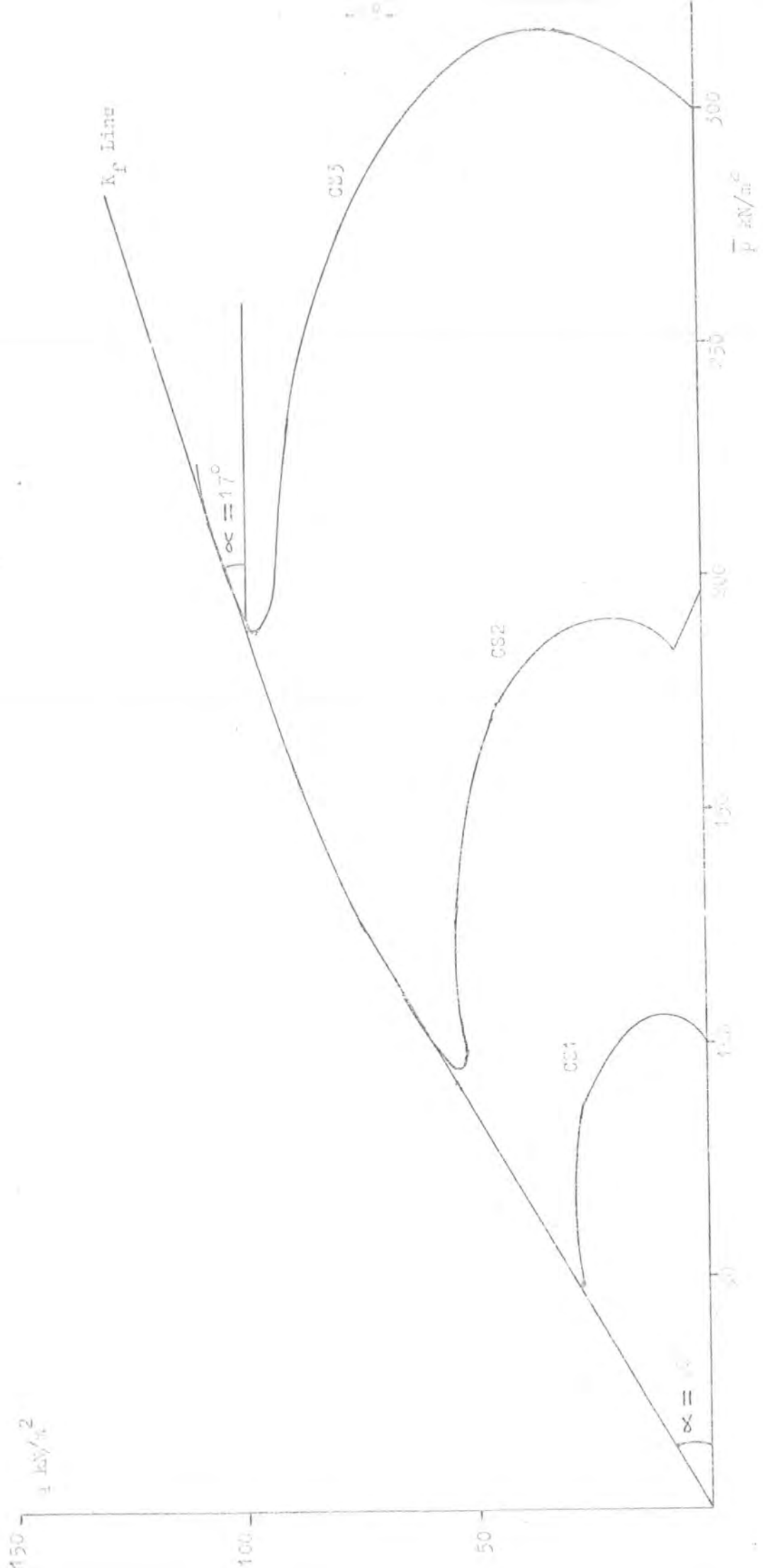
$\tau \ kN/m^2$

K_p Line

$\alpha = 17°$

CS3

CS2

CS1

$\bar{p} \ kN/m^2$

$\alpha =$
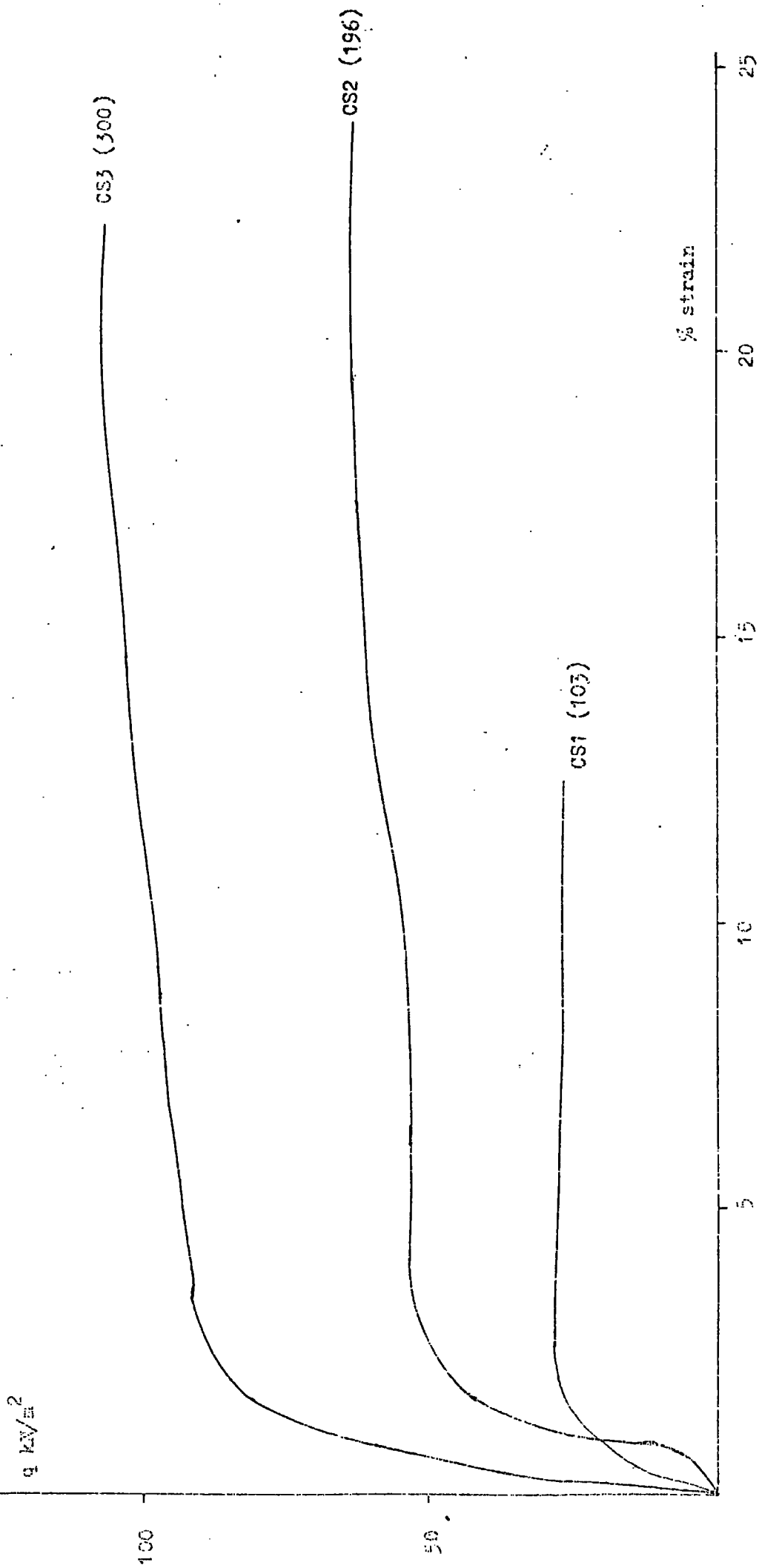
Figure 6.2 Stress/Strain Curves for Controlled Strain Tests on Gedling Coarse Discard.
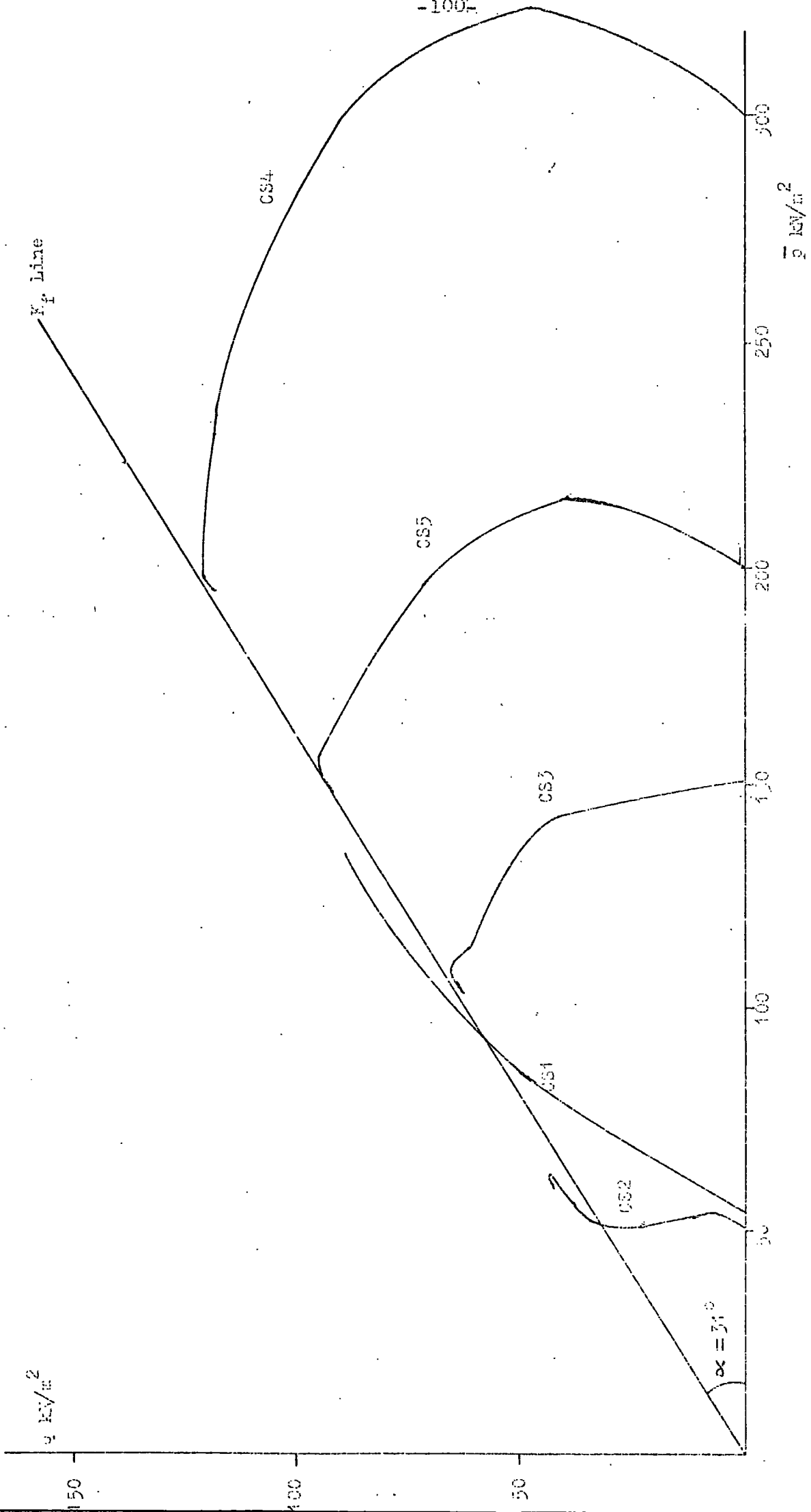
Figure 6.3 Stress Paths for Controlled Strain Tests on Aberrant Coarse Discard.
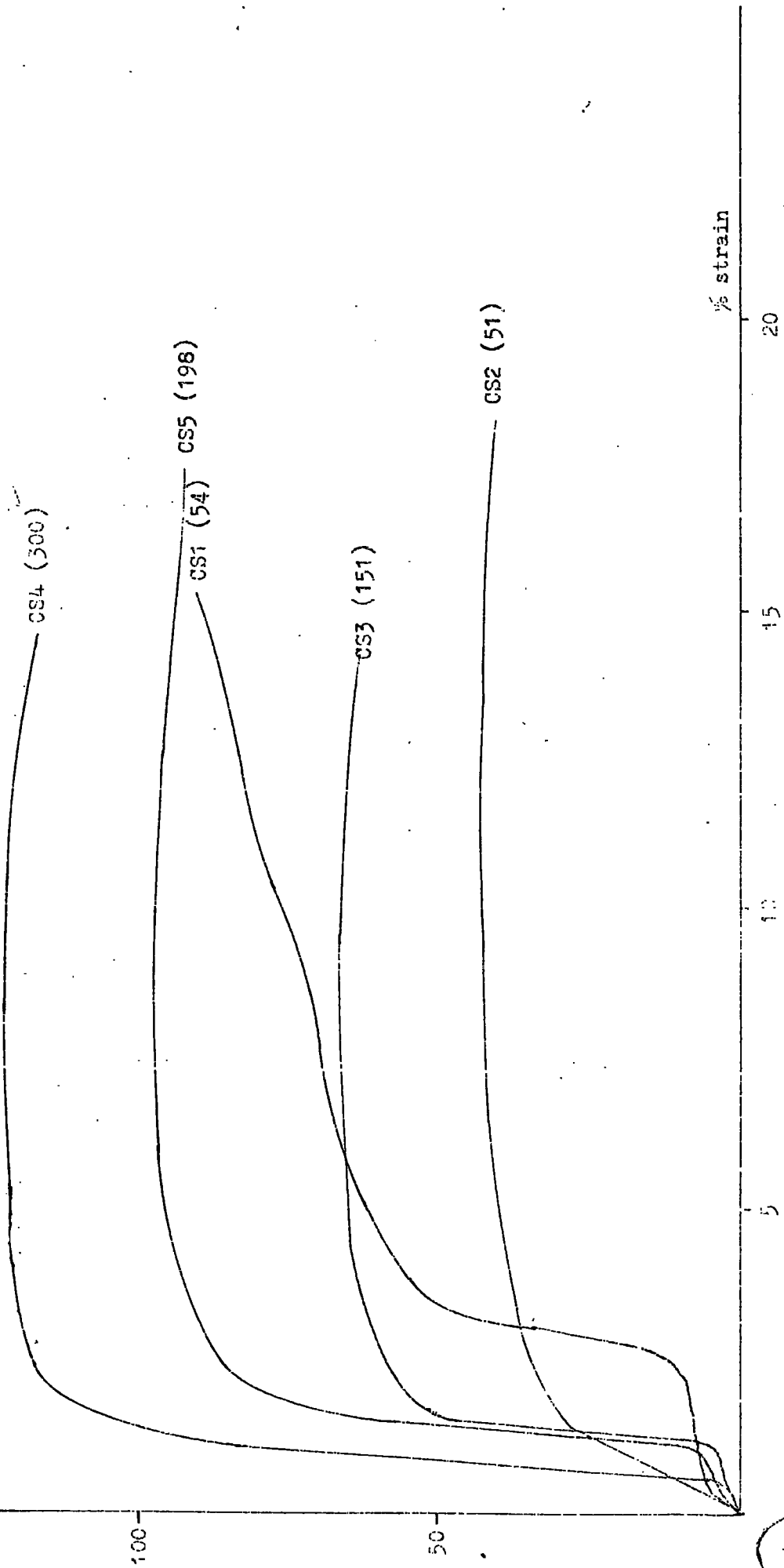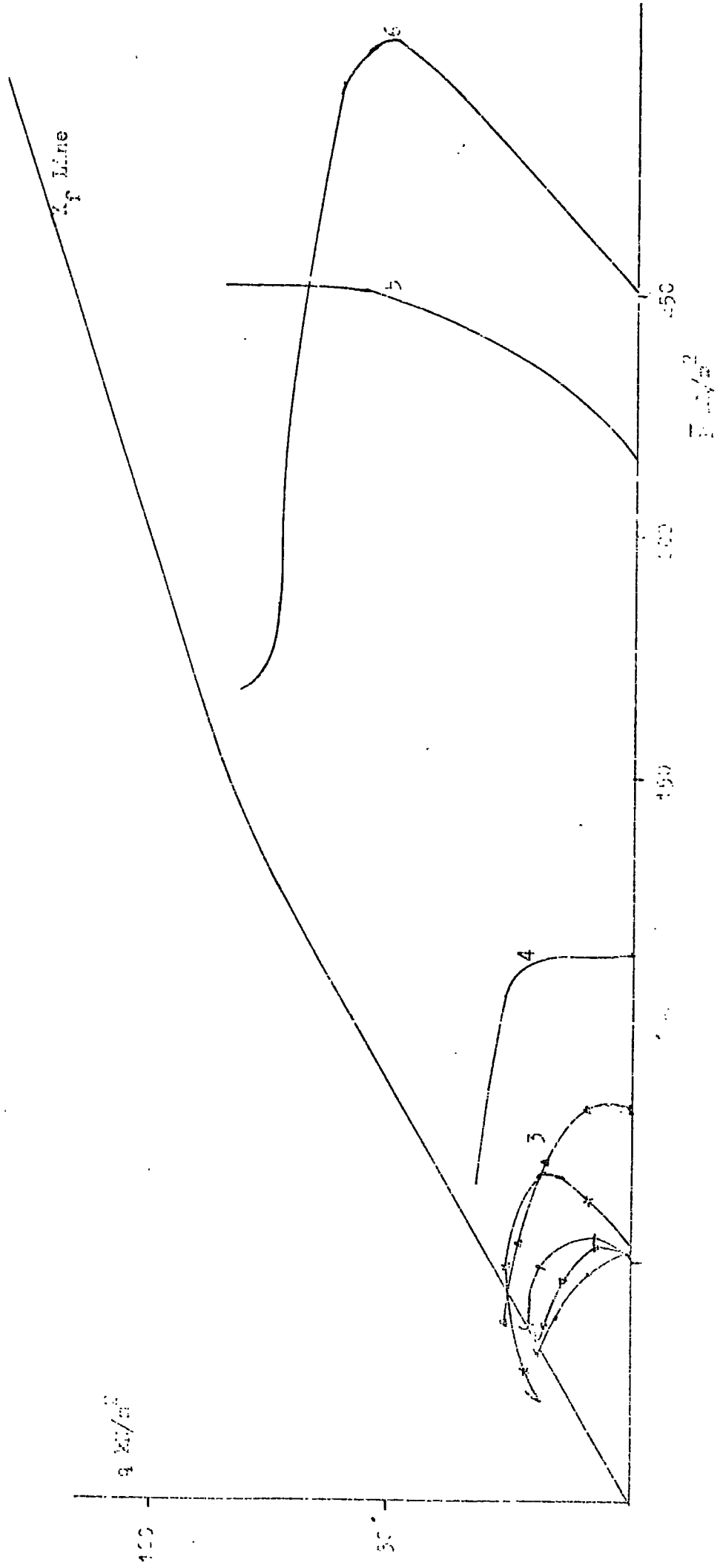
Figure 6.4 Stress/Strain Curves for Controlled Strain Tests on Abutment Coarse Discard.

q kn/m²

100

50

Z_f Line

5

6

4

3

450 500 550

$F = v/g²$

No. 1

No. 3

No. 4 No. 5

No. 8

Figure ... Pressure volume ratio for ... (From the Signal A Investigation).

Figure 4.2 Stress Paths for Controlled Load Tests on Gedling Coarse Discard (from Previous Investigation).
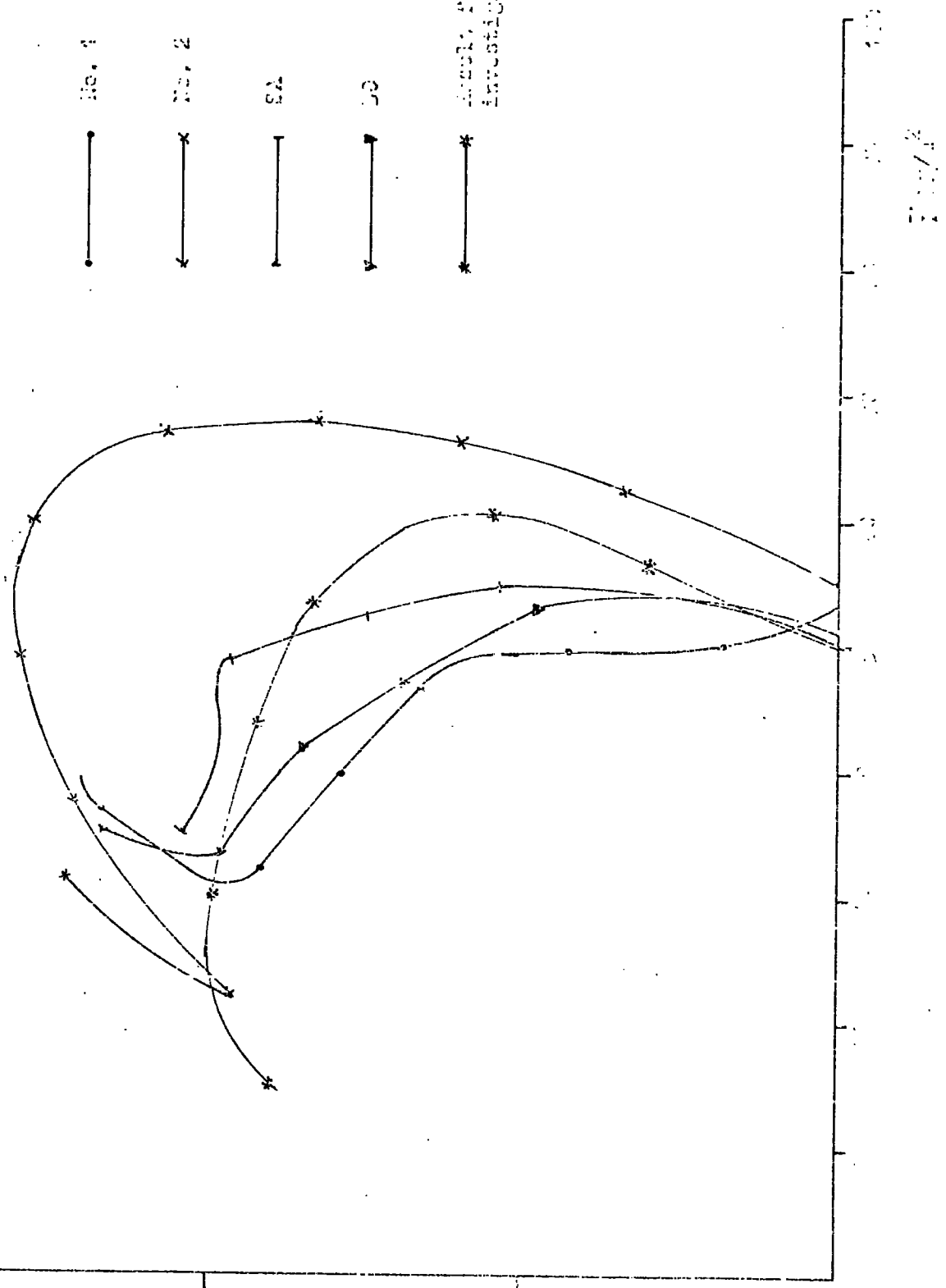
No. 1 •———•

No. 2 ×———×

No. 3 |———|

No. 4 ▼———▼

Mach, Max. Review
Investigation ✱———✱

Q Kg/m²

100

50

Time from Rock to 20,0 strain

1   25 sec.   4
2   35 sec.   5   50,55,85 sec.
3   20 sec.   6   115 min.
4   40 sec.

No.1
No.2
No.3

Figure — Aging Curves for Compacted Clay ... (from the 9-point investigation).

Figure 6.3 Stress/Strain Curves for Controlled Load Tests on Gedling Coarse Discard.

2 (241)

3 (196)

1 (234)

4 (143)

5 (101)
9 (47)
6 (101)
10 (54)
7 (53)
8 (31)

Area Peak No. (columns)
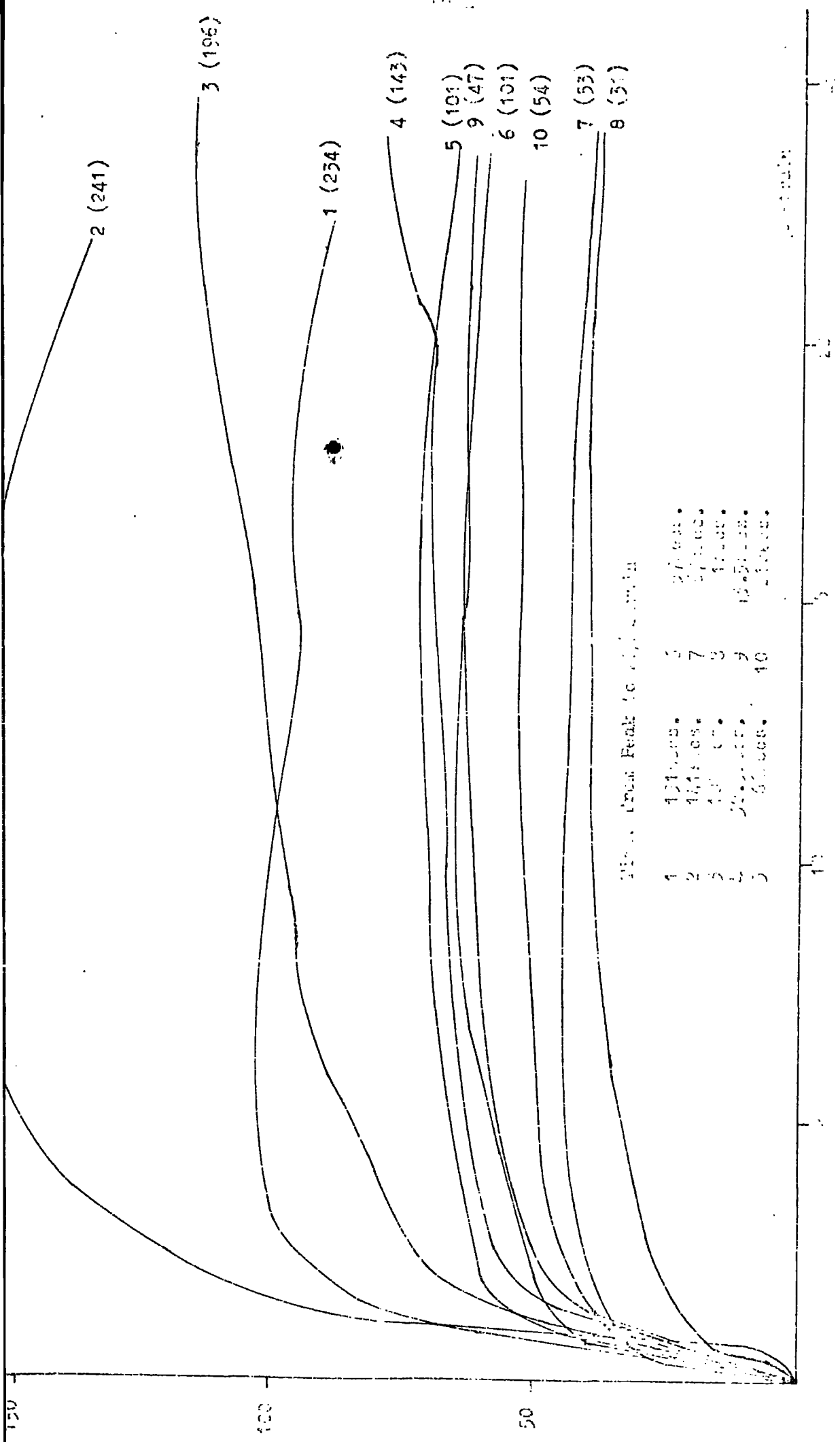
Figure 6.12 Stress Paths for Controlled Load Tests on Durham Shale, Durham Seatearth and Aberrant/Seatearth Mixtures.

All tests performed at a nominal consolidation pressure of 50 kN/m², except SH2 for which $P_c = 97$
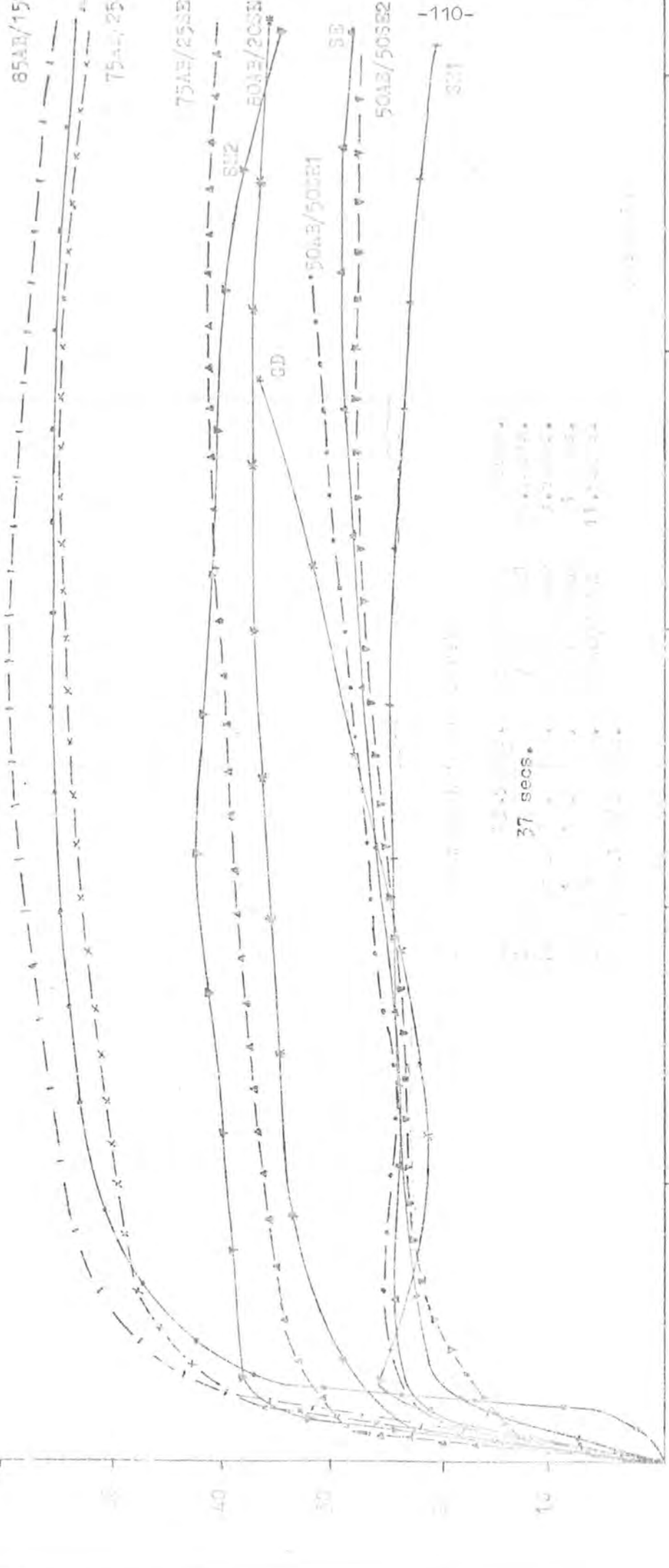
q kN/m²

kN/m²

85AB/15S

75AB/25S

75AB/25SB2

SB2

50AB/20SSB

SE

50AB/50SB2

SH1

50AB/50CB1

GD

5.0

4.0

3.0

2.0

1.0

37 secs.

Gedling No. 4 (P$_c$ =114)

Gedling No. 2 (P$_c$ = 55)

Abernant No. 9 (P$_c$ = 47)
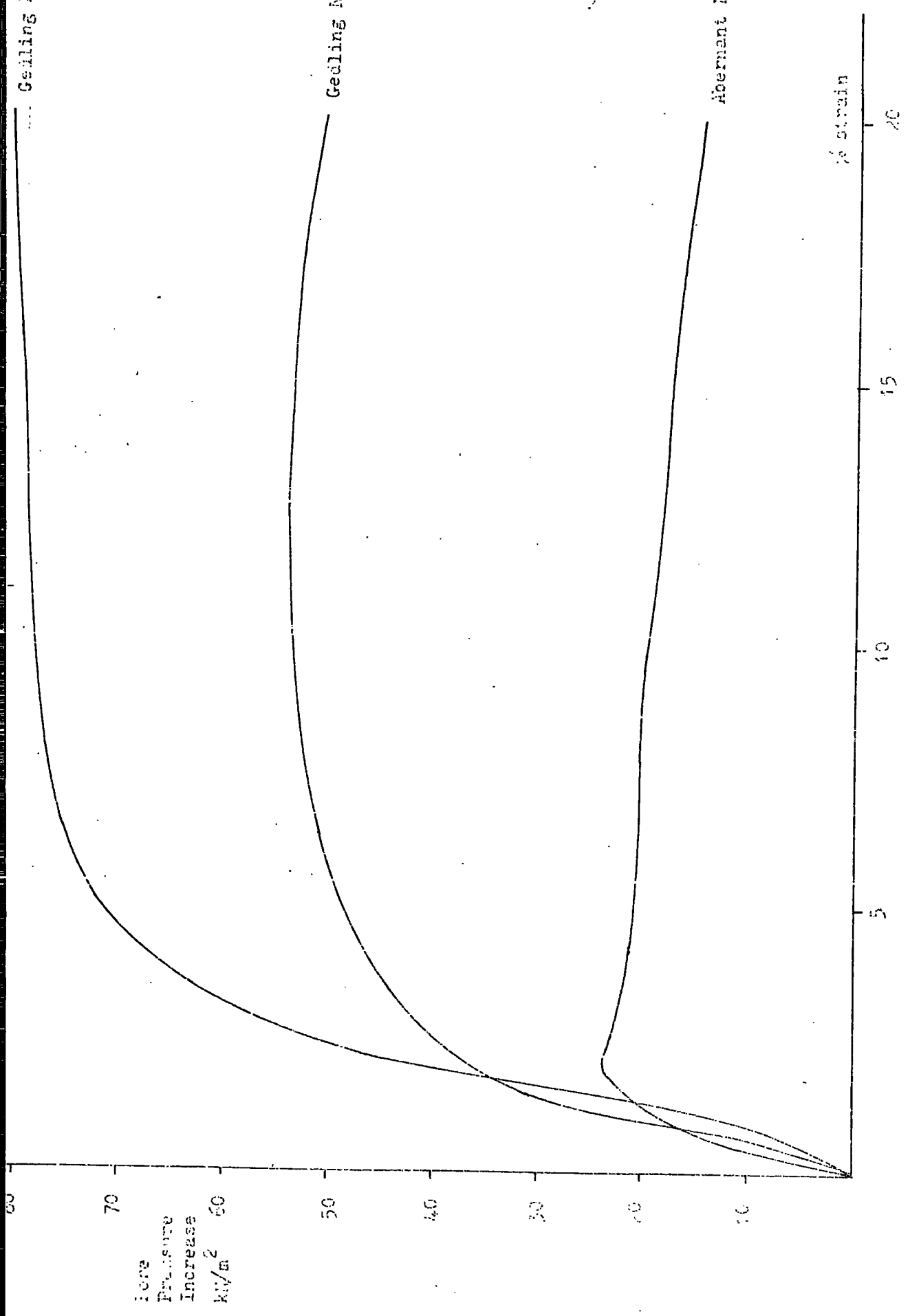
Core
Pressure
Increase
kN/m²

80
70
60
50
40
30
20
10

% strain

5   10   15   20
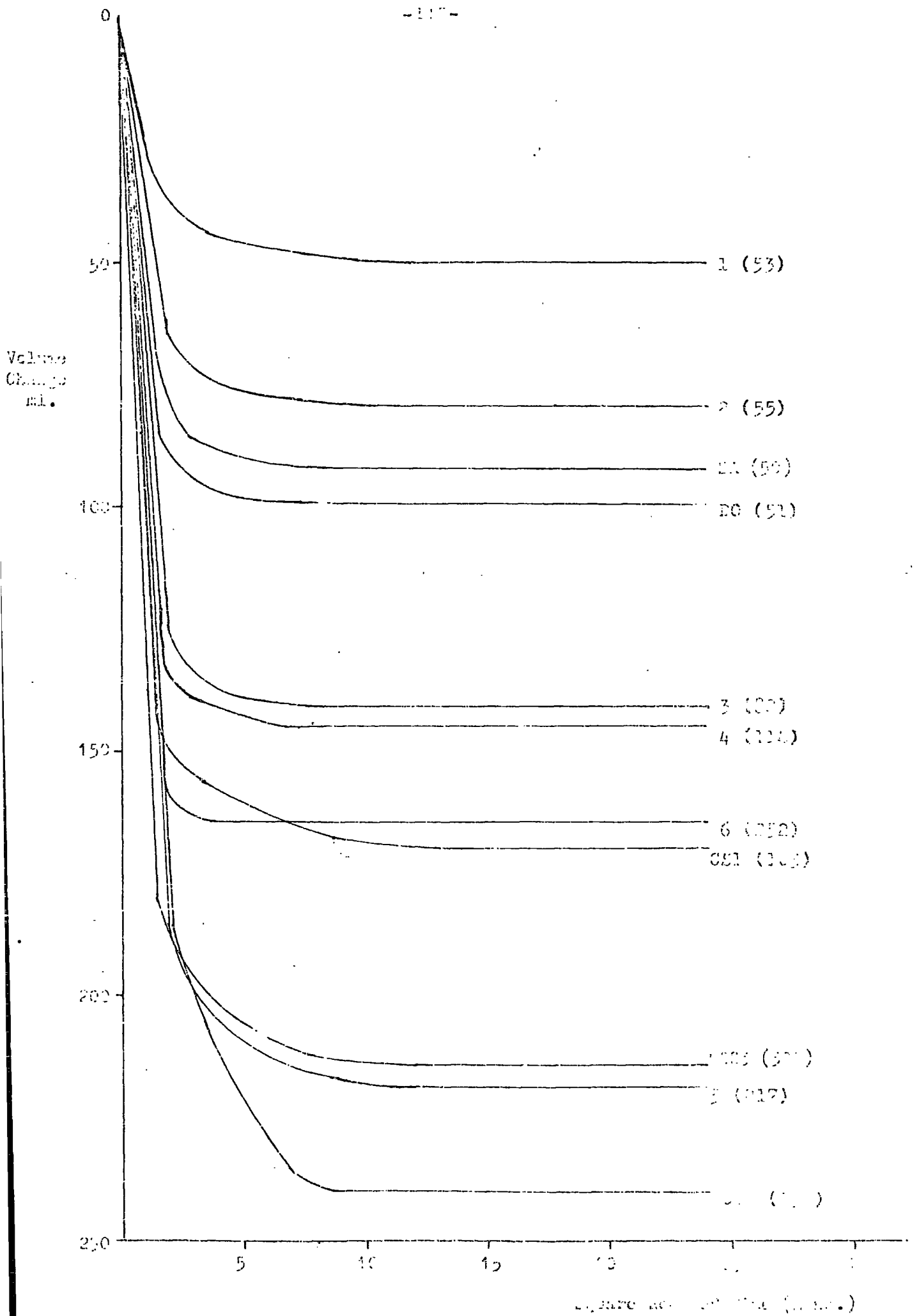
Figure C.15 Consolidation Curves for Scutic, Row ? ....
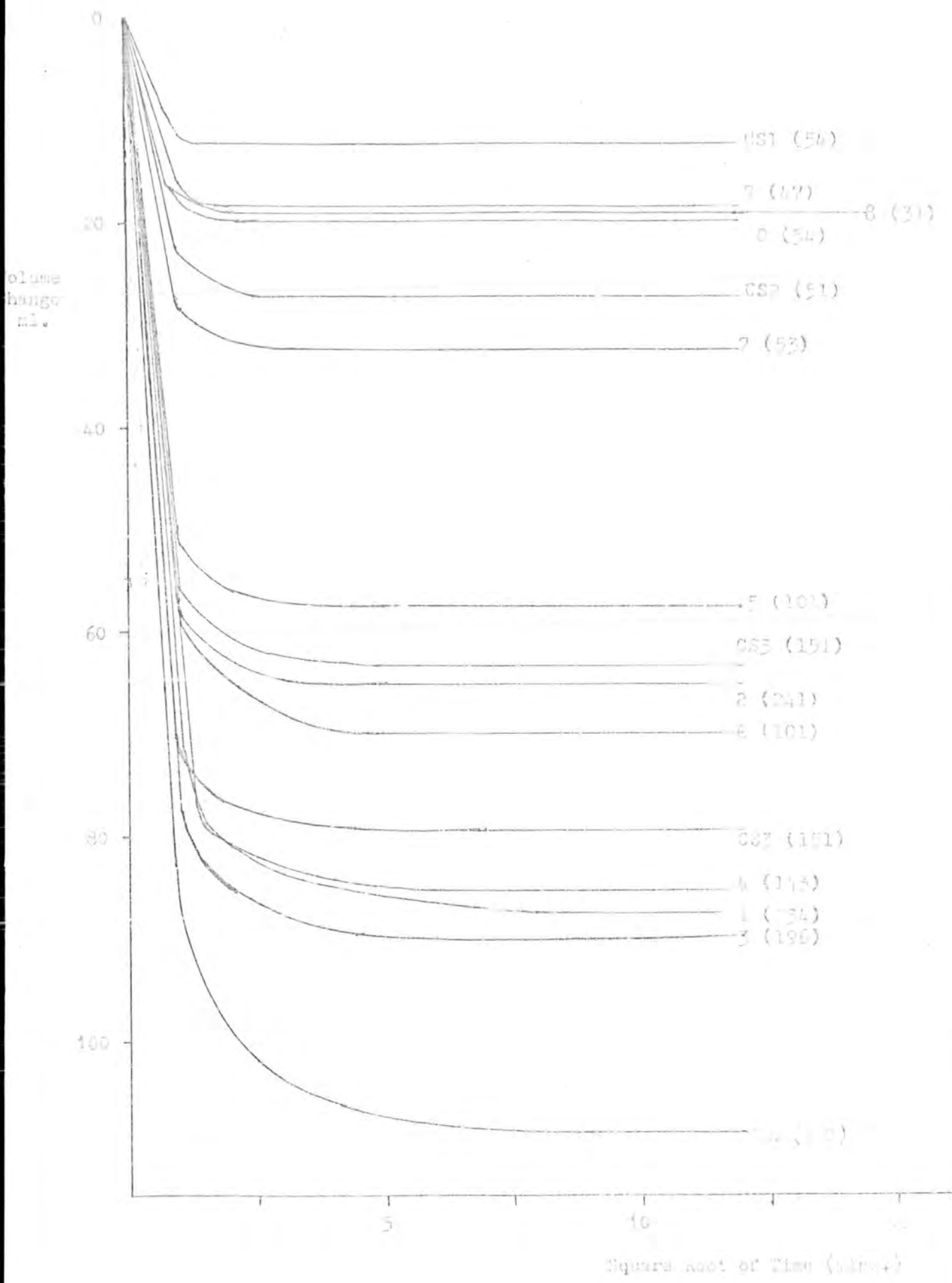
Figure 6.16 Consolidation Curves for Abutment Coarse Discard
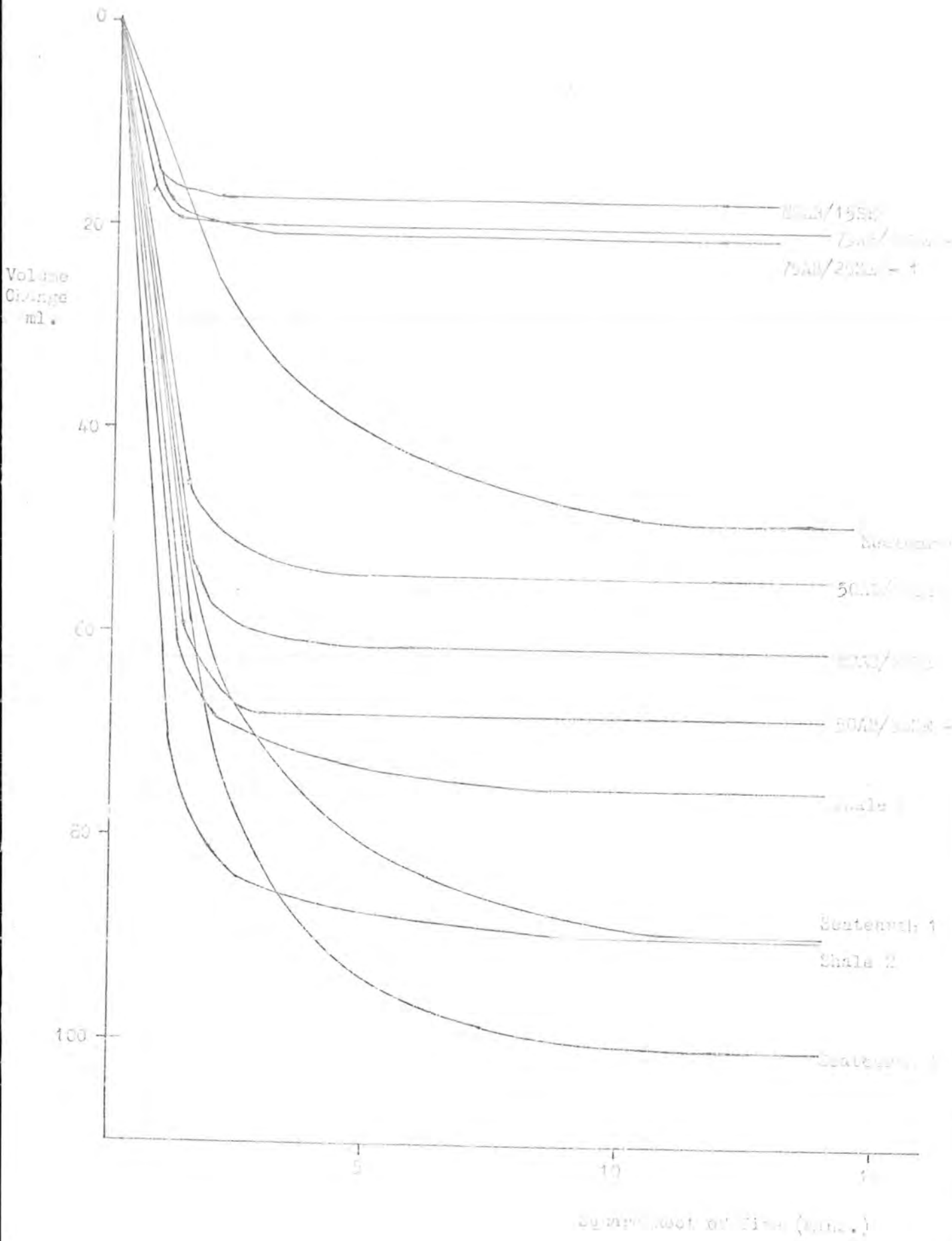
Figure 6.17 Consolidation Curves For Durham Shale, Durham Sandstone and ...

Sample No.	Initial Moisture Content %	Consolidation Pressure kN/m²	Dry Density Mg/m³		Void Ratio		Relative Compaction %		Time to 20% strain secs	Volume change ml.	c_v (m²/year)	Comments
			Initial	Final	Initial	Final	Initial	Final				
1	15.7	53	1.291	1.403	0.842	0.694	73.88	77.08	23	50.18	216.6	
2	11.4	55	1.345	1.479	0.766	0.607	73.96	81.26	37	79.67	160.09	Piston stuck for 14 secs during straining.
3	11.45	82	1.323	1.462	0.796	0.626	72.69	80.33	37	141.20	145.27	Estimated time due to loss of timer bars.
4	11.79	114	1.351	1.500	0.759	0.584	74.23	82.42	40	144.32	171.40	
5	11.83	217	1.324	1.553	0.795	0.530	72.45	85.33	-	215.77	216.67	Did not strain
6	11.83	252	1.318	1.484	0.803	0.602	72.43	81.54	43	164.16	172.81	
5A	8.96	50	1.352	1.452	0.758	0.637	74.29	79.78	38.5	72.15	121.95	Sample sieved after testing
DO	10.00	51	1.322	1.417	0.798	0.677	72.64	77.86	11	98.95	194.87	Sample dried out & remoulded
CS1	10.11	103	1.359	1.536	0.749	0.547	74.67	84.40	-	169.55	190.03	
CS2	10.53	196	1.331	1.550	0.736	0.533	73.13	85.16	-	239.87	118.97	
CS3	10.66	300	1.339	1.565	0.775	0.519	73.57	85.99	-	214.63	143.04	

Sample No.	Initial Moisture Content %	Consolidation Pressure kN/m²	Dry Density Mg/m³ Initial	Final	Void Ratio Initial	Final	Relative Compaction % Initial	Final	Time to 20% strain secs.	Volume change ml.	c_v (m²/year)	Comments
1	10.0	234	1.299	1.379	0.687	0.589	81.19	86.19	191	87.33	447.26	
2	10.0	241	1.430	1.493	0.532	0.468	89.38	93.31	141	65.59	664.67	Made up to higher density
3	10.00	196	1.299	1.382	0.687	0.585	81.19	86.36	100	90.16	559.94	
4	10.00	143	1.345	1.424	0.629	0.539	84.06	89.00	30.5	85.34	433.13	
5	10.00	101	1.339	1.391	0.636	0.575	83.69	86.94	66	57.56	567.43	
6	10.00	101	1.329	1.391	0.649	0.575	83.06	86.94	57	69.75	519.84	
7	10.00	53	1.327	1.356	0.651	0.616	82.94	84.75	67	32.61	568.65	
8	10.00	31	1.312	1.328	0.670	0.650	82.00	83.00	61	19.28	579.27	
9	5.61	47	1.573	1.586	0.393	0.382	98.31	99.13	47.5	18.43	1127.85	Sample sieved after testing
10	8.52	54	1.411	1.430	0.553	0.532	88.19	89.38	21	19.85	653.83	
CS1	10.00	54	1.283	1.293	0.708	0.695	80.19	80.81	-	12.48	682.97	
CS2	10.00	51	1.306	1.329	0.678	0.649	81.63	83.06	-	47.22	528.36	
CS3	10.00	151	1.338	1.395	0.638	0.571	83.63	87.19	-	63.51	146.42	
CS4	10.00	300	1.340	1.440	0.635	0.522	83.75	90.00	-	108.88	565.37	
CS5	10.00	198	1.563	1.437	0.607	0.525	85.19	89.81	-	79.67	516.98	

Sample No.	Consolidation Pressure kN/m²	Dry Density (Mg/m³) Initial	Final	Void Ratio Initial	Final	Time to 20% strain (secs)	c_v (m²/year)	Volume change ml.	Comments
Gedling 2	55	1.345	1.479	0.766	0.607	38	160.09	79.67	
100 SE1	51	1.496	1.608	0.732	0.611	22.5	80.22	89.31	
100 SE2	50	1.661	0.727	0.560	0.500	30.5	82.60	48.77	
100 SE3	49	1.599	1.719	0.620	0.507	18.5	102.96	100.65	
50AB/50SE1	60	1.541	1.600	0.622	0.563	7.5	206.93	54.15	
50AB/50SE2	53	1.528	1.601	0.636	0.562	6.0	246.06	58.05	
75AB/25SE1	58	1.628	1.650	0.464	0.444	26.5	463.63	20.70	
75AB/25SE2	56	1.464	1.484	0.628	0.606	9.5	721.72	20.13	
80AB/20SE1	50	1.485	1.549	0.615	0.549	18	198.83	61.81	Non-representative volume change
85AB/15SE1	51	1.521	1.540	0.549	0.530	11.5	549.52	17.58	
Abernant 7	53	1.327	1.356	0.651	0.616	67	568.65	32.61	
Abernant 9	47	1.573	1.586	0.393	0.382	43.5	1127.85	18.43	
Abernant 10	54	1.411	1.430	0.553	0.532	21	653.83	19.85	
100 SH 1	49	1.636	1.729	0.621	0.534	16.5	230.12	75.14	
100 SH 2	97	1.645	1.753	0.512	0.513	9	238.95	89.31	

CHAPTER SEVEN

RESULTS FOR FINE DISCARDS.
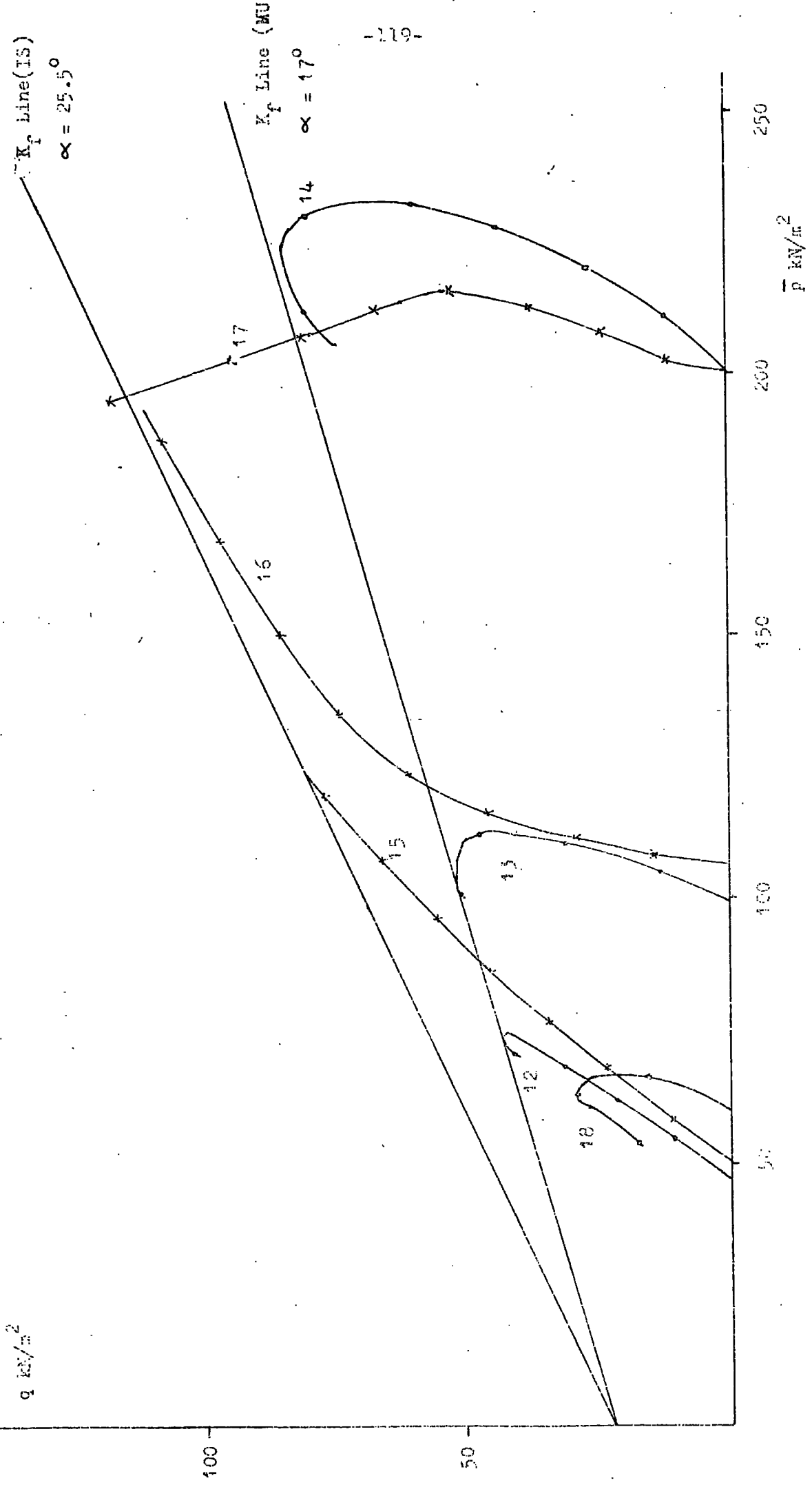
Figure 7.1 Stress Paths for Controlled Load Tests on Peckfield Slurry.

Stress-Strain Curves for pre-stretched samples of Standard Fibres.

Made-up Samples   Times from Peak to 20% Strain

In-situ Samples

12 17.5 secs.   15 79 secs.
13 17 secs.   16 78 secs.
14 7 secs.   17 48.5 secs.
18 24.5 secs.
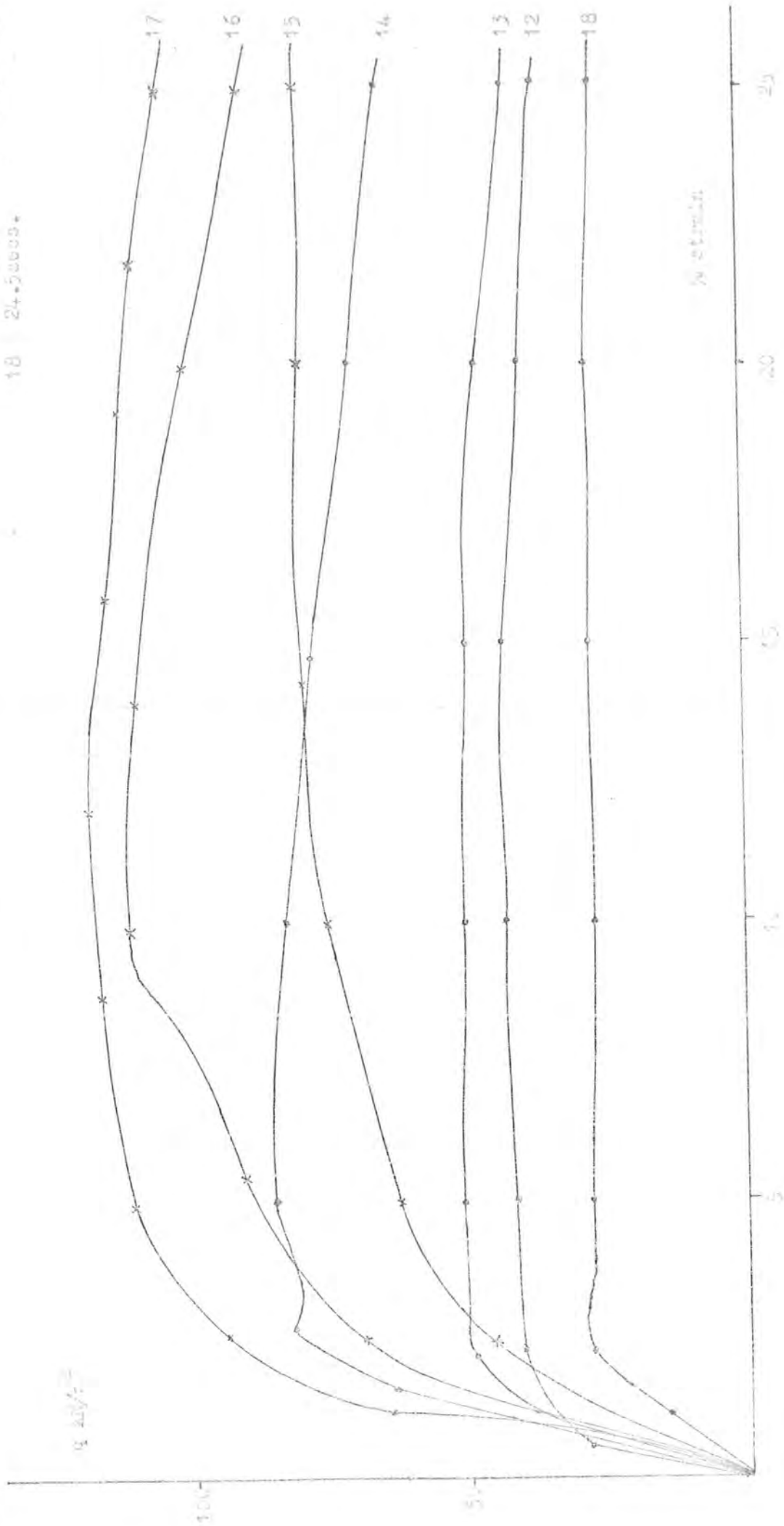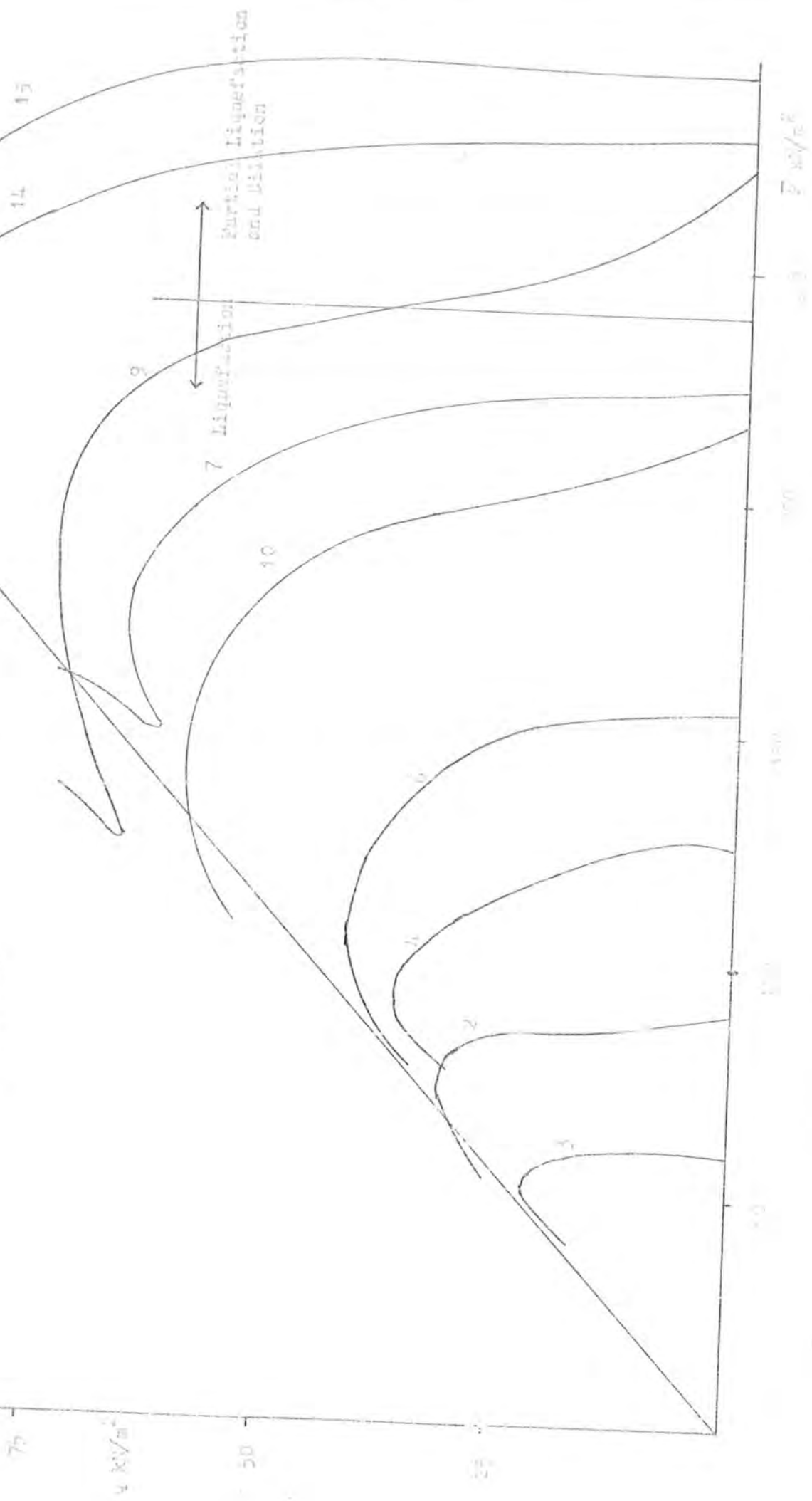
Photo Forwarded by L.P. Ginzex

q kW/m²

75

50

25

13   14   15

Partial liquefaction and mistion

7 Liquefaction

9

10

2   4   6   8

T kW/m²

Plots reproduced by L.B. Gordon

K_p Line

q kN/m²

$\bar{P}$ kN/m²
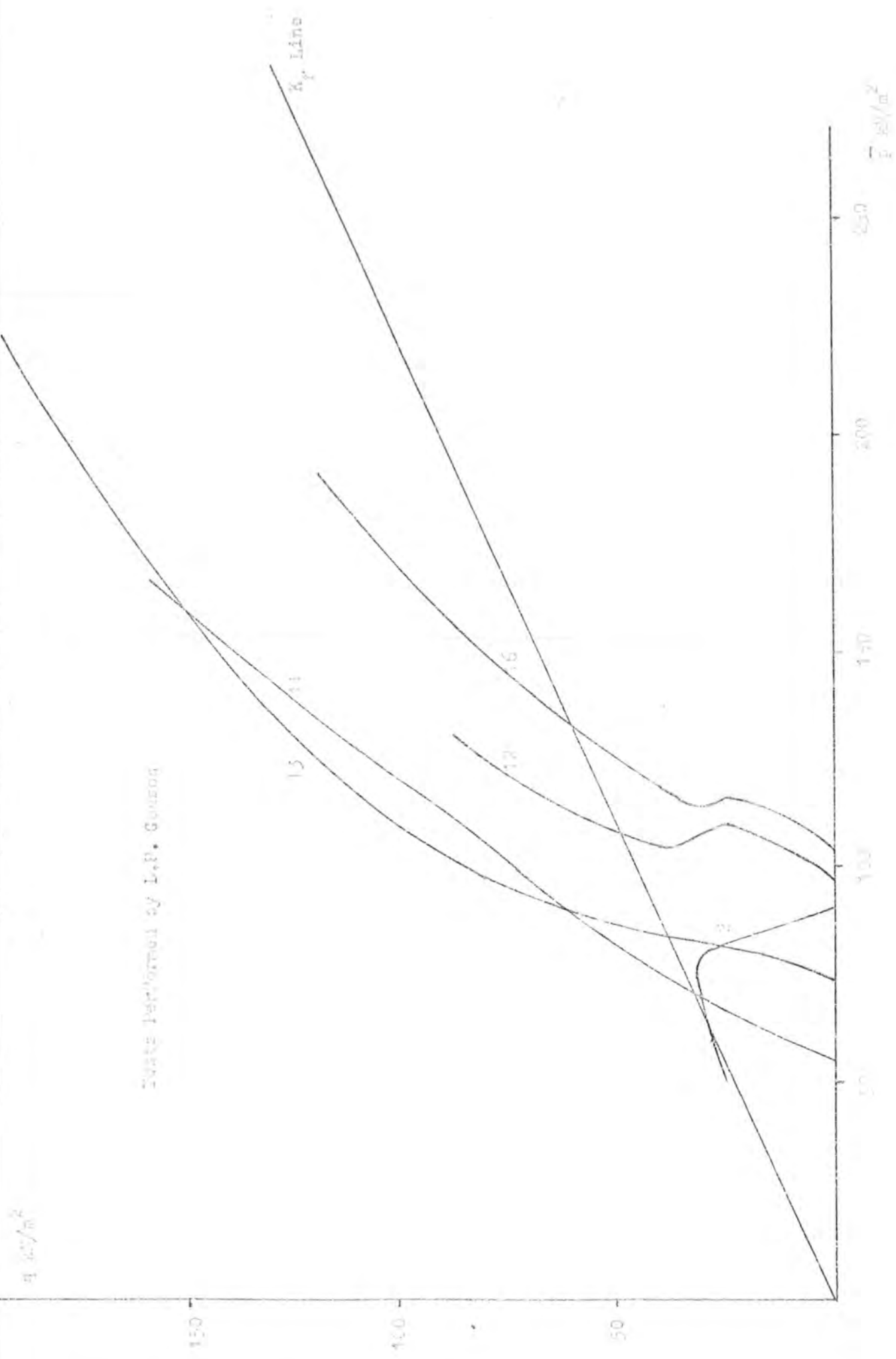
Percentage Loss in q
from Peak to Failure

2   21.97%
3   26.66%
4   14.51%
6   30.47%
7   41.64%
9   47.41%
10   35.00%
14   5.01%
15   33.07%

Time from Peak to
Failure

2   4.5sec.
3   5.5secs.
4   5secs.
6   7.5secs.
7   9.5secs.
9   21.5secs.
10   12.5secs.
14   25.5secs.
15   8.5secs.

q kN/m²

80

60

40

20

% strain

10   20   30   40   50

15
9
10
7
6
4
2
3

Controlled .... tests .... strain rate controlled tests ... of ... kaolinite ... remoulded samples.

q kN/m^2
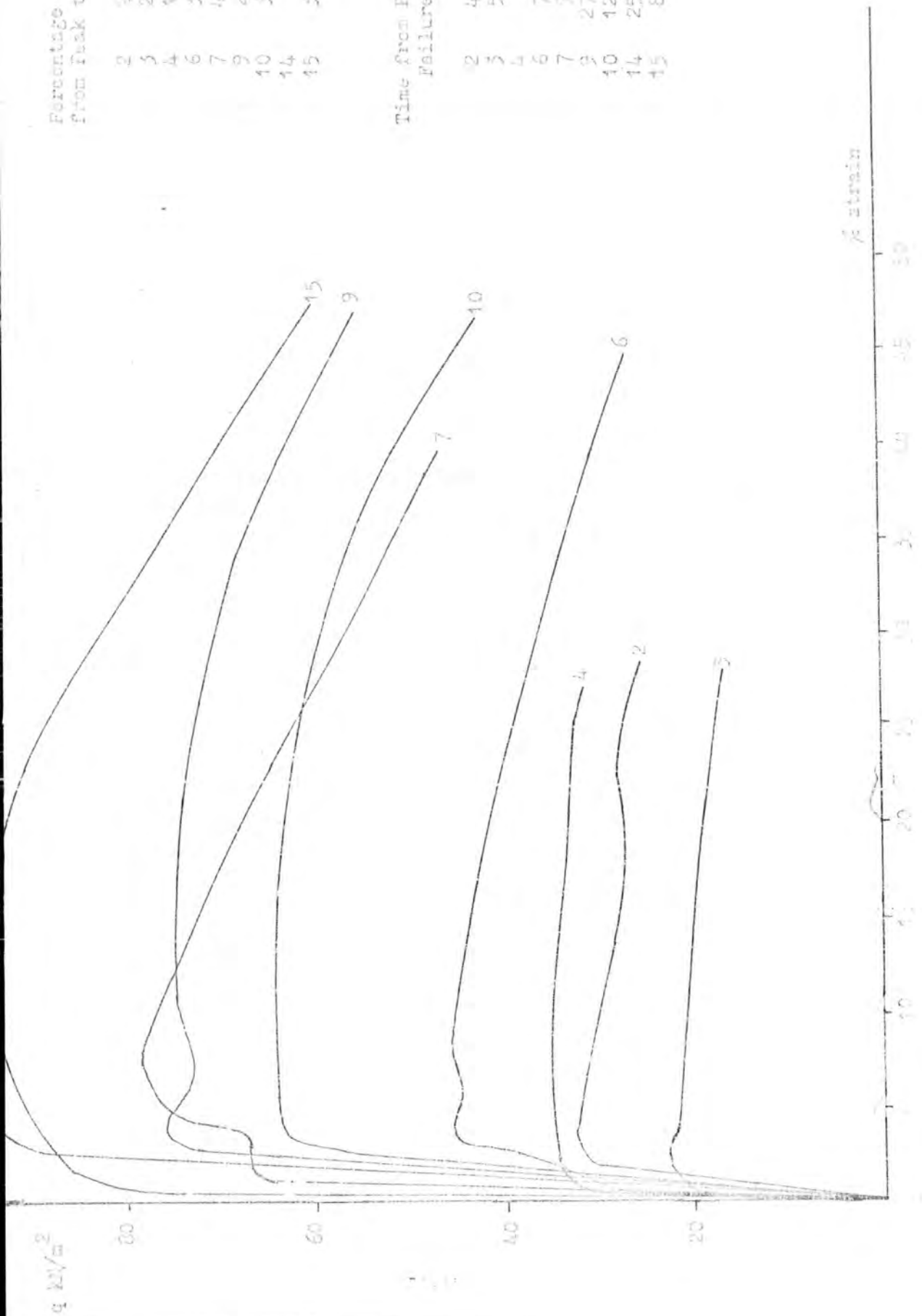
N.B. The losses in strength shown in this figure for samples which dilated are due to the difficulty in making lead during the later stages of shrinking

Time from Peak to Failure

2   4.5secs.
12   2.5secs.
16   18.5secs.

γ strain
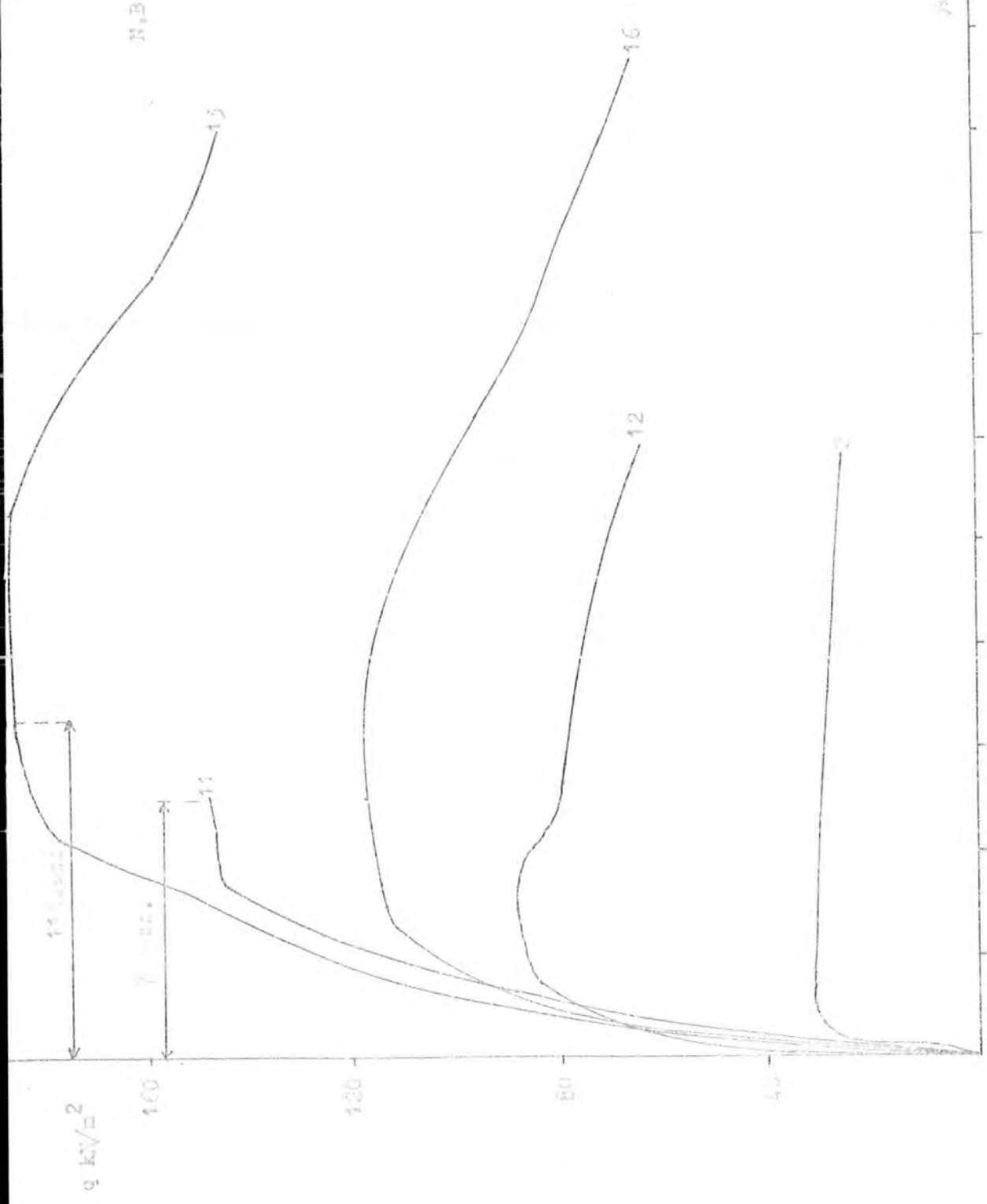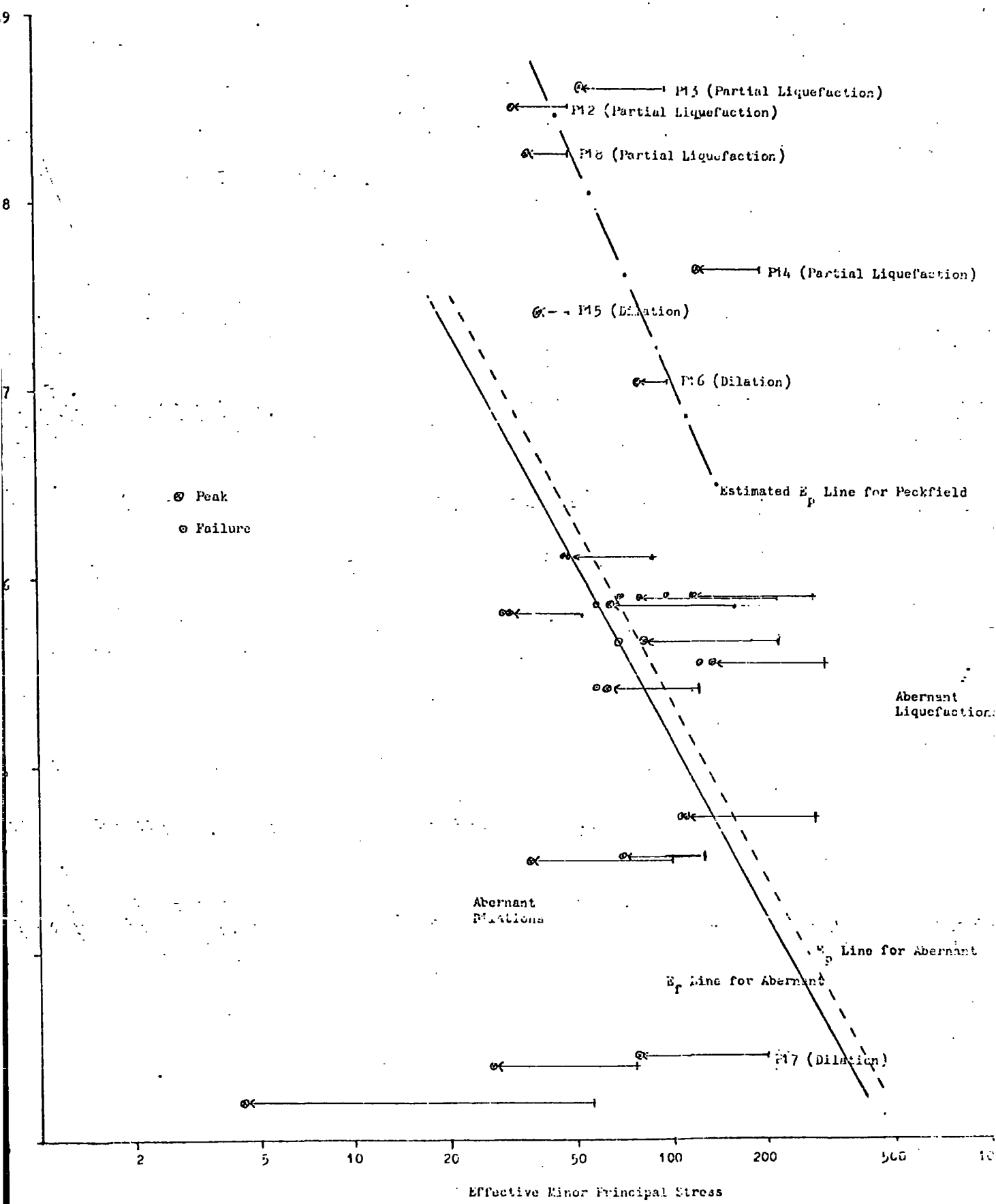
Figure 7.7 E_f and E_p Lines for Fine Discards.
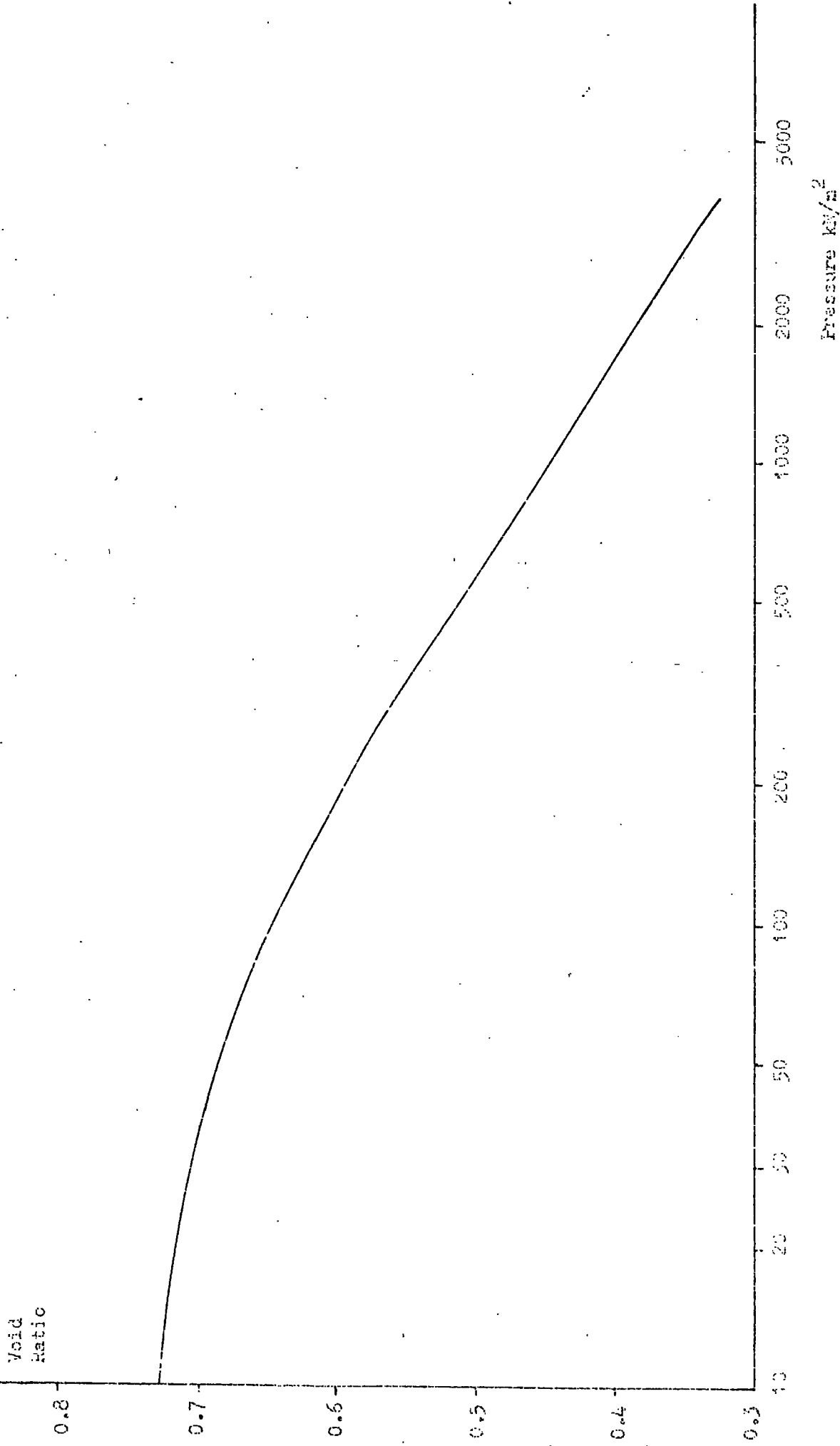
Figure 7.8 Pressure against Void Ratio Curve from Consolidation Test on Aberrant Fine Discard.
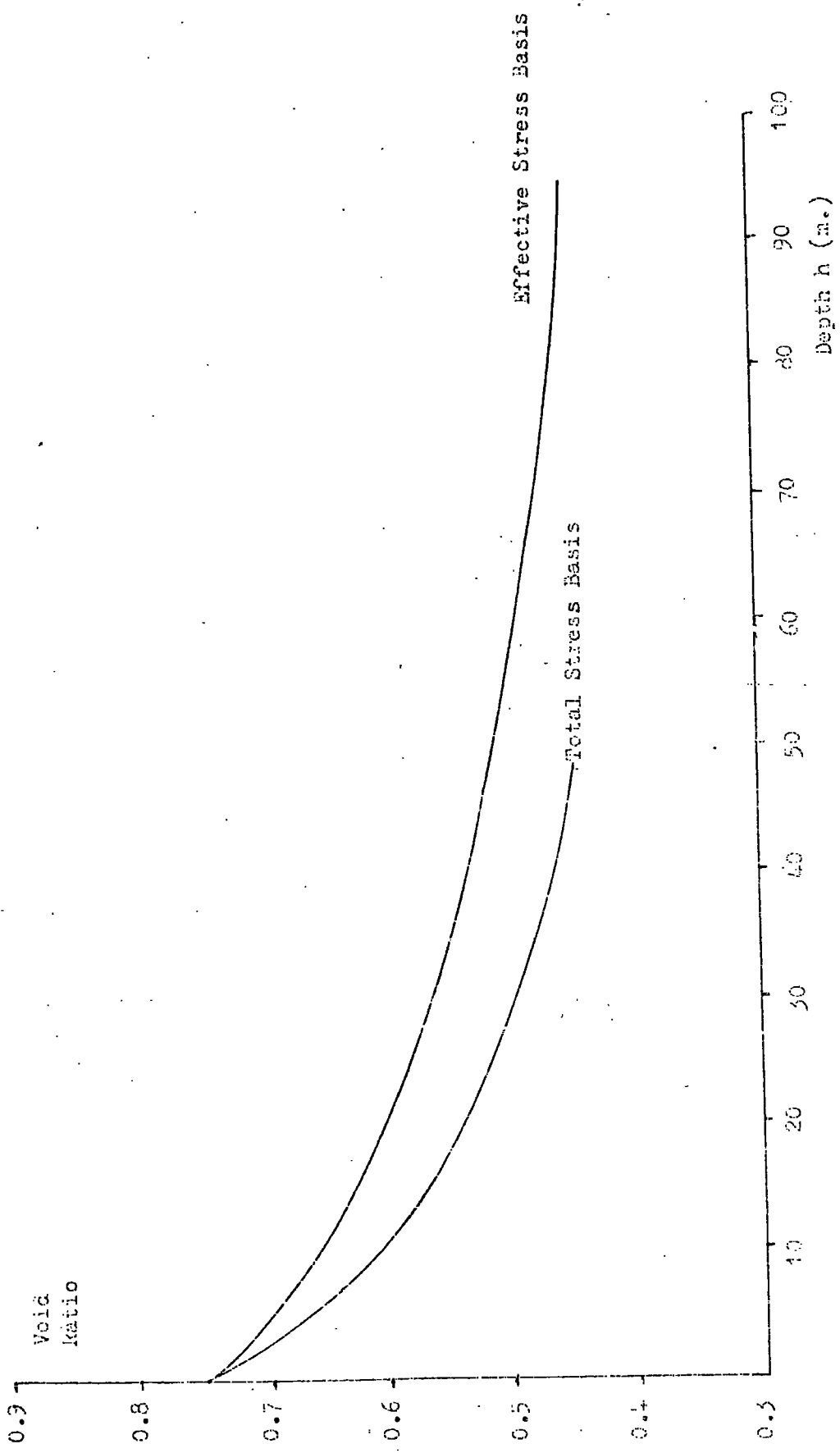
Figure 7.9 Depth of Sediment against Void Ratio for Aberrant Fine Discard.

Table 7.1 Summary of Results for Peckfield Slurry

Sample No.	Original M.C. (%)	Consolidation Pressure kN/m²	Back Saturation Pressure kN/m²	B Value.	Volume Change ml.	Dry Density (Mg/m³) Initial	Dry Density (Mg/m³) Final	Void Ratio Initial	Void Ratio Final
12	10	47	450	0.97	1.05	1.273	1.289	0.871	0.848
13	10	100	450	0.92	1.95	1.249	1.280	0.807	0.861
14	10	202	350	0.93	2.60	1.307	1.351	0.822	0.763
15	17.12	50	300	0.94	0.75	1.358	1.370	0.754	0.739
16	22.70	106	400	1.00	2.85	1.351	1.399	0.763	0.703
17	14.11	202	300	1.00	14.10	1.428	1.773	0.668	0.543
18	10	58	350	0.98	1.80	1.293	1.306	0.842	0.824

Sample No.	Relative Compaction% Initial	Relative Compaction% Final	Peak Strain %	Time to 20% Strain (sec)	u Peak kN/m²	$\bar{\sigma}_1$ Peak kN/m²	$\bar{\sigma}_3$ Peak kN/m²	$\sigma_1-\sigma_3$ Peak kN/m²
12	76.92	77.89	8.97	17.5	482.14	120.42	33.26	87.16
13	75.47	77.34	7.83	17	509.82	157.20	54.28	102.92
14	78.97	81.63	6.75	7	440.29	297.00	125.74	171.26
15	82.05	82.78	19.11	79	319.64	197.14	38.80	158.34
16	81.63	84.53	9.92	78	430.00	303.66	80.80	222.86
17	86.28	107.13	10.95	48.5	430.92	312.70	78.14	234.56
18	78.12	78.91	2.24	24.5	376.79	95.02	37.22	57.80

Non-representative volume change

Table 7.2 Summary of Results for Abernant Fine Discard.

Sample No.	Consolidation Pressure kN/m²	Back Saturation Pressure kN/m²	B Value	Volume Change ml.	Dry Density Mg/m³		Void Ratio		Relative Compaction (%)	
					Initial	Final	Initial	Final	Initial	Final
2	90	300	0.99	0.54	1.564	1.573	0.621	0.611	90.66	91.19
3	58	200	0.98	0.40	1.596	1.604	0.589	0.581	92.52	92.99
4	125	300	0.98	0.70	1.631	1.645	0.555	0.541	94.55	95.36
6	153	300	0.99	0.50	1.590	1.601	0.595	0.584	92.17	92.81
7	222	300	1.00	0.55	1.609	1.620	0.576	0.565	93.28	93.91
9	272	250	0.98	0.55	1.586	1.596	0.599	0.589	91.94	92.52
10	220	250	0.98	0.15	1.595	1.597	0.590	0.587	92.46	92.58
11	56	300	1.00	0.40	1.912	1.922	0.326	0.319	110.84	111.42
12	98	300	0.97	0.45	1.747	1.757	0.452	0.447	101.27	101.86
13	73	300	0.99	0.20	1.892	1.897	0.340	0.337	109.68	109.97
14	280	150	1.00	1.10	1.697	1.722	0.494	0.473	98.38	99.83
15	307	150	0.99	0.70	1.618	1.633	0.567	0.553	93.80	94.67
16	164	300	0.98	0.10	1.749	1.751	0.451	0.448	101.39	101.51

Table 7.2 cont...   Summary of Results for Aberrant Fine Discard.

Sample No.	Peak Strain %	Time from peak to failure (sec)	u Peak kN/m²	σ̄₁ Peak kN/m²	σ̄₃ Peak kN/m²	σ₁-σ₃ Peak kN/m²	Failure Strain %	u Fail kN/m²	σ̄₁ Fail kN/m²	σ̄₃ Fail kN/m²	σ₁-σ₃ Fail kN/m²
2	4.06	4.5	369.97	112.67	48.43	64.24	6.88	390.29	111.44	49.08	62.36
3	2.33	5.5	229.46	77.28	31.76	45.52	7.10	252.57	72.58	29.92	42.66
4	2.07	6.0	369.97	133.27	64.17	69.10	11.79	408.35	128.31	58.89	69.42
6	3.52	7.5	394.80	156.29	65.47	90.82	5.87	408.35	147.51	58.89	88.62
7	7.81	9.5	480.58	226.44	70.28	156.16	14.18	455.75	231.16	84.66	146.50
9	3.80	27.5	401.23	271.69	121.51	150.18	7.77	430.58	246.07	98.16	147.91
10	7.17	12.5	412.52	198.38	70.92	127.46	3.03	398.98	205.28	80.98	124.30
11	8.07		372.23	302.42	4.42	298.00					
12	8.48		430.92	212.74	36.32	176.42					
13	19.07		349.66	428.99	26.99	402.00					
14	14.93	25.5	389.27	315.42	109.16	206.22	10.77	375.73	317.99	112.70	195.29
15	7.00	8.5	339.61	348.21	137.91	210.30	10.53	382.50	332.51	126.38	206.13
16	13.53		342.88	308.35	70.35	238.00					

CHAPTER EIGHT

DISCUSSION FOR COARSE DISCARDS

8.1 General

All the tests were carried out on remoulded (fabricated) samples which had been screened through a 19mm sieve; the Gedling material was obtained wet from the colliery, and tested in this state. This was also true for later samples from Abernant. Earlier samples from Abernant and the shale and seatearth from County Durham were dry and were re-wetted before testing. The question arises as to the validity of tests under these conditions as compared to the actual conditions in which there would be considerable amounts of material of greater size than 19mm.

The National Coal Board's Review of Research on Properties of Spoil Tip materials (1972), gives the results of tests performed on Gedling material. It compares laboratory shear strength results on screened material with field shear box results. The results of this comparison show a very good correlation between laboratory and field shear strengths, suggesting that the effect of screening is not very great. The Review concludes that the standard 100mm diameter triaxial test does give a good indication of the actual field behaviour.

The Review also shows that the effect of variations in relative density for values below British Standard Compaction was very small.

8.2 Controlled Strain Test Results

8.2.1 Gedling

During the controlled-strain tests there was a considerable and rapid build up in pore pressure during the early stages. This was accompanied by a build up in the load. The initial period was followed by a long period

·of steady load, during which the pore pressure continued to rise, but more slowly than at first.   In the later stages of the test the pore pressure began to fall off slowly while the load increased again.   This basic type of behaviour was the same for all three consolidation pressures used.

The stress paths show the effect of the pore pressure build up and steady load by moving to the left at an almost constant value of q.   The failure envelope was reached at a considerably lower effective stress than the original consolidation pressure.   The final fall in pore pressure and rise in load are shown by the movement of the stress path up the failure envelope indicating a gain in strength and characterising a dilation.

The K_f line produced from these tests shows a very considerable degree of curvature from $\propto = 30^\circ$ at the origin to $\propto = 17^\circ$ at $\bar{p} = 300kN/m^2$ ($\emptyset' = 35^\circ$ to $\emptyset' = 19^\circ$).   It also implies that cohesion is zero.   Results given in the N.C.B.'s Review also show some degree of curvature for Gedling, from $\emptyset' = 32^\circ$ to $\emptyset' = 23^\circ$.

The results presented here (Figure 6.1) confirm the general observation of a curved envelope for Gedling material.   However, the degree of curvature is considerably greater, giving a lower value which is well outside the general range of $\emptyset'$ values for spoils in England (39° to 25.5°). Two main reasons have been suggested for the curvature of failure envelopes. Firstly the breakdown of inter-particular contacts at higher confining pressures, leading to reduced shearing resistance, and secondly lack of full saturation (Taylor, 1973).   It is likely that the first of these effects is acting in Gedling material, leading to some curvature of the failure envelope, and this will be discussed later in this chapter.   The over-emphasis of the effect producing the low value of 19° could probably be due to the samples not being fully saturated, as mentioned in Section 4.2.5.

The lack of total saturation could be due to air trapped within the particles, which are relatively fissured.   This could also explain the observation of a decrease in B value after the initial B test.   After a B test the back pressure is reduced to its original value and this could lead to some of the air within the particles coming out of solution and thus decreasing the degree of saturation.

The stress-strain curves (Figure 6.2) show the levelling off of the stress after the initial rapid increase, followed by a smaller rise in stress when the failure envelope is reached.   The strain attained a value of 25 per cent without any significant fall in stress level, indicating a plastic mode of failure.

8.2.2   Abernant

In the tests on the material from Abernant (Figs 6.3 and 6.4) there was also a fairly rapid rise in pore pressure in the initial stages.   The rate of this increase was less than for Gedling.   The stress rose fairly rapidly in this initial stage, reaching a higher value than for the Gedling specimens at the same consolidation pressure.   The stress and pore pressure continued to rise at a slower rate after the initial period.   At the end of the test the pore pressure levelled off and the stress fell slightly.   The tests were terminated when the stress level fell.

The stress paths show the smaller level of pore pressure build up than for Gedling as they reach the failure envelope much closer to the original consolidation pressure, without the flat section moving to the left. However, there was not the same movement up the failure envelope after this point had been reached, although further straining might have produced this effect after the small drop in stress on reaching the failure envelope.

The first test proved an exception to this general trend of behaviour. The stress rose continuously throughout the test and after an initial early

build up of pore pressure there was a fall off, producing a movement up the K_f line.

There was no noticeable curvature of the K_f line, which had a slope of $\alpha = 31^{\circ}$ ($\emptyset' = 37^{\circ}$). This falls well within the range of 25.5° to 41.5° given by the N.C.B. Review for Welsh spoils. As there were no problems with saturation, there should have been no envelope curvature due to this. From these results it would appear that there is no significant crushing out of inter-particular contacts in this material. In a similar manner to Gedling there appeared to be no cohesion intercept. The Abernant material would appear to have a greater shear strength than Gedling, as shown by the higher stress levels reached and the higher value of $\emptyset'$, especially at higher confining pressures. These results are in line with the findings of Taylor and Cobb (1977), who have shown that Mohr envelopes are sensibly linear (with c'=0) in the case of burnt shales and strong brittle shales, whereas those of the weaker spoils are more distinctly curved.

The stress strain curves for Abernant (Fig.6.4) show the steady state of stress reached and the extent to which it was maintained during the major part of the straining. Although a drop in stress level occurred at the end of the tests, there was no sign of failure, other than the barrelling effect of a plastic failure.

8.3   Gedling Controlled Load Tests

8.3.1   Consolidation

The Gedling samples (Fig. 6.15) exhibited initial large and rapid volume changes lasting for about 5 minutes. This was followed by a continuing slower volume change lasting up to about an hour or an hour and a half. The amount of volume change increased with consolidation pressure, reaching a 'cut-off' for pressures in the region of 200 to 300 kN/m^2.

There was a certain amount of scatter in the final densities and void ratios reached, but there was a general increase in final density with consolidation pressure, as would be expected. The values of c_v calculated give an average of about 170 m^2/year, which represents a relatively low rate of pore pressure dissipation.

8.3.2 Behaviour during Testing

For the samples tested at a consolidation pressure of 50 kN/m^2 there was a steady rise in pore pressure from the start of loading, becoming greater just before the sample started to strain. The rate of increase levelled off during straining and the pore pressure finally reached a steady value somewhat below the cell pressure. Towards the end of straining the pore pressure decreased slightly. The cell pressure remained generally fairly constant, although there was some rise during the straining period due to piston plunge. The straining period was about 25 seconds from the start of straining to 20 per cent strain, which although fairly rapid is not particularly so in terms of the time periods associated with liquefaction failures (see Fig. 6.5). The specimen which was dried out and then re-wetted (specimen DO Fig. 6.5) showed the same basic behaviour although it strained more quickly(11 seconds to 20 per cent strain).

As the consolidation pressure increased, the basic trend of behaviour was maintained. However, the degree of pore pressure build up became less, reaching levels well below the cell pressure. The load required to produce straining increased, and the rate of straining decreased; the strain taking 45 seconds to reach 20 per cent strain at 250 kN/m^2. The greater load and the smaller pore pressure build up with higher consolidation pressures would be expected. In the test performed at 217 kN/m^2 the specimen took all the load that could be added without showing any sign of straining or pore pressure build up. This sample had a slightly higher final density than

other samples, and would therefore have had an especially stable structure
(see Table 6.1).

There did not appear to be any kind of shearing during these tests.
The samples all showed a 'barrelling' type of deformation, associated with
a plastic failure.

8.3.3 Stress Paths and Stress-Strain Curves.

The stress paths and stress strain curves shown in Figures 6.5 to 6.9
are those from this investigation, together with results from some previous
tests carried out on Gedling material. These earlier tests were carried
out on the same rig, but with an external load cell, and a smaller strain
capacity.

The stress paths from the current investigation (Fig. 6.5) fit quite
well with the failure envelope obtained from the controlled strain tests.
All except that for test No. 5 ($P_c = 217$ kN/m^2) show a movement to the
left exhibiting a long flat section, characterising pore pressure build up.
The form of the stress paths above effective cell pressure of about 100 kN/m^2
was very similar to those produced from the controlled strain tests, except
that there was no dilation at the end of the test. In these tests a stress
level close to the failure envelope was reached in the early stages of
straining and was maintained with very little change in stress levels. It
is possible that insufficient load was added to produce dilation. The
previous tests at these pressures had shown larger stresses and had reached
the K_f line near the original consolidation pressure. It is probable that
this material was taken from the bunker or when the washery was producing
somewhat different material. This demonstrates the danger of possible
variations in the characteristics of material taken from the same tip. The
material for this previous investigation was rewetted before testing and

this could also have had some effect on the behaviour.

The samples tested at lower consolidation pressures show some differences in behaviour. The sample from the previous investigation tested at 50 kN/m^2 and sample No. 2 of the current investigation (Fig. 6.7) show a maximum stress level which is followed by a fall-off down the K$_f$ line, which is equivalent to a drop in strength of about 10 per cent. This drop in strength was followed by a further increase in strength, to a steady stress level, which was maintained for the major part of the straining period. Other tests at this consolidation pressure do not show any significant drop in strength, although the majority of the paths indicate that during this time the stress level is oscillating around a constant stress level close to the failure envelope. The two tests showing a drop in stress suggest that partial liquefaction is occurring. The final gain in strength and relatively long time period involved however, show that they are not total liquefactions. These results demonstrate that there is some potential danger of partial liquefaction at low confining pressures. For a bulk density of around 1.6 Mg/m^3 this represents a depth of spoil equivalent to about 3m in depth. The general trend is for this material to reach a steady state of stress without significant rises or falls. In order to produce a significant drop in strength the rate of straining would need to be greater. The test performed at an intermediate consolidation pressure of 80 kN/m^2, shows a mode of behaviour similar to specimens tested at higher confining pressures.

The stress-strain curves (Figs 6.8 and 6.9) indicate that stress levels are maintained over most of the straining period. Test No. 6 shows a gradual rise in deviator stress during this period. Test No. 2 shows a peak stress followed by a fall and then a final increase. The form of the stress-strain curves is the same as those obtained in the controlled strain tests, and the deviator stresses reached are about the same at equivalent consolidation

pressures. The observation of similarity between the stress-paths and stress-strain curves from controlled strain and controlled load tests when liquefaction does not occur conforms with the findings of Hird and Humphries (In press),who show that a similar behaviour applies to mica residues from the China Clay industry.

8.3.4 Possible implications of a Partial Liquefaction

The demonstration of a potential for partial liquefaction of Gedling spoil at low effective confining pressures poses the question as to what effect this might have in the field.

In the laboratory test the partial liquefaction produces a drop in strength which is followed by a final increase in strength (dilation). The question arising is the pertinence of this final dilation in a liquefied material. Assuming that the material flows as a result of the initial liquefaction will the dilation arrest this flow? The answer to these questions is considerably more complex than might at first meet the eye.

For the case of a tip which is built on flat ground, the effect of a total liquefaction is to produce a flow which only stops when the slope angle of the tip is equivalent to the reduced shear strength of the material. In the case of partial liquefaction in these circumstances the friction angle of the material will increase when the dilation occurs and hence the slope/which it will come to rest is equivalent to this friction angle at rather than the very much reduced one associated with the liquefied state.

A more complex problem is involved in the case of a tip which is built on sloping ground. This was the case at Aberfan (a slope of $12\frac{1}{2}^{o}$) and is also true at Gedling. In these circumstances the material will be flowing downhill and not on the flat (Figure 8.1).
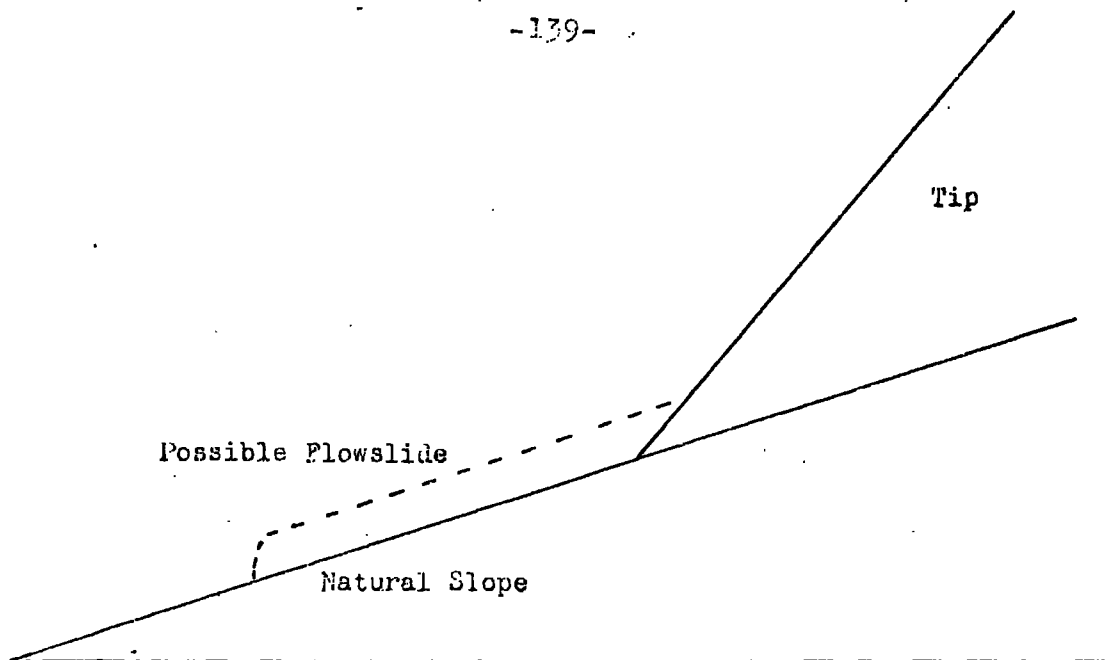
Figure 8.1   Tip Founded on a Slope.

The material in this case will be accelerating under gravity down the slope.   Thus, by the time a possible dilation occurs it will have developed considerable momentum.   In this case one has to determine whether the dilation will be sufficient to arrest the flow on the slope.

In considering this problem it is necessary to know at what stage the dilation occurs so as to calculate how much momentum will have been achieved.   Another important factor is at what rate does the increase in strength of the material occur.   When considering the possible arrest of the flow it is not the static friction as measured by the friction angle which is involed but the kinetic friction which is generally less.   Another problem is that of considering a 'tongue' of material rather than a single mass.

The points mentioned above show the complexity of this problem and that it is not possible to do a simple calculation to produce an answer. A considerable amount of work would be needed to relate the readings from the laboratory test to the field situation in order to answer the first two points.   As well as that the calculations which would be involved in the second part of a solution are beyond the bounds of elementary mechanics,

and were not thereforepossible in the time available during this investigation.

It seems quite possible that the gradual increase in strength likely to occur in such circumstances would not be sufficient to stop a large mass of rapidly moving spoil when it is flowing downhill. If this is the case the dangers of a partial liquefaction are much the same as for a total liquefaction. In many respects this is also the conclusion drawn by Casagrande (1976).

As well as a slope reducing the likelihood of a dilation arresting a flow once it had started, it also increases the possibility of a partial liquefaction occurring since a smaller proportion of the load needs to be transferred to the pore water before straining can start (Bishop et al. 1969).

Bishop drew the logical conclusion that the reduction in the proportion of the load that needed to be carried by the pore water would be equivalent to:

$$\frac{\tan \theta}{\tan \phi'} \times 100\%$$

where θ = angle of slope
ϕ' = friction angle of material.

Using this approach the percentage rise in pore pressure required to cause straining can be calculated.

In test No. 2 in which a drop in strength was recorded, the value of ϕ' at peak was 28°, and the straining started when the rise in pore pressure was 50 per cent of the original effective consolidation pressure. Figure 8.2 illustrates the relationship of slope angle versus percentage pore pressure increase required to start straining.

This shows that the effect of a slope angle on the required pore pressure increase is very great and that the potential for a liquefaction induced flowslide is enhanced in these circumstances.

For example, in the case of a slope angle of $12\frac{1}{2}°$ the build up of pore pressure required is only 29.4 per cent of the cell pressure. Thus, for an effective consolidation pressure of 50 kN/m^2, the pore pressure only needs to increase by 14.7 kN/m^2 to induce straining.

8.4 Abernant Controlled Load Tests

8.4.1 Consolidation

For the Abernant specimens (Fig. 6.16) the initial rapid period of volume change lasted for about one or two minutes. The period of further volume change depended on the consolidation pressure, being about 10 minutes at 50 kN/m^2 and about an hour at 200 kN/m^2. Overall the volume change was quicker than that for Gedling and produced values between a third and a half of those for Gedling at the same consolidation pressure (Table 6.2). The amount of volume change increased with consolidation pressure reaching a constant value at around 200 to 250 kN/m^2. The change in density was accordingly smaller than for Gedling. The final densities were again rather variable, but tended to increase with consolidation pressure. The sample was made up to a higher density (No. 2) and showed a reduced degree of consolidation, as would be expected. The average value of c_v was about 550 $m^2/year$, which is significantly higher than for Gedling, and is more in line with drainage rates measured in the large Rowe Cell (700-800 $m^2/year$; Taylor and Cobb, 1977).

8.4.2 Behaviour during Tests

The behaviour of the Abernant material, although showing some similarities in basic characteristics, did show some significant differences from the

Gedling material.

As for Gedling there was a pore pressure build up during the initial

stages of loading.   The rate increased before the start of straining,

and then dropped reaching a steady level during straining.   The pore

pressure finally fell towards the end of straining.   In general the rate

of build up was much less than for Gedling at the same consolidation pressure

and the final value reached was much further below the cell pressure.

The rate of pore pressure build up in the tests at high consolidation

pressures was very slow.   The amount of load required to produce straining

was considerably greater than for Gedling and at high consolidation pressures

it exceeded the amount that could be added to the hanger.   Extra load was

added by applying pressure to the loading beam.   The load was generally

maintained during straining and extra load could still be taken during this

period.   The period taken during straining was considerably longer than for

Gedling, being about a minute even at a consolidation pressure of 30 kN/m^2,

and reaching 3 minutes at 235 kN/m^2.   There did not appear to be any

significant differences in behaviour between samples made up from wet

material, and those which were re-wetted.

Like the Gedling specimens the deformation generally took the form of

barrelling, although at least one sample (No. 9, Fig. 6.10) failed in shear.

8.4.3   Stress Paths and Stress/Strain curves

The stress paths (Fig. 6.10) from the controlled load tests agree very

well with the failure envelope from the controlled strain tests.   The type

of behaviour shown is basically the same throughout the range of consolidation

pressures used.

The deviator stress increases throughout the tests, except at the very

end when it is not possible to apply sufficient load to maintain the increase.

The failure envelope is reached at effective pressures close to the original consolidation pressures. The amount of movement to the left is greater at higher consolidation pressures, showing the pore pressure increases to have a greater effect at these pressures. On reaching the K_f line the stress paths exhibit dilation. This trend of behaviour is maintained down to a consolidation pressure of 30 kN/m^2. This shows that there is not likely to be any drop in strength or significant pore pressure build ups to lead to liquefaction failure phenomena, hence this material is safe from liquefaction.

Despite variations in the densities achieved the type of behaviour and the proximity to the K_f line do not seem to be significantly affected, confirming the observations referred to by McKechnie Thomson and Rodin (1972) concerning the effects of density variation and the resultant effective shearing resistance.

The sample which was fabricated to a significantly higher density (No. 2, Fig. 6.10) (close to the maximum dry density), shows a higher load and a smaller effect due to pore pressure build up, reaching the K_f line at a higher deviator stress than in the more conventional test at a similar consolidation pressure (No. 1. Fig. 6.10). It also crosses the K_f line, inferring that at higher densities the shear strength possibly increases somewhat.

The stress-strain curves (Fig. 6.11) generally confirm the gradual continued rise in deviator stress throughout the tests. They also show the significantly higher loads attained than samples from Gedling. The larger load carried by the denser sample is clearly shown. The form of the curves is again very similar to those from the controlled strain tests, and the stresses achieved are also very similar. The two sets of stress paths also show similar types of behaviour in the two types of test (Figs. 6.3 and 6.10).

From these results it can be concluded that the material from Abernant has a higher shear strength than that from Gedling. Also in a controlled load triaxial test it is likely to dilate at all consolidation pressures showing it to be safe insofar as liquefaction is concerned. The material from Gedling shows some signs of partial liquefaction at low confining pressures, and no significant dilation at higher confining pressures.

8.5 Pore Pressure versus Strain Plots

Figure 6.14 shows pore pressure versus strain plots for three tests representative of the types of behaviour observed. The plots are compensated for changes caused by cell pressure increases due to piston plunge.

Gedling No. 2 was a partial liquefaction. The plot shows the initial increase in pore pressure, continuing at a reduced rate up to a strain of about 12 per cent, followed by the final pore pressure decrease, representing the final gain in strength. The pore pressure reaches a value very close to the confining pressure showing a very low effective pressure during this type of failure.

Gedling No. 4 was typical of the tests in which a steady state of stress was reached. The plot shows an initial increase in pore pressure followed by a period of almost constant pore pressure, representing the major part of the straining period. The pore pressure reached is well below the confining pressure.

Abernant No. 9 shows the behaviour of a dilating sample. The pore pressure rises fairly rapidly initially, reaching a peak at a relatively low strain. The pore pressure then decreases for the remainder of the test. This is shown by the gain in strength and movement to the right on the stress path.

8.6   The Durham Seatearth and Shale Investigation

The significantly different types of behaviour between the samples

from Gedling and Abernant have been discussed above.   It was decided to

try and demonstrate the reason behind these differences in behaviour.

The most obvious difference between the two types of material was that

one type was shale-rich (Abernant) and the other seatearth-rich (Gedling).

In order to demonstrate the difference it was decided to use two

pure materials of shale and seatearth obtained locally.   Having demonstrated

the different behaviour it was hoped to test mixtures of the two materials

to determine how much seatearth was required to cause a significant change

in behaviour.   However, the results were somewhat unexpected.

The two samples were crushed down and made up to the same grading as

the equivalent spoil to eliminate any effects due to major differences in

grading.

As is shown in the next section the shale did not behave as expected,

and so in order to explore the effect of mixing the two types of material

Abernant shale-rich spoil was mixed with the Durham seatearth.   Possible

factors affecting the behaviour of the various materials are discussed in section

8.10.

8.7   The Durham Shale

The behaviour of the Durham Shale differed considerably from Abernant,

being more like that of Gedling.   The first test was carried out at a nominal

consolidation pressure of 50 kN/m^2 as this was the pressure at which the

most significant differences in behaviour had occurred between the two

colliery spoils.

On consolidation (Fig. 6.17) there was a rapid volume change for

about 5 minutes followed by a slower change lasting for up to about an

hour.   The actual volume change was of the same order as for Gedling (90 ml)

and the c_v value was about 230 m^2/year, which although slightly higher than

that of Gedling is much less than for Abernant, indicating a slower

dissipation of excess pore pressure.

In the test there was a fairly large initial rise in pore pressure,

followed by an increase in the rate of rise prior to the start of straining.

The pore pressure continued to rise during the first part of straining

leading to a large overall increase in pore pressure, much larger than

for Abernant samples but of the same order as for Gedling samples.   There

was a levelling off followed by a slight fall in the later stages of straining.

The load taken was fairly small compared to those for Abernant, and the

straining was quicker (16.5 seconds) than either Abernant or Gedling.

The stress path and stress-strain curve (Figs.6.12 and 6.13) show that

there is a definite loss of strength and considerable build up in pore

pressure, before a slight gain in strength at the end of the test.   This

shows a partial liquefaction failure, which is more definite than the one

noted for Gedling colliery spoil.

In order to investigate the extent of this type of behaviour, a second

test was carried out at a consolidation pressure of 97 kN/m^2.   The same

type of behaviour was again observed in this test.   A substantial build up

in pore pressure occurred and only a relatively small load was carried.

The straining period in this test was especially fast at 9 seconds to 20

per cent strain.   The stress path shows that there was again a drop in

strength at this pressure and a partial liquefaction was observed (Fig.6.12).

From these tests it was obvious that the material type (namely shale)

was not sufficient evidence to preclude the possibility of liquefaction

in a spoil, and that other properties would have to be examined before more

definite conclusions could be drawn.

8.8   The Durham Seatearth.

Three tests were carried out on the Durham Seatearth all at nominal consolidation pressures of 50 kN/m^2.   With the amount of material used in the first test it proved very difficult to produce a uniform sample, so more material was used in the last two tests producing more uniform samples, although their densities were not very much higher, giving voids ratios of the same order as for other samples.

The amount of volume change was of the same order as for Gedling samples, but took much longer - up to about 2 hours.   This produced a less steep volume change versus root time curve (Fig. 6.17) and hence a lower value of c_v of around 80 m^2/year, indicating a lower drainage rate.

The behaviour in the tests was similar to the Gedling samples at the same consolidation pressure.   There was a quite large initial pore pressure increase up to the start of straining, followed by a levelling off during straining with a slight fall at the end of the test.   The overall pore pressure increase was quite large, being of the same order as that of the requisite Gedling samples.   The load carried was relatively small and the straining period was about the same as for Gedling.

The stress path and stress-strain curve (Figs.6.12 and 6.13) show a similar form to Gedling samples.   A steady state of stress is reached during straining and this is maintained with certain fluctuations.   There is no definite drop in strength and there is some indication of dilation at the end of the tests.   The actual strength is slightly higher than that exhibited by the Gedling specimen.

These tests show that the Durham Seatearth models the behaviour of seatearth-rich Gedling spoil quite well.

8.9   The Seatearth/Abernant Mixtures

All tests described in this section were at a nominal consolidation pressure of 50 kN/m^2 (Figs. 6.12 and 6.13).

The first tests were carried out on a mixture of 50 per cent by weight of each material, to see if either type of behaviour was dominant.

The consolidation behaviour of the 50-50 mixtures showed an intermediate behaviour between the two extremes.   The amount of volume change was less than for the seatearth and the time taken considerably less.   This produced a value of c_v around 220 m^2/year, indicating a drainage facility lower than that of Abernant colliery spoil.

The behaviour during loading was more characteristic of the seatearth. The pore pressure build up was rapid and of a similar size to that of the seatearth.   The straining period was considerably shorter than for the pure samples of Abernant or Seatearth.   The stress paths (Fig. 6.12) show that although the tendency was for little change in the state of stress during the straining period, there was a slight trend of increasing deviator stress (i.e. dilation) similar to that of the seatearth.   It was not as definite as for Abernant samples, however.   The stress-strain curves (Fig. 6.13) show that the load carried was about the same as for the seatearth and considerably less than for Abernant samples.

From these tests it was concluded that the seatearth was the dominating influence, and that further tests should be carried out with larger proportions of Abernant material.

The next two tests were carried out on mixtures of 75 per cent Abernant material and 25 per cent Durham seatearth.   The first was performed at a density which was higher than the general range used in these tests.   The density of the second sample was slightly low.

The volume change of both these samples was quite short and relatively small, being of the same order as for Abernant samples. The values of c_v produced were also in the same range as for Abernant (Table 6.3).

The behaviour of the two samples during the tests differed considerably. The denser sample showed a slow build up in pore pressure with a levelling out during straining. The amount of build up was less than the previous mixtures. The straining was quicker than that exhibited by Abernant spoil, but slower than the previous mixtures. There was a noticeable fall in pore pressure at the end of the test and the behaviour appeared closer to that of Abernant samples. The stress path (Fig. 6.12) confirms this, showing no movement to the left and continued upward movement in deviator stress throughout the test. Both the stress path and stress-strain curve (Figs 6.12 and 6.13) show that the strength is very similar to that of Abernant.

The looser sample showed a more rapid build up in pore pressure, especially during straining, although there was a greater change in cell pressure than usual, accounting for some of the pore pressure rise. The straining was quite quick, again being quicker than either individual end components. A smaller load was carried although some increase was maintained during straining. The stress path (Fig. 6.12) shows that an almost constant state of stress is reached in a similar way to the seatearth with a slight upward trend. The stress-strain curve (Fig. 6.13) illustrates the intermediate value of stress attained. The small change in state of stress during straining shows a characteristic of the seatearth, while the lack of movement to the left shows an Abernant characteristic. Hence, this sample shows an intermediate type of behaviour. The difference between these two last samples shows that density can be significant in these mixtures.

The next test was carried out on a mixture of 80 per cent Abernant and 20 per cent seatearth. The volume change of the specimen was not representiative as accidental straining during saturation led to excess pore pressures, which took longer to dissipate. This explains the larger volume change and low value of c_v (Table 6.3).

The behaviour of the specimen tended towards that of Abernant, the rate of pore pressure build up being quite slow. The pore pressure build up was maintained during straining leading to a slightly larger overall increase than that for an Abernant sample. The pore pressure decreased towards the end of straining; which was quicker than for an Abernant sample. The load taken was about the same as for the second 75/25 sample although some increase was maintained during straining.

The stress path (Fig. 6.12) again shows no movement to the left and an upward movement symptomatic of dilation. The stress level is in fact slightly lower than the second 75/25 sample. The type of behaviour is fairly close to Abernant showing more definite tendencies than the previous mixture.

The final test was carried out on a mixture of 85 per cent Abernant and 15 per cent seatearth. The volume change and resulting c_v value were very similar to those for Abernant samples (Table 6.3).

The behaviour during the loading stage also showed strong similarities to Abernant samples. The build up in pore pressure was slow and was maintained at a reduced rate during the early part of straining. This was followed by a decrease in pore pressure at the end of straining. The load carried was quite large, and continued increasing during straining. The only major difference from an Abernant sample was the rapid rate of strain.

The stress path (Fig. 6.12)shows a great similarity to that of the Abernant sample with no movement to the left, and a fairly large dilation maintained in the latter parts of the test. The stress-strain curve (Fig.6.13)

shows that the load carried was similar to, and in fact slightly larger

than the Abernant Sample.   In this mixture the seatearth has little

effect on the overall behaviour.

The two extreme types of behaviour observed are a definite dilation

and the maintenance of a steady state of stress with little loss or gain

in strength.   From these tests it appears that the transition between

these two types of behaviour occurs when the mixture contains about

20 to 25 per cent additional seatearth, the actual percentage depending

on the density of the specimen prepared.   The only major difference noted

was the large strain rates in the mixtures compared with the constituents

alone.   This is possibly due to the production of less stable structure

at failure due to interfaces between the differing materials.

8.10   Discussion of differences in material properties influencing the behaviour in the controlled load tests.

8.10.1   Shape

A factor which has been thought to have an important influence on the

behaviour of granular materials with respect to liquefaction is the shape

of the particles.   Hird and Humphries (In press) have shown that for mica

tailings from the China Clay industry the flat 'platey' particles inhibit

susceptibility to liquefaction due to the increased compressibility they

produce.

The shape distributions   for the materials used in this investigation

are shown in Figs 2.10 to 2.13.   The plot for Gedling shows both the

material used in this investigation and that used in the previous liquefaction

investigation.   These measurements show that there is a noticeable

difference in the shape, the previous sample studied being more rounded

than the new one, which is more platey.   This difference could in part

account for the differences in behaviour noted . in section 8.3. i.e. their

taking higher loads and showing a smaller amount of pore pressure build up.

The Abernant material is shown to be relatively platey, only a very small proportion having a thickness greater than half the length, and a significant proportion having a length to thickness ratio between 8:1 and 4:1. There is a good degree of scatter in the distribution.

The Durham seatearth shows a very even distribution with 80 per cent having a length to thickness ratio between 2:1 and 4:1 and a length to breadth ratio beteen 1:1 and 2:1. This again shows a platey material, although not to the same extent as Abernant.

The Durham shale has a distribution pattern which is very similar to that of Abernant, showing a platey material with some scatter in the type of particles.

From these results it would appear that the particle shape is not playing a major part in the behaviour of these particular materials in the controlled-load tests. All the materials were basically 'platey', and the most susceptible and least susceptible have almost identical shape distributions. It is possible that the platey nature of the Gedling material, the seatearth and the shale has some influence on their behaviour in combination with other factors, whilst for the Abernant material the shape factor is obviously over-ridden by other influences. However, it must be concluded that for materials of this particle size a 'platey' material will not necessarily be susceptible to liquefaction, and that shape cannot be taken as a major factor on its own merits.

8.10.2 Grading

Another factor which has been shown to affect the behaviour of materials with respect to liquefaction is the particle size distribution. Various criteria have been put forward to relate the grading of a material to liquefaction potential (Terzaghi and Peck, 1948). However, these generally give a requirement of a uniformly graded material, which in general coarse colliery spoils are not.

Terzaghi and Peck (1948) state that flow or liquefaction slides usually occur in uniformly graded material in the fine sand range, and among the criteria proposed were:

$D_{10} < 0.1mm$ and $D_{60}/D_{10} < 5$ (Uniformity coefficient)

where: D_{10} is the diameter equivalent to the 10 per cent passing on a grading curve and D_{60} is the 60 per cent passing size. Hutchinson (1967) pointed out that the range could obviously be extended since D_{10} for Aberfan was slightly greater than 0.1 mm and the uniformity coefficient was about 10. Hutchinson also showed that the D_{10} size of a liquefaction slide which occurred in PFA at a site in South Wales had a uniformity coefficient of approximately 10 and a D_{10} size of 0.15mm. Some indication of the state of looseness of liquefaction slides can be gained by comparing in situ dry densities with maximum dry densities obtained from B.S. compaction tests (B.S. 1377, 1975).

	Maximum Dry Density Mg/m^3	In Situ Dry Density Mg/m^3	% maximum
PFA slide Jupille(Belgium)	1.170	0.897	77
" " (S.Wales)	0.994	0.785	79
Aberfan Tip 7	1.939	1.587	82

It is unlikely that grading differences caused any of the variations noted in this investigation as the seatearth and the shale were made up to the same nominal gradings as Gedling and Abernant material, respectively.

8.10.3 Strength

A factor which may have a fairly large bearing on the behaviour of materials in the controlled-load tests is the material strength. This includes both the strength of the material in shear and the strength of

the individual particles.

From the stress-strain curves and the stress paths it can be seen that the material from Abernant has a considerably higher shear strength than any of the other three materials. It has already been noted that Gedling has a curved shear strength envelope, showing a reduction in strength at higher confining pressures. An explanation put forward for this was the crushing out of interparticle contacts during the test. In order to investigate the possibility of this phenomenon occurring in all the materials investigated, samples were sieved after testing (all at nominal consolidation pressures of 50 kN/m^2). The final grading was compared to the original. The two sets of curves are shown in Figs 2.5 to 2.8. Although it was suspected from the curved failure envelope that crushing out did occur in Gedling material, this is not shown up on the grading curves. However, both gradings were produced by wet sieving, and the effect of rewetting Gedling material has been noted in the past (National Coal Board, 1972; see also Section 8.10.4.). A considerable degree of breakdown was noted when sieving the Gedling material, and on sieving the tested sample there appeared to be less breakdown. It is likely that wet sieving has the effect of breaking this material down to the same grading whatever the grading is in a dry condition, and so any change in grading due to crushing out will not be shown up. However, from the smaller amount of breakdown in the second sieving and the curved failure envelope it would appear that crushing out is a reality.

Some differences are visible between the two gradings for Abernant. However, the after testing curve shows less fine material, which would not be possible if the grading before testing was as shown. It is therefore likely that the differences between the two gradings are due to the

sievings having been carried out on samples from different batches of material. The relatively small quantity of silt size material (10%) suggests that there is not likely to have been any great amount of crushing out. The linear failure envelope confirms this view.

The Durham seatearth shows considerable differences between the two grading curves. Although part of this effect may be due to water (see Section 8.10.4) it seems likely that such a large difference as that illustrated is, at least in part, due to crushing out during the test.

The Durham shale also shows a significant difference between the two grading curves. It is again possible that some of this difference is due to the action of water, although there is also some effect due to crushing out in the test.

Lawrence (1972) has shown that there is some connection between the material strength given by the aggregate impact test and its shear strength. It also seems likely that there will be a connection between individual particle strength and any tendency to crush out during the test. The aggregate impact values shown in Table 2.2 imply that the Gedling material and the Durham seatearth have lower values of A.I.V. than either the Abernant material or the Durham shale. The shale has a slightly lower strength than the Abernant material (a higher A.I.V. indicates a lower strength). From these results it would be expected that Abernant would have the highest material strength and would therefore be least likely to undergo crushing out, and this is confirmed in practice. The seatearth and Gedling material would be expected to be weaker and more susceptible to crushing out and this is again the case. The shale, although it is weaker than the Abernant material, is not sufficiently so to account for large differences in behaviour. However, as will be shown in the next section water can also have a significant effect.

8.10.4   The Effects of Water

The effects of water on a material's structure and its particle strength could be another factor connected with the behaviour in the controlled load tests.

The slaking tests (Table 2.2) which were carried out (following Taylor and Spears, 1970) show the potential effects of water on the stability of the material. The original test using the No. 14 sieve confirms that Gedling is susceptible to considerable particle breakdown in the presence of water. However, no significant difference is shown between the other materials. It was thought that the difference in strength was probably the main reason for the seatearth behaviour differing from that of the Abernant material. For this reason it was decided that it was not necessary to investigate the behaviour of this material or Gedling in the presence of water any further.

The main factor that required an explanation was the reason for the difference in behaviour between the Durham Shale and the Abernant material. It was noted that in the No. 14 Slaking test, the shale had shown some degree of deterioration but not sufficient to be accentuated by this sieve. Therefore, these two materials were re-tested on the No. 7 sieve. The results (Table 2.2) show that there is in fact a greater degree of breakdown in the case of the shale than for the Abernant material. The second test carried out was an A.I.V. test on pre-saturated material, to enhance any change in strength under the influence of water. The results (Table 2.2) show that both materials suffer a reduction in strength, but this is significantly greater for the Durham shale. This confirms that water has a greater effect on the Durham shale than on the shale-rich colliery spoil from Abernant. This change in behaviour in the presence of water seems to be a significant contributory factor to the differences in controlled-load

test behaviour. It is likely that as the seatearth is a similar

material to the shale, coming from the same seam, it is likely to undergo

similar changes in behaviour to those noted above.

It seems that a material's strength and its stability in water are

major factors involved in its behaviour in a controlled-load test.

However, it is probable that the overall behaviour is governed by a

combination of inter-connected factors and that these two alone are not

sufficient to account for the overall behaviour under test. Other factors

which could be involved are discussed in the following sections.

8.10.5 Pore Pressure Dissipation

As the build up in pore pressure plays an important part in liquefaction

failures, it seems probable that the dissipation of pore pressure within a

material is likely to play an important part in its susceptibility to lique-

faction.

The values of c_v (Tables 6.1, 6.2 and 6.3) calculated for the materials

used in this investigation show that the Abernant material has a

significantly higher value of c_v than any of the other three materials.

This indicates that there are less likely to be centres of excess pore

pressure build up in an Abernant specimen during loading, i.e. pore pressures

will more readily equilibriate. This is also shown on the Abernant stress

paths by the smaller degree of movement to the left, (Fig. 6.12). This

suggests that the pore pressure equilisation is playing an important

part in the differences in behaviour noted between these materials.

Differences in pore pressure dissipation and volume change are due

to differences in the soil structure and its changes under consolidation.

It appears that the fabricated Abernant materials have a relatively stable

structure with little potential for change during consolidation.   The

other three materials have less stable structures allowing greater volume

changes.

It is probable that there is again some crushing out and particle

breakdown during the consolidation of these materials.   Allen (1973)

recorded that weaker spoils exhibited a higher degree of breakdown during

consolidation than more brittle types.

8.10.6   Chemistry and Mineralogy.

There are two striking things noticeable from the chemistry and

mineralogy.   The first is that the Abernant material has considerably

more organic carbon (coal) than any of the other materials.   The second

is that the Durham rocks are kaolinite-rich, while the Abernant material

has a low kaolinite content.

Although it could be expected that kaolinitic rocks are more stable

in water than those containing degraded illite and mixed-layer clay (Taylor

and Spears, 1970), the latter authors showed that the fabric (i.e. structure)

of the rock was equally as important.   In the current work a straight

mineralogical comparison of the kaolinite-rich Durham shale and the

illitic Abernant shale is not meaningful because Abernant has a high coal

content, whilst the Durham material is devoid of coal.   Coal is an

important contributor to peak shear strength to the extent that McKechnie

Thomson and Rodin (1972) showed that coal-rich tailings had a higher shear

strength than the coarse discard (of lower coal content) from the same

colliery.   Taylor (1974) also showed conclusively that coal content is

the major control in so far as peak shear strength is concerned.   It is

probably also a major factor in the results obtained in the current work.

8.11   Conclusions.

From the tests on the seatearth-rich   Gedling colliery spoil

it can be concluded that this is a relatively weak spoil, as is generally

the case for seatearth-rich discards. The Mohr envelope for this material is curved indicating crushing out of particle contacts at the higher confining pressures. In the controlled-load tests it showed a possible susceptibility to partial liquefaction at low confining pressures and generally showed a type of behaviour in which a steady state of stress close to the failure envelope was maintained with little variation.

The Abernant material was shown to be considerably stronger than that from Gedling, and there was no indication of a curved failure envelope. The controlled-load tests induced a dilatant response and confirmed that this was a considerably stronger material.

The results of tests on Durham seatearth and shale showed that the differences in behaviour were not necessarily due to the contrast between seatearth-rich and shale-rich discards, since the Durham shale showed tendencies to partial liquefaction. The behaviour of the seatearth was similar to that of Gedling and suggests that the response is typical of weak seatearth type spoils.

The results of tests on mixtures of Abernant and Durham seatearth show that the transition in behaviour of the two end members occurs when the mixture contains between 20 per cent and 25 per cent seatearth. It is also dependent on the density.

The main factors which appear to influence the behaviour in the controlled-load tests are the material strength, its behaviour in water and its ability to dissipate (i.e. equilibriate) pore pressures. The Abernant material has a high particle strength, partly in response to its high coal content, is little affected by water and is free draining (i.e. high c_v). The remaining materials have lower strengths, are significantly affected by water and exhibit lower values of c_v implying that pore pressures are not necessarily uniform within a sample under test. Particle shape and grading seem to have little influence in this size range.
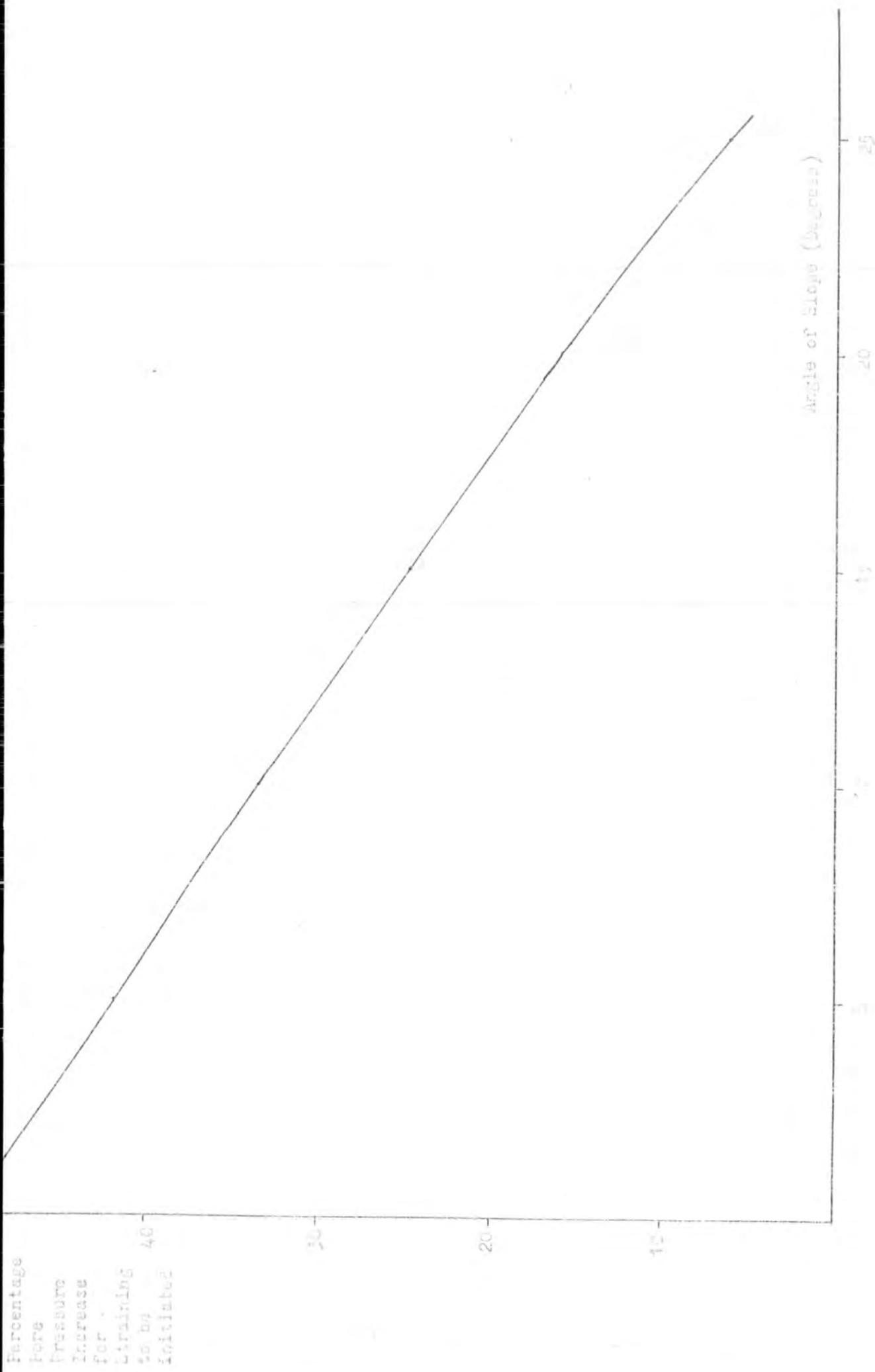
Percentage
Pore
Pressure
Increase
for
Draining
to be
Initiated

CHAPTER NINE

DISCUSSION OF FINE DISCARDS

9.1   General

Two fine discards were investigated, with two main objects in mind.

As both in situ and bulk samples could be obtained from Peckfield it

was decided to investigate the differences in behaviour between made-up

and in situ samples in the light of Seed's (1977) findings.   Since

in situ samples could not be obtained from Abernant the investigation

of Peckfield material would enable the reliability of the results from

made up Abernant samples to be gauged.

The investigation of Abernant material was carried out varying the

consolidation pressure at approximately constant density and varying the

density at constant consolidation pressure.   This enabled the effects of

variations in these to parameters on the behaviour with respect to

liquefaction to be seen.

It was also hoped to be able to correlate any differences in

behaviour with differences in material properties.   Also in the case

of Abernant it was hoped to show any similarities or differences with

the coarse discard from the same colliery.

The degree to which results of these tests are related to the actual

behaviour in the field is of interest.   The validity of the use of made-

up samples has been questioned by Seed (1977) and others, and is illustrated

again here.   Seed has also raised the validity of the use of small (38mm)

diameter samples, at least in terms of cyclic liquefaction, and has used

large scale cyclic shear boxes in his recent investigations (1977).

However, in the static situation the effects of boundary conditions on pore pressure are not likely to be as large, and previous investigations (Castro, 1969) seem to have produced acceptable results.

Another point brought out by this investigation is the use of a vacuum in sample preparation. The results for Abernant, when a vacuum was used, and from previous investigations (Castro, 1969), (J.M.P. Shorten, in preparation), show that liquefaction failures can be produced when a vacuum is used. However, tests carried out on Leighton Buzzard Sand at the time of this investigation suggested that the vacuum was preventing liquefaction by densifying the sample (see Chapter 4). It would appear that the vacuum only has this effect on materials which are very susceptible to liquefaction and are in very loose states. Materials which are less susceptible to liquefaction are not affected by the vacuum, and can be liquefied in the controlled-load test. Materials in the second category seem to have more rigid initial structures, possibly due to differences in particle shape. Earlier tests on Peckfield (see next section) using the vacuum produced similar results to tests not using the vacuum, again suggesting that it is only very sensitive materials which are significantly affected. Another factor involved is the subtlety of technique involved in sample preparation, involving such points as the rate and amount of vacuum applied. It is possible that previous investigators have had better control of these factors than the present writer, enabling them to produce liquefactions despite the use of a vacuum.

9.2 Peckfield Slurry.

For clarity the results of only a limited number of the Peckfield tests are shown here. The results of the earlier tests tend to confirm the conclusions drawn from the results shown here. Due to the smaller

size of the sample, the volume changes involved were considerably

smaller than those for the coarse discard. For this reason it was

not readily feasible to take readings to produce consolidation curves,

and hence estimates of c_v and pore pressure dissipation characteristics

cannot be made.

9.2.1 The Made-up Samples

Four made-up samples are illustrated in Figures 7.1 and 7.2, the

fourth (No. 18) being carried out as a check after saturation difficulties

had been experienced in the previous samples due to the use of an

unnecessary porous disc in the revised apparatus. Three nominal consolidation

pressures, 50, 100 and 200 kN/m^2 were used. The amount of material used

was such as to produce approximately the same dry density as the in situ

samples, as estimated from previous measurements. The actual densities

produced (Table 7.1) were slightly lower than those of in situ samples.

The first three tests showed some undersaturation effect, when the

pore pressure failed to follow the increasing cell pressure during the

final straining period. However, the final test showed that the general

pattern of behaviour in a fully saturated sample was the same, with a

slightly larger overall pore pressure increase.

The general behaviour was the same in all the tests. There was an

initial build up in pore pressure to a constant value some way below the

cell pressure (in test no. 18 the pore pressure was nearer to the cell

pressure, Fig. 71). In all cases the straining period was quite long

in terms of liquefaction failures and considerable strains were reached.

The load taken increased with consolidation pressure as would be expected.

The pore pressure remained constant or rose slightly during straining

until it climbed sharply and then fell rapidly as a result of cell pressure

changes caused when the sample collapses and hits the side of the cell.

The stress paths and stress-strain curves (Figs 7.1 and 7.2) show that for these tests there is some loss of strength, suggesting some degree of liquefaction. The limited loss in strength and the relatively long straining periods suggest that these are partial liquefactions, although no final gain in strength occurs. This could be due to the fact that it is not possible to add loads to the sample in the later stages of straining when it could be regaining strength; this was also noted for the dilations and partial liquefactions of Abernant samples. The results of Test No. 18 show a lower stress although the form of the curves is the same. The slight loss in strength is common to all the four samples.

The results of these tests suggest at least some susceptibility to liquefaction, and an estimated K_f line drawn from these stress paths has a slope of 17° with some cohesion (20 kN/m^2). The equivalent value of $\emptyset'$ is about 18°, which is a very low friction angle. The results of TestNo. 18 suggest a smaller cohesion and/or an increased friction angle. As noted for the Gedling coarse material lack of saturation produces reduced friction angles, and this could partly account for the low value. Even so, the results suggest a relatively weak material.

The failure of these samples was by a gradual barrelling which is more characteristic of a plastic failure.

9.2.2   The In Situ Samples

Three in situ test results are shown here (Figs 7.1 and 7.2). They are from three tubes taken from the same horizon of the same 'U100', and were tested at nominal consolidation pressures of 50, 100 and 200 kN/m^2 for comparison with the made-up samples.

The volume change and finally density of Sample no. 17 seems unlikely as the settlement one would expect for such a volume change did not occur. This type of behaviour is a characteristic of a leak in either the sheath or a line. However, in this case the excessive volume change terminated and the test was completed conventionally, possibly due to some particle blocking whatever was causing the leak. The final values of density, voids ratio and relative compaction are probably nearer to those of the other samples than the values shown.

The behaviour of these three samples was noticeably different from the equivalent three made up samples. Although there was some pore pressure build up, this was less than in the other tests and reached a value further below the cell pressure. The pore pressure also decreased near the end of the tests, the amount of decrease being greater at higher confining pressures. The load carried was much greater than the equivalent made-up sample. In fact, as can be seen from the stress-strain curves (Fig. 7.2) the final loads reached in all three tests were greater than any of those in the other four. The straining was much slower in all the tests (see Table 7.1), until the end when all the samples failed suddenly in shear, showing another major difference in behaviour from the made up samples.

The stress paths and stress-strain curves (Figs 7.1 and 7.2) emphasise the difference in behaviour. There is no drop in strength until the shear failure at the end and the trend is one of continual increase in strength. This shows a strong dilatant tendency. The estimated K_f line again shows a cohesion of about 20 kN/m^2, but also has a slope

of 25.5°, equivalent to a $\emptyset'$ of 28.5°, which is a much more reasonable value and shows a much higher shear strength for the _in situ_ samples.

9.2.3   Reasons for the Differences

Observations made before the test might lead one to the conclusion that the made up sample would have a higher strength.   The sample produced by compaction in the Denison machine appears to be rigid and gives the impression of stability.   The sample extracted from the U100 appears considerably less stable and is in fact much softer, due to its higher moisture content.   The made up sample is considerably easier to handle and set up.

The results of the tests show that these observations are completely erroneous.   Although overall the _in situ_ samples have a higher average density, this is unlikely to account for such a marked difference in behaviour.   The probable reason behind the difference in the behaviour of the two sets of samples is the different soil structures produced by the processes of deposition in the field and the compaction of a sample in a mould in the laboratory.   The former is more likely to produce a preferred orientation structural mode, whereas the latter is more likely to produce a random orientation.   It has already been shown by Seed (1977) that such differing structures can exist at the same density and void ratio.   The process   of pumping a slurry into a lagoon and allowing it to settle out is likely to produce some kind of preferred orientation.   Associated with this is the stratification which occurs in lagoon sediments.   Even in small triaxial samples a certain degree of layering or zoning can be seen, these being due to differences in materials deposited due to variations in washery processes and a certain amount of differential settlement.   These layers of similar materials and

particle sizes produce additional stability. In a remoulded sample the different materials are completed mixed and randomly distributed, and so this effect is lost. These seem to be the most likely specific factors affecting lagoon sediments out of Seed's (see section 1.4.3) list of possible reasons.

9.2.4 Conclusions

From these results it can be concluded that a made up (fabricated) sample will have a greater susceptibility to liquefaction, and hence will give a conservative result. However, the large discrepancies between the results are such that unnecessary alarm may be caused, and hence whenever possible in situ samples should be tested to give a more accurate guide to actual field behaviour.

9.3 Abernant Fine Discard

Because of the field conditions described in Chapter 2 all the tests were carried out on made up samples, and the results should be viewed with regard to the conclusions of the previous Section.

Tests 2 to 10, 14 and 15, were carried out at approximately the same density while tests 11, 12, 13 and 16 were carried out at increasing consolidation pressures (see Figs 7.3 and 7.4).

9.3.1 Behaviour during the tests

In test No. 3 at a consolidation pressure of 58 kN/m^2, there was a steady initial build up in pore pressure, the rate of which increased before failure. The sample collapsed rapidly at a relatively small load and the overall build up in pore pressure was quite large. As the consolidation pressure was increased the basic pattern of behaviour was the same. The rate of pore pressure build up became less and the overall amount was smaller. The load also increased with consolidation pressure and the rate of straining decreased, although it was still quite rapid

compared with Peckfield slurry or any of the coarse materials.   In test

No. 9 at 272 kN/m^2 there was some decrease in pore pressure in the later

stages of the test.   In test No. 14 the pore pressure again decreased

in the later stages and the straining period was much longer, being of

the same order as for other materials.   The foregoing observations refer

to the tests in which the density was approximately constant.

In the tests with increasing density at a nominal consolidation pressure

of 100 kN/m^2, densities well in excess of the maximum dry density obtained

from the compaction tests were obtained.   The effect of increasing the

density was similar to that of increasing the consolidation pressure.

The amount and rate of pore pressure build up were smaller and there was

some decrease in pore pressure at the end of the tests.   The load carried

increased with increasing density and except for Test No. 12 the rate of

strain was much slower.

In the samples which underwent rapid collapse, bulging occurred which

led to strains of up to 40 or 50 per cent.   The other tests produced

characteristic plastic failures.

9.3.2   Stress Paths and Stress-Strain Curves (Figs 7.3 to 7.6)

In Figs 7.3 and 7.4 the K_f drawn was obtained from a set of ordinary

controlled-strain triaxial tests and has a slope of $\propto = 23.5^{\circ}$ ($\emptyset' = 26^{\circ}$).

This is less than the Peckfield in situ samples but greater than the

Peckfield remoulded samples, although as mentioned previously the low

value could be due to lack of saturation.   It should also be noted that

the K_f lines drawn for Peckfield were estimates from the stress paths.

The Abernant stress paths in Fig. 7.3 (the constant density tests) fit

reasonably well with this K_f line.   Those in Fig. 7.4 go well above

the K_f line, showing that in a fine discard the increase in density has a greater effect on shear strength characteristics than it has in a coarse discard.

The stress paths for Tests 2, 3, 4, 6, 10 (Fig.7.3.) show some movement to the left, reaching a peak stress, followed by a considerable fall off. The stress-strain curves also show this peak followed by fall-off. Shown on the stress-strain curves are the times from peak stress to the end of the test and the percentage fall off in stress. These show that the failure is rapid and the loss in strength considerable. These facts and the amount of pore pressure build up noted during the tests suggest complete liquefaction failures.

The stress path for test no. 7 shows some gain in strength after the initial fall, suggesting a partial liquefaction failure. The stress-strain curve shows a considerable loss in strength in the later stages and a fairly rapid collapse, both of which suggest total liquefaction. These observations suggest that this particular sample lies close to the borderline between liquefaction and partial liquefaction at this density.

The stress paths for Test 9 and 14 show increases in strength after the initial loss, and the stress strain curves show slower rates of strain and in the case of No. 14 a much smaller percentage strength loss. Test No. 9 shows a levelling off in stress level at the end of the stress-strain curve. In both these tests there was a smaller degree of pore pressure build up with some fall off at the end of the test. These characteristics indicate partial liquefaction failures for these specimens. These results produce a 'cut-off' between liquefaction and partial liquefaction at consolidation pressures in the region of 220 kN/m^2 to 240 kN/m^2 for samples with densities of the same order as those used here.

Fig. 7.4 shows the results of the tests at higher densities. All these tests show typical dilatant failures with the stress paths moving up and to the right after small initial movements to the left, and they contrast well with the stress path for test No. 2, also shown on this Figure. The stress-strain curves show the longer time periods involved in these tests and the much higher stress levels attained. The drop in stress indicated at the end of the test is due to the fact that load cannot be added to the straining sample quickly enough to produce stresses equivalent to its increased strength. The same point was shown by the Peckfield tests.

These tests indicate that the cut-off in terms of density lies somewhere around a relative compaction of 100 per cent, since the tests at 102 per cent show dilation, but with fairly rapid straining.

The stress paths show a number of samples starting at $\bar{p}$ values well below the nominal consolidation pressure from which they should start. This is partly due to inaccuracies in setting the consolidation pressure and also the early termination of the consolidation leading to the build up of pore pressure before loading commences.

9.3.3 The E_f Line

As an indication of the behaviour of Abernant fine discard with respect to liquefaction an E_f line was plotted as described by Casagrande (see Section 1.4.1). This is a plot of voids ratio against the logarithm of the effective minor principal stress. Two points are plotted for the tests in which liquefaction occurred; the first represents the peak condition and the second the point of failure. In plotting these points failure was defined as the point at which the pore and cell pressure traces on the ultra-violet chart crossed.

The points were run through a linear regression programme, which gave slopes of about 62° (on the scales used) for both the E_f and E_p lines. Thus the E_p line lies parallel and slightly above the E_f line. The accuracy of the lines plotted is probably no better than $\pm 5^{o}$, since the points are very sensitive to the third decimal place of the void ratio, which is difficult to determine with certainty. Also a greater number of tests would have to be carried out to produce a more certain line as there is a good deal of scatter on the points used.

The arrows plotted on this graph show the movement in the state of stress during the test. The starting point is the original consolidation pressure. It can be seen that in general samples lying originally above the E_f line undergo liquefaction moving to a position close to the line and that points lying below the line undergo dilation. This is as would be expected from Casagrande's findings.

The points from the Peckfield tests are also shown on this graph. Only a point equivalent to peak stress is shown, as it was not possible to obtain a failure point on the same basis as used for Abernant, since the two traces only crossed at very high strains. This was due to the slower straining rates involved. A rough estimate of the E_p line for Peckfield from these points would appear to have a similar (or slightly steeper) slope to the Abernant line, but to lie somewhat above it, showing less susceptibility to liquefaction. Also from these lines it can be seen that the Peckfield samples had higher void ratios than those from Abernant. This again shows less susceptibility to liquefaction.

9.3.4   Effects of Liquefaction

In order to assess the potential danger of liquefaction of the lagoon sediment a one dimensional consolidation test was carried out as described in B.S. 1377 (1975).

The material was initially moulded into the ring at a moisture content equivalent to the liquid limit.   The results of the test enabled a plot of void ratio against depth of sediment to be made using the effective pressure/void ratio plot produced from the test. The range of loads chosen was such as to cover the consolidation pressures used in the controlled load tests.   The two curves are shown in Figs. 7.8 and 7.9.

The depth of sediment versus void ratio plot is shown on both a total and an effective stress basis.   The first case represents a condition with a low water table and the second case represents the saturated condition of high water table.   The latter is more likely to be the case at Abernant.

The depths of sediment were calculated using the relationships between pressure and depth of sediment in the lagoon.

$P = gh \, (\rho_{sat} - \rho_w)$ for effective stress condition

$P = gh \, \rho_{sat}$ for total stress condition

P = pressure

h = height

ρ_{sat} = saturated mass density = $(\dfrac{G_s + e}{1 + e})$

G_s = specific gravity

e = void ratio

ρ_w = density of water.

For the density used in these tests the 'cut-off' for liquefaction was around 240 kN/m^2, which from Figs 7.8 and 7.9 represents a depth of sediment of 25m on an effective stress basis and 12.5m on a total stress basis. Both results indicate a considerable danger from liquefaction in terms of the likely depths of sediment concerned.

9.3.5 Conclusions

As indicated in the previous section the results imply that this lagoon sediment exhibits a considerable danger from liquefaction. However, since all these tests were carried out on made up samples, it is likely that the true susceptibility to liquefaction may be less than that indicated here. However, it would still appear that there is a risk of liquefaction occurring since the degree of liquefaction is greater than that exhibited by remoulded samples from Peckfield.

The results with respect to higher densities show the importance of compaction (consolidation) of sediments in the reduction of liquefaction potential.

9.4 Factors affecting behaviour

The factors which dominate the behaviour of fine discards in controlled-load tests are likely to be different from those dominating the behaviour of coarse discards. For instance the strength of the individual particles seems less likely to be of importance than the overall grading or the shape of individual particles. These latter factors are therefore discussed in this section.

9.4.1 Grading

As was mentioned in section 8.10.2 criteria for liquefaction involving grading have been put forward in the past. Although these are probably not applicable to coarse discards they could have a much greater

bearing on the behaviour of fine discards, since they were postulated as a result of work carried out on fine grained materials.

It has generally been shown that uniformly graded materials have a greater susceptibility to liquefaction. The grading curves for Peckfield and Abernant discards in Fig. 2.9 show that Abernant discard does have a more uniform grading, with a steeper curve and much less fine material.

A criterion for liquefaction given by Terzaghi and Peck (1948) was in terms of the sorting factor D_{60}/D_{10} where D_{60} is the diameter equivalent to 60 per cent passing and D_{10} is the diameter equivalent to 10 per cent passing. They postulated that materials for which $D_{60}/D_{10} < 5$ would be susceptible to liquefaction.

For Peckfield discard:

D_{60} = 0.32mm and D_{10} = 0.002mm

$$\frac{D_{60}}{D_{10}} = 160$$

For Abernant discard:

D_{60} = 0.43mm and D_{10} = 0.048mm

$$\frac{D_{60}}{D_{10}} = 8.96$$

They also give $D_{10} < 0.1$mm as a condition for liquefaction susceptibility, this condition is met by both these materials.

This shows very well the great difference in uniformity between the two materials. Although the Abernant discard does not fall within the range given by Terzaghi and Peck, it is quite close, and the results imply that the greater uniformity of the Abernant sediment is one reason for its greater susceptibility to liquefaction.

9.4.2 Shape

The shape of the particles is shown on the photographs of slides made of the materials (Figs 2.18 & 2.19). It is difficult to make any definite statements about differences between the particles of these two materials, since these slides show them to be very similar in appearance. In both materials there is a mixture of relatively uniform particles and long thin particles, the more uniform particles generally being smaller. There seems to be more fine grained material in the Peckfield sample (as is shown by the grading curve). If anything the Peckfield material is slightly more angular. From the feel of the materials that from Peckfield is possibly slightly less platey than the Abernant material, which is similar to the coarse discard in this respect. However, there is not a great deal to choose between the two materials in either of the aspects mentioned above and it would be wrong to make any definite statements concerning the effect of these differences on the behaviour of the two materials.

9.4.3 Plasticity

Another factor which could have some bearing on the liquefaction potential of a material is the plasticity. An indication of the plasticity is given by the plasticity index. A material with a low plasticity index is less likely to behave plastically than a material with a higher plasticity index, and consequently should have a greater susceptibility to liquefaction.

However, it can be seen from Table 2.1 that both the materials under consideration here have very similar, and low, plasticity indices, and so it would appear that plasticity is not a major contributory factor in this case.

9.4.4   Chemistry and Mineralogy.

The chemistry and mineralogy of the two fine discards does not

seem notably different.   The Peckfield slurry has slightly higher

kaolinite and quartz contents, but the combined silica to alumina ratio

is the same.   There is a small amount of dolomite or ankerite in the

Peckfield slurry but this is not likely to have a significant effect

on the behaviour.   There does not appear to be anything in the chemistry

or mineralogy to suggest widely differing modes of behaviour.

One of the most important aspects of the chemistry and mineralogy

for the coarse discards was the difference in organic carbon content.

The results for the fine discards (Table 2.1) show that both these discards

had relatively low organic carbon contents.   The Peckfield slurry does

have a higher carbon content which could in part account for its higher

strength.   The higher specific gravity of the Abernant discard with its

lower carbon content confirms the results of Lawrence (1972) that the

specific gravity is inversely proporitional to organic carbon.

9.5   Links with Coarse Discard.

The expected correlation between coarse and fine discards from the

same colliery was not shown.   The coarse Abernant material showed strong

dilatant behaviour while the fine discard showed considerable susceptibility

to liquefaction.   This was in spite of the fact that the two materials

showed the chemical and mineralogical similarities that would be expected

from materials from the same colliery.

The reason for the difference in behaviour of the kind noticed is

the strong probability that different properties are significant in the

different size ranges involved.   For the coarse discard particle and

material strength and stability in water seem the most important properties, while for the fine discard the grading and possibly the shape of the material are the most important.

This shows that it is not possible to correlate the behaviour of the two different types of discard from the same colliery, and that they should be treated separately.

9.6 Conclusions

The main conclusion concerning the investigation of Peckfield slurry is that there are significant differences in behaviour between _in situ_ and remoulded samples. The latter generally give conservative results in terms of liquefaction susceptibility and material strength. From the results of the _in situ_ tests the Peckfield material tested has a low susceptibility to liquefaction in a static controlled-load situation.

The results from the Abernant tests show that this material has a considerably greater susceptibility, although the degree may well have been overemphasised by the enforced use of remoulded samples.

The main factor which appears to cause the differences in behaviour between the two materials is the uniformity of grading, the Abernant material having a considerably more uniform sorting. Other factors such as particle shape, plasticity and mineralogy do not seem to be major influences in this case.

There does not appear to be any correlation between coarse and fine discards from the same colliery, the important influences being different for the two different size ranges.

CHAPTER TEN

CONCLUSIONS

The controlled load tests on the coarse discards showed that the seatearth-rich material from Gedling has a certain susceptibility to liquefaction at low consolidation pressures. The implications of such a partial liquefaction in a tip built on a slope could be just as serious as a total liquefaction. This is because it seems unlikely that a dilation occurring at the end of an episode of partial liquefaction would arrest a flowslide. Also the effect of a downhill gradient is to reduce the amount of pore pressure increase necessary to induce a flowslide. The tests on the material from Abernant showed that this shale-rich discard is not susceptible to liquefaction, a dilatant response being obtained at all consolidation pressures used.

Tests carried out on a seatearth and shale from County Durham, showed that the difference in behaviour between the two discards was not necessarily due to the contrast between a seatearth-rich discard and a shale-rich discard, as might have been expected. Both the County Durham materials behaved in a similar fashion to the Gedling material at low consolidation pressures. In fact, the shale showed a more definite partial liquefaction response than the Gedling material.

A comparison of properties was made for the four materials which had been tested. This indicated that the main reasons for the differences in behaviour noted, were material and particle strength, stability in water and the ability for pore pressure equalization within the specimen. The Abernant discard was shown to be stronger than the other three and to be more stable in water. It also had a higher c_v value, indicating

a greater ability to equalize pore pressures. A major reason for the greater material strength and stability is the higher organic carbon (coal) content of this material. Properties such as shape and grading do not seem to be very important influences on the behaviour of these materials.

Tests carried out on mixtures of Abernant discard and the Durham seatearth show that a transition between the behaviours of the two end materials occurs for mixtures containing between 20 and 25 per cent seatearth, the exact value depending upon the density of the specimen.

The controlled load tests on the fine discard from Peckfield Colliery showed that there were significant differences in behaviour between samples fabricated in the laboratory and those obtained from the field. The former showed some tendency to partial liquefaction, whereas the latter showed strong dilatant behaviour. The main reason for these differences is believed to be variations in structure between material deposited in the lagoon and that remoulded in the laboratory.

The tests on fine discard from Abernant showed that this material has a high susceptibility to liquefaction, and even though this may be partly due to the use of remoulded samples, the susceptibility seemed considerably greater than that of the remoulded Peckfield samples. At relative compactions of between 90 and 95 per cent liquefaction occurred up to consolidation pressures of 240 kN/m^2, which represents a depth of sediment of 25m on an effective stress basis. This shows a very real danger from liquefaction under shock loading conditions. Relative compactions of over 100 per cent appear to reduce liquefaction potential and shows the importance of consolidation of lagoon sediments or the

necessity for a high compactive effort if these materials are used for construction purposes. The results of these tests show that it is not feasible to predict the behaviour of fine discards from the same colliery on the basis of coarse discard response under controlled load triaxial testing.

The most significant difference between the two fine materials, which appears to influence behaviour, is the particle size distribution as represented by the sorting coefficient (D_{60}/D_{10}). The Abernant discard has a value of about 9, representing a reasonably-well graded material, while Peckfield discard has a value of about 160 showing this to be quite the opposite. This appears to be the only significant difference between these two types, since their shape, plasticity and mineralogy are very similar.

The tests on the fine discards raised the question of using a vacuum in setting up fine-grained materials for controlled load testing, because of possible densification effects. This led to the development of an alternative method which has been used subsequently.

A behaviour difference noted between the coarse and fine discards was the effect of density on the effective K_f line. The coarse discards fitted a common K_f line, despite density variations. McKechnie Thomson and Rodin (1972) had noted that there was little variation in peak effective shear strength with density for coarse discards. In the case of fine discards however, the current work shows that there are significant variations in the K_f lines obtained at differing densities.

APPENDIX I

CALIBRATION OF INSTRUMENTATION
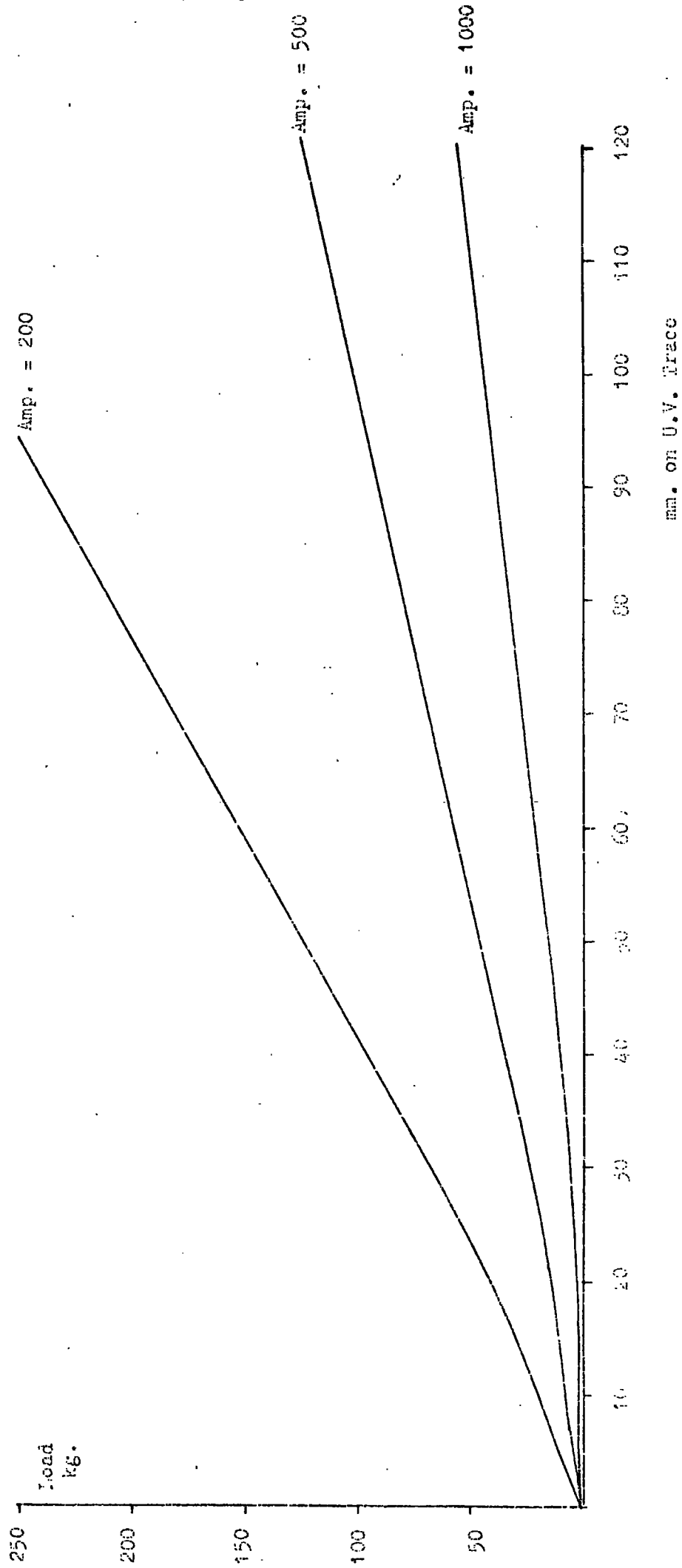
Figure A.1   Calibration of Transducers Load Cell No. 4438 used on the Large Controlled-Load Rig.

Fig. A5.1 Calibration of transducers used in the Large Consolidation Load Cell.
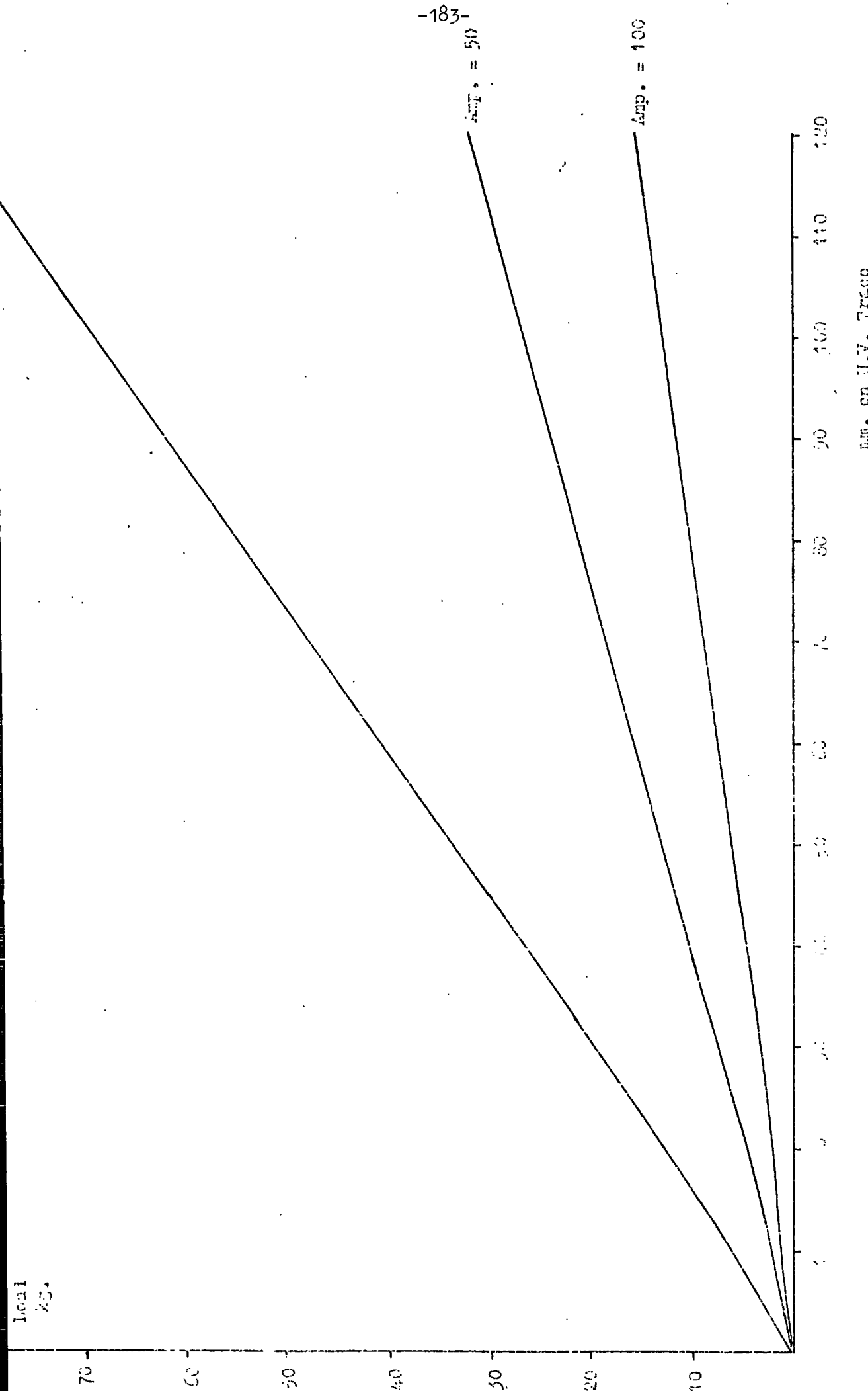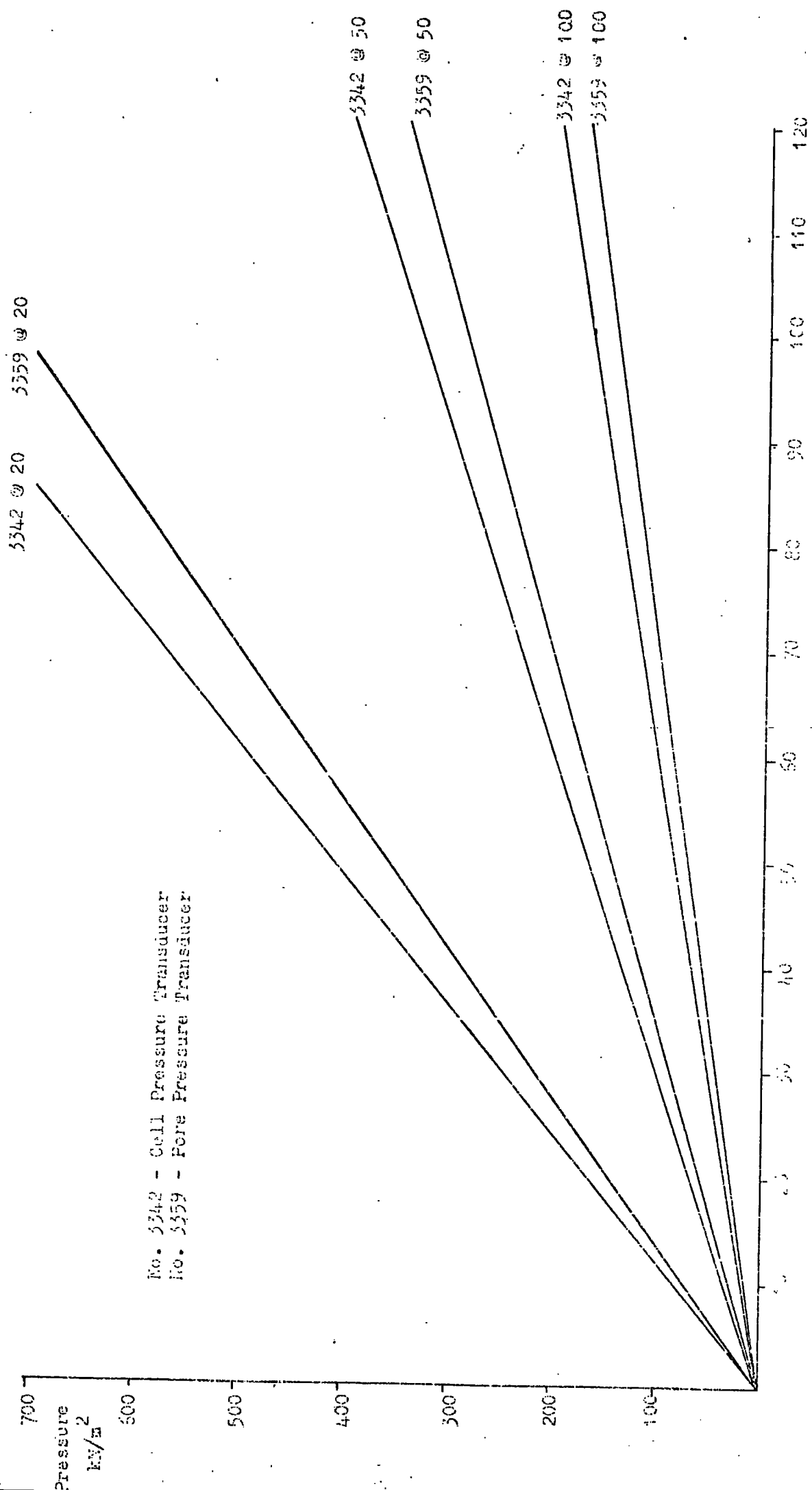
No. 3342 - Cell Pressure Transducer
No. 3359 - Pore Pressure Transducer

Calibration of Transducers No. 4202 and No. 3346 connected to Load rig.
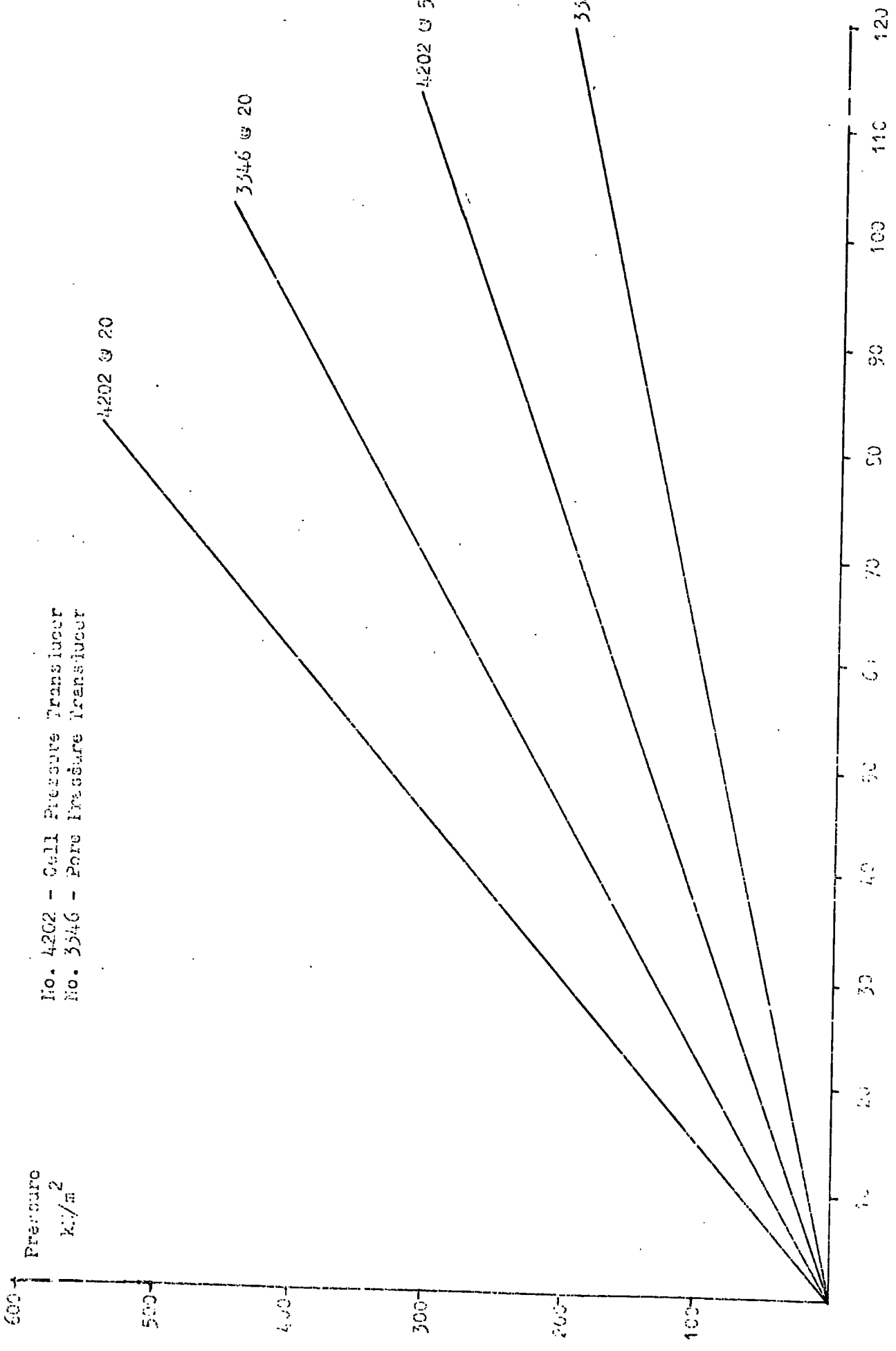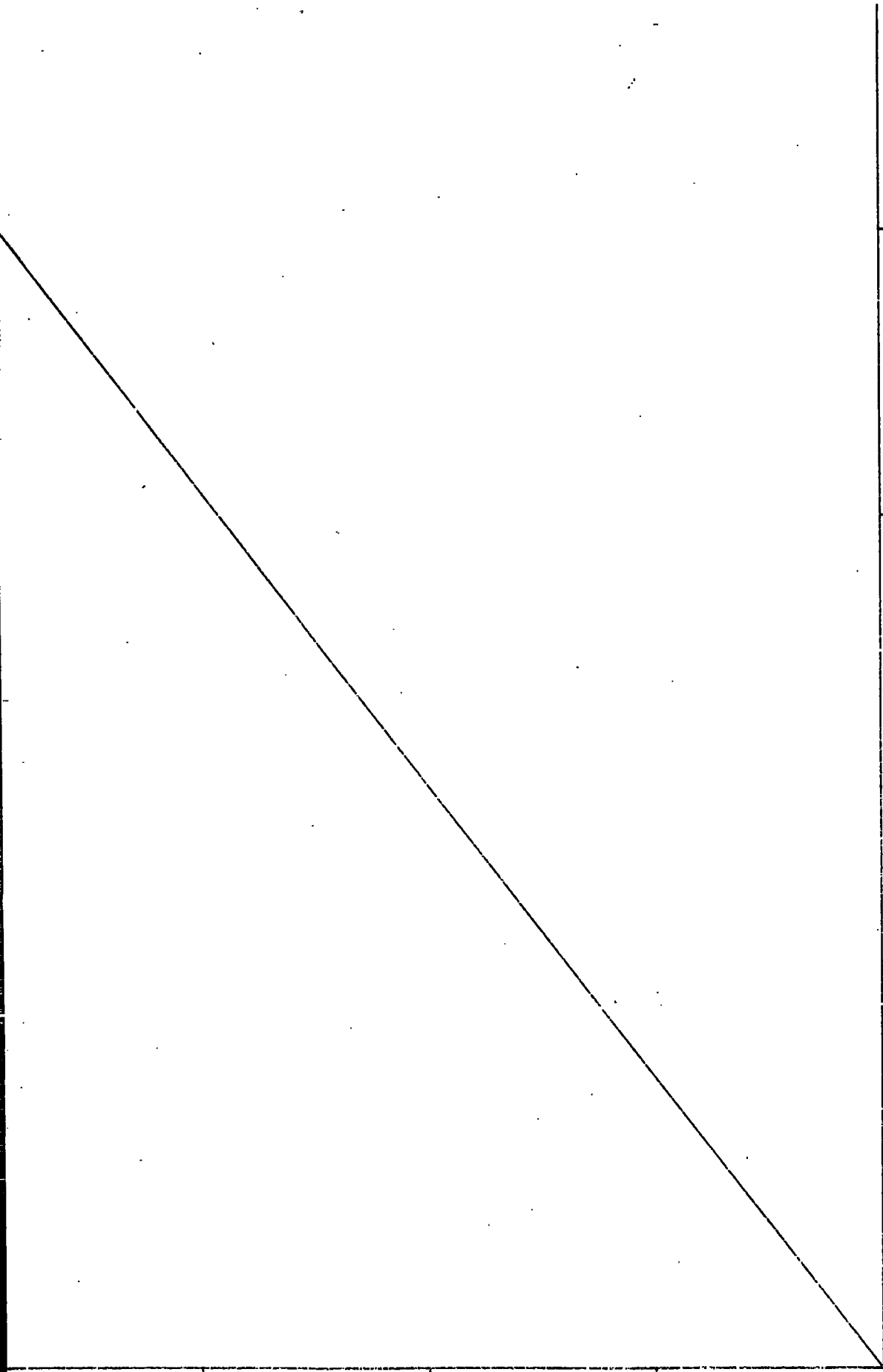
Figure A.3 Calibration of Saunders L.V.D.T. No. 1004 (with in-line resistance of 150Ω).

Linear
Strain
mm.

APPENDIX II

RESULTS OF CONTROLLED STRAIN TESTS

Gedling Sample CS1

$\bar{p}$	q	%strain
103.37	0	0
105.83	6.92	0.17
106.07	8.99	0.23
105.69	10.71	0.29
104.63	11.74	0.35
105.12	13.81	0.40
104.39	15.18	0.46
103.58	16.20	0.52
102.51	17.23	0.58
101.70	18.25	0.63
100.88	19.27	0.69
99.99	19.95	0.75
98.93	20.63	0.81
97.67	21.30	0.87
94.62	22.98	1.04
90.93	25.32	1.27
88.97	25.97	1.38
86.19	26.61	1.56
78.76	27.83	2.08
71.07	28.00	2.65
66.81	28.20	3.12
62.73	28.05	3.63
59.43	27.90	4.15
56.61	27.71	4.82
55.18	27.58	5.25
53.73	27.45	5.71
52.22	27.25	6.40
50.64	26.98	7.33
49.92	27.31	8.37
49.42	27.33	9.35
48.63	27.33	10.39
48.63	27.59	11.54
48.08	27.30	12.46

Gedling Sample CS2

$\bar{p}$	q	%strain
196.29	0	0
190.00	2.10	0.17
187.46	3.50	0.35
183.25	5.57	0.69
186.80	11.49	0.75
188.61	16.70	0.81
189.12	18.78	0.84
189.54	20.51	0.87
189.43	22.25	0.90
188.72	23.63	0.92
187.92	24.66	0.95
187.99	26.57	0.98
187.36	27.77	1.01
187.08	28.81	1.04
186.28	29.84	1.07
185.82	31.22	1.10
184.93	31.90	1.13
184.22	32.76	1.15
183.22	34.65	1.21
181.44	36.01	1.27
179.57	37.03	1.33
178.05	38.39	1.39
176.18	39.41	1.44
174.65	40.76	1.50
172.78	41.78	1.56
170.82	42.44	1.62
168.95	43.45	1.67
167.25	44.12	1.73
165.29	44.78	1.79
163.34	45.44	1.85
161.64	46.10	1.91
159.68	46.25	1.96
158.07	46.74	2.02
156.64	47.39	2.08
142.94	50.22	2.60
131.51	51.63	3.15
123.87	52.39	3.64
117.48	53.08	4.22
112.77	52.82	4.68
108.55	52.54	5.20
104.66	52.58	5.72
101.45	52.26	6.29
97.50	51.97	7.39
95.79	52.09	8.31
94.63	52.77	9.35
94.81	53.74	10.39
98.01	57.47	11.43
99.49	58.94	12.47

Gedling Sample CS2

$\bar{p}$	q	%strain
100.79	59.45	13.51
101.87	60.54	14.55
102.84	60.99	15.59
104.20	61.56	17.21
107.60	63.64	17.67
109.10	64.09	18.71
108.90	63.89	19.75
110.54	65.01	20.79
111.56	64.98	21.83
110.84	63.74	22.87
111.14	63.25	23.91

Gedling Sample CS3

$\bar{p}$	q	%strain
300.00	0	0
303.89	5.21	0.09
308.64	11.81	0.12
312.61	17.36	0.15
314.66	21.52	0.18
315.65	25.67	0.21
316.84	28.44	0.24
317.23	31.20	0.27
317.62	33.97	0.29
317.05	36.04	0.32
317.09	38.45	0.35
315.60	42.24	0.41
313.84	46.02	0.47
311.47	49.45	0.53
309.28	52.53	0.59
306.65	54.92	0.65
304.37	57.64	0.71
301.48	60.02	0.77
298.84	62.40	0.82
296.13	64.43	0.88
293.2	66.81	0.94
290.68	68.49	1.00
281.35	70.17	1.06
284.54	71.84	1.12
281.66	73.17	1.18
279.03	74.50	1.24
276.67	75.83	1.30
273.69	76.81	1.35
270.80	78.14	1.41
268.88	79.12	1.47
266.16	80.10	1.53
263.45	81.08	1.59
256.65	82.98	1.77
249.66	85.22	1.94

Gedling Sample CS3 cont..

$\bar{p}$	q	%strain
243.82	86.77	2.12
237.82	87.63	2.30
232.88	88.49	2.47
227.40	89.34	2.65
220.79	90.11	2.92
215.75	90.88	3.18
206.83	91.72	3.71
200.27	92.54	4.24
195.65	92.66	4.80
192.73	93.71	5.42
191.27	94.61	5.83
189.59	95.05	6.36
188.76	96.07	7.42
189.37	97.99	8.48
190.82	99.18	9.72
193.09	99.60	10.60
196.15	101.54	11.66
198.91	102.52	12.75
203.52	103.70	13.78
208.23	104.72	14.90
210.66	105.83	15.90
214.30	107.37	17.20
215.94	107.15	18.02
219.68	107.73	19.08
221.74	107.16	20.14
224.54	107.84	21.26
225.56	107.28	22.26

Abernant Sample CS1

$\bar{p}$	q	%strain
53.73	0	0
59.24	6.05	0.51
59.54	6.62	1.02
59.53	6.89	1.53
59.91	8.34	2.04
62.20	13.33	2.54
79.14	42.74	3.05
87.10	53.36	3.56
91.49	57.75	4.07
94.77	60.49	4.58
96.63	62.62	5.09
100.23	64.86	5.60
101.86	66.23	6.11
105.61	68.90	7.12
107.90	70.38	8.14
112.36	74.29	9.16
116.71	78.10	10.18
120.01	80.86	11.19
12 .98	81.67	12.21
127.60	84.95	13.23
130.80	87.34	14.25
134.58	90.04	15.26

Abernant Sample CS2

$\bar{p}$	q	%strain
51.26	0	0
53.57	8.40	0.50
51.92	22.08	1.01
51.30	29.39	1.51
50.96	32.49	2.01
52.35	34.67	2.51
53.66	36.25	3.02
54.94	37.51	3.52
55.60	38.19	4.02
56.82	39.14	4.53
57.73	39.79	5.03
57.81	39.86	5.53
58.43	40.22	6.03
59.64	40.91	7.04
60.58	41.58	8.05
61.21	41.94	9.05
62.36	42.83	10.06
62.69	43.16	11.06
61.67	42.94	12.07
60.39	42.71	13.08
60.68	42.47	14.08
60.44	42.23	15.09
60.75	41.23	16.09
60.23	41.23	17.10
58.67	40.73	18.10

Abernant Sample CS3

$\bar{p}$	q	%strain
150.73	0	0
150.44	1.83	0.51
149.49	2.73	1.01
141.68	46.47	1.52
124.91	56.14	2.02
117.06	59.14	2.53
113.55	60.91	3.03
112.69	62.37	3.54
111.39	63.51	4.04
110.32	63.76	4.55
110.20	64.44	5.05
109.50	64.53	5.56
109.20	64.76	6.06
109.14	65.49	7.08
108.76	65.90	8.09
108.46	65.88	9.10
107.08	65.28	10.11
105.82	64.82	11.12
105.49	64.49	12.13
104.75	63.74	13.14
103.74	63.00	14.15

Abernant Sample CS4				Abernant Sample CS5		
$\bar{p}$	q	%strain		$\bar{p}$	q	%strain
300.20	0	0		197.82	0	0
301.50	3.42	0.51		199.61	3.11	0.26
305.02	9.31	0.66		200.05	4.34	0.51
311.37	18.31	0.68		199.63	5.25	1.02
315.15	26.06	0.71		202.48	10.48	1.14
318.72	34.12	0.74		209.69	24.02	1.19
322.72	43.41	0.77		211.78	29.57	1.22
320.74	46.19	0.80		212.39	33.87	1.25
319.82	50.82	0.83		212.98	38.17	1.28
319.74	55.76	0.86		212.13	41.54	1.31
318.20	59.77	0.88		210.74	44.91	1.33
316.92	63.78	0.91		210.63	47.97	1.36
315.33	67.48	0.94		209.94	50.73	1.39
312.85	70.55	0.97		207.47	55.92	1.45
310.63	73.63	1.00		206.43	58.06	1.48
308.95	76.70	1.03		205.13	60.19	1.51
303.36	82.22	1.08		203.74	61.71	1.53
299.46	84.66	1.11		202.12	63.53	1.56
296.18	87.73	1.14		200.73	65.05	1.59
294.02	91.38	1.20		199.38	66.87	1.62
292.75	93.83	1.23		197.99	68.38	1.65
289.38	94.42	1.26		196.55	69.59	1.68
285.27	97.45	1.31		195.37	70.79	1.70
281.16	100.47	1.37		192.98	72.90	1.76
276.08	102.26	1.43		190.85	75.00	1.82
271.83	104.36	1.48		187.62	76.79	1.87
268.85	106.14	1.54		186.20	78.27	1.93
264.16	107.00	1.60		184.55	80.06	1.99
260.66	108.78	1.66		182.55	81.24	2.04
257.63	110.26	1.71		180.82	82.41	2.10
253.51	111.42	1.77		177.26	84.14	2.22
250.29	112.43	1.83		173.16	86.13	2.39
246.76	113.13	1.88		170.38	88.10	2.56
244.70	113.98	1.94		166.15	89.69	2.81
242.38	114.84	2.00		163.76	91.27	3.07
239.45	115.08	2.05		160.66	93.19	3.58
230.40	116.61	2.31		158.23	94.19	4.09
223.42	117.82	2.57		157.36	95.18	4.60
217.37	118.12	2.82		156.68	95.56	5.11
213.21	118.71	3.08		156.38	96.57	5.85
206.42	119.59	3.60		156.52	96.98	6.30
202.82	120.75	4.11		155.71	96.97	7.16
199.74	121.38	4.79		155.26	97.05	8.18
198.28	121.24	5.14		155.03	96.82	9.20
197.42	121.17	5.65		154.81	97.13	10.22
197.11	121.39	6.16		154.54	96.85	11.25
195.94	121.80	7.19		152.35	95.19	12.27
196.36	122.75	8.22		151.25	94.62	13.29
195.57	122.22	9.25		151.20	94.04	14.31
195.01	121.40	10.27		149.54	92.92	15.34
195.01	121.40	11.30		148.42	91.79	16.36
194.69	120.81	12.33		148.60	91.70	17.38
193.27	119.40	13.35				
191.06	117.45	14.38				

APPENDIX III

RESULTS OF CONTROLLED LOAD TESTS

ON COARSE MATERIALS

Gedling Sample No. 1

$\bar{p}$	q	%strain
53.33	0	0
50.01	3.62	0.33
49.09	8.53	0.44
49.50	12.00	0.66
39.13	15.52	0.89
35.71	17.10	1.99
34.63	17.96	3.10
32.32	18.43	4.21
31.66	18.88	5.32
30.94	19.27	6.65
32.75	19.42	7.65
34.17	20.28	8.53
31.98	20.59	9.75
32.63	20.96	10.86
33.27	21.32	11.97
33.86	21.64	13.18
33.94	21.72	14.19
33.90	21.68	15.40
34.49	22.27	16.63
34.50	22.55	17.73
35.14	23.19	18.62
36.75	23.41	19.84
36.73	23.39	20.96
36.65	23.31	22.05
37.71	23.27	23.16
41.79	23.18	24.27
41.33	23.55	24.94
42.61	23.72	25.15

Gedling Sample No. 2

$\bar{p}$	q	%strain
55.24	0	0
60.24	5.00	0.11
63.08	9.27	0.34
68.01	15.62	0.56
66.51	21.27	0.67
49.87	26.06	1.35
39.32	24.08	2.47
38.06	24.02	3.93
27.11	21.40	4.93
22.12	19.02	4.93
24.50	21.40	4.93
28.31	23.55	5.83
28.00	23.24	7.07
29.98	23.31	8.19
29.17	23.70	9.20
32.12	24.98	10.43
31.44	26.91	11.44
29.35	28.39	12.67
35.96	29.53	13.91
41.99	31.03	14.80
39.15	31.77	16.15
39.57	33.14	17.16
39.74	34.74	18.28
40.12	36.79	19.51

Gedling Sample No. 3

$\bar{p}$	q	%strain
82.38	0	0
82.56	3.63	1.10
84.29	3.69	1.10
77.42	5.52	1.33
79.42	7.28	1.54
81.25	9.11	1.65
77.83	10.93	1.77
79.80	12.77	1.77
78.17	14.60	1.77
74.98	16.41	1.88
74.36	17.46	1.88
71.80	18.23	1.99
68.43	18.19	2.21
67.80	19.23	2.21
63.75	20.29	2.43
60.13	21.67	2.65
53.78	23.78	3.09
49.77	24.65	3.75
51.68	24.78	4.75
40.75	25.51	6.07
39.34	25.53	7.19
37.47	25.21	8.39
38.69	26.07	9.05
38.86	26.00	10.60
38.01	26.70	11.48
38.88	27.34	12.70
39.17	27.38	13.69
39.51	27.61	15.01
37.78	27.54	16.12
38.33	27.86	17.2
38.57	28.10	18.32
40.27	28.01	19.43
40.52	28.26	20.42
41.01	28.75	21.64
40.89	28.75	2 .52
41.01	28.92	23.62
41.09	28.93	24.29

Gedling Sample No. 4

$\bar{p}$	q	%strain
114.28	0	0
113.14	2.18	0.11
113.30	4.02	0.55
112.75	5.13	0.66
113.02	8.73	0.89
113.34	12.38	1.10
113.89	14.61	1.10
113.82	17.87	1.21
109.68	20.40	1.33
107.95	23.67	1.33
104.16	26.55	1.55
91.19	28.93	2.10
81.97	31.50	2.99
75.81	31.875	3.98
72.61	32.03	4.65
71.47	32.18	5.31
69.75	31.88	6.20
69.64	31.67	6.86
69.92	31.82	7.30
69.80	31.59	7.97
70.01	31.80	8.41
70.28	31.95	8.85
68.79	32.00	9.73
67.26	32.14	10.18
67.42	32.29	10.73
67.57	32.45	11.29
67.82	32.58	11.73
67.96	32.72	12.28
67.96	32.72	13.05
68.47	33.23	13.39
68.68	33.36	13.94
68.85	33.48	14.49
68.65	33.18	15.27
68.76	33.28	15.71
68.66	33.19	16.37
66.95	33.14	16.93
66.70	33.01	17.92
66.85	33.155	18.36
66.71	33.02	18.70
64.80	32.93	19.58
64.72	32.93	20.36
66.21	32.75	20.80
64.05	32.38	21.68
64.20	32.53	22.68
64.40	32.86	23.23

Gedling Sample No. 5

$\bar{p}$	q	%strain
216.99	0	0
220.13	5.44	0
227.12	12.43	0
233.68	18.99	0.25
238.33	23.64	0.25
237.98	27.96	0.25
240.72	32.94	0.25
241.13	35.65	0.25
242.68	37.20	0.25
246.55	41.07	0.25
245.07	46.50	0.25
247.41	51.15	0.25
252.10	60.45	0.25
250.17	67.72	0.38
245.56	67.72	0.38
246.76	73.53	0.38
249.79	81.16	0.51
249.82	85.80	0.51

Gedling Sample No. 6

$\bar{p}$	q	%strain
251.89	0	0
258.27	6.38	0.12
265.54	13.65	0.24
271.89	20.00	0.37
277.31	25.42	0.49
283.67	31.77	0.49
289.97	38.08	0.61
294.46	42.56	0.73
297.12	45.22	0.86
299.77	47.88	0.98
301.52	49.62	1.10
304.99	53.10	1.35
290.30	63.74	1.59
262.55	65.94	2.32
244.33	70.75	3.06
221.97	73.73	3.79
204.82	72.70	5.14
188.52	72.52	6.48
170.43	77.46	7.71
168.84	80.48	9.05
167.80	81.74	10.40
168.99	82.93	11.75
168.86	82.81	12.72
163.10	81.65	13.95
160.31	83.46	15.29
162.03	85.18	17.37
172.07	88.31	19.33

Gedling Sample No. 6 cont...

$\bar{p}$	q	%strain
183.11	87.83	20.43
181.58	86.30	21.17
182.66	82.78	21.78
189.32	84.83	22.51
189.91	85.43	23.25
190.62	86.14	23.86
195.96	90.96	24.47

Gedling Sample S.A.

$\bar{p}$	q	%strain
50.05	0	0
53.43	3.38	0.12
53.60	8.26	0.24
54.37	10.88	0.36
48.79	19.43	0.71
44.58	19.34	1.19
37.58	20.58	2.38
36.09	21.78	3.57
36.05	22.58	4.77
35.29	22.66	5.96
35.78	23.07	7.15
34.83	23.46	8.34
34.11	23.16	9.53
33.72	23.19	10.72
35.17	23.21	11.91
34.59	23.55	13.11
34.91	23.87	14.30
33.65	23.54	15.49
33.95	23.34	16.68
34.22	24.11	17.87
34.48	24.37	19.06
29.57	20.47	20.02
28.00	18.06	20.02
24.96	17.46	20.02

Gedling Sample D.O.

$\bar{p}$	q	%strain
51.48	0	0
54.18	5.98	0.48
53.32	9.33	0.60
48.75	12.66	0.84
44.27	15.59	1.19
41.97	16.98	1.67
39.98	18.70	2.39
36.00	18.83	3.58
33.79	19.31	4.77
32.48	19.77	5.97
34.73	20.92	7.16
33.15	22.03	8.36
33.79	22.08	9.55
33.91	22.12	10.74
34.37	22.49	11.94
34.80	22.84	13.13
33.14	22.53	14.32
36.32	22.84	15.52
33.55	23.77	16.71
34.22	23.43	17.91
34.49	23.70	19.10
34.14	23.35	20.29

Gedling Sample D.O.   cont..

$\bar{p}$	q	%strain
38.89	23.59	21.49
34.86	23.23	22.68
33.77	23.16	23.87
34.09	23.09	25.07
35.00	23.54	26.26
35.31	23.43	27.46
34.87	23.58	28.65
33.02	21.90	28.89

Abernant Sample No. 1

$\bar{p}$	q	%strain
234.49	0	0
236.93	2.44	0.38
237.88	5.69	0.50
239.63	9.75	0.63
240.03	17.06	0.63
241.89	23.52	0.76
242.28	30.82	0.76
244.29	39.75	0.76
240.44	40.51	0.88
239.89	44.56	0.88
237.71	46.99	0.88
239.08	59.87	1.01
226.44	67.96	1.01
206.84	80.60	1.39
197.05	86.94	1.51
181.50	89.81	1.89
171.17	95.61	2.52
169.97	101.32	3.15
162.01	100.27	4.16
165.74	104.00	5.05
163.59	104.15	6.31
150.02	102.89	7.44
159.65	102.51	8.45
158.80	101.67	9.21
158.10	100.96	9.84
158.12	100.98	10.47
157.55	100.42	10.98
156.84	99.70	11.61
156.41	99.28	11.98
155.56	98.42	12.74
151.70	96.86	13.50
150.29	95.45	14.13
141.74	86.90	14.26
146.30	93.77	14.38
151.97	99.44	15.52
151.07	98.54	16.27
150.04	97.51	17.16
149.14	96.61	17.91
145.74	93.21	18.54
149.34	96.81	19.43
149.77	97.24	20.69
142.71	90.18	21.19
141.99	89.46	21.82
141.55	89.02	22.20

Abernant Sample No. 2

$\bar{p}$	q	%strain
241.40	0	0
249.77	8.37	0.12
248.06	15.87	0.35
244.61	21.64	0.71
246.67	28.30	0.71
248.68	34.92	0.82
248.37	41.52	0.94
245.93	49.00	0.94
249.43	56.40	1.06
246.21	64.70	1.06
245.11	70.50	1.06
244.56	74.56	1.18
243.45	80.36	1.18
242.23	86.06	1.30
238.53	89.26	1.41
234.92	92.57	1.41
231.21	95.76	1.53
229.25	100.71	1.53
224.69	103.07	1.65
219.47	107.06	1.77
218.03	110.22	1.88
212.79	114.20	2.00
210.37	116.38	2.24
207.12	122.35	2.71
217.05	134.58	3.30
230.56	146.81	4.83
231.33	146.38	6.12
245.77	160.82	7.77
252.66	161.82	8.95
253.36	161.24	10.13
250.88	159.87	11.30
251.51	159.21	12.48
245.49	157.80	13.60
243.33	155.64	14.84
242.38	153.49	16.01
235.84	149.26	17.19
233.72	147.13	18.37
229.57	142.99	19.55
228.81	142.23	20.72
222.77	136.18	21.90
227.34	117.72	22.84
174.71	100.26	22.84
165.39	94.44	22.84

Abernant Sample No. 3

$\bar{p}$	q	%strain
195.92	0	0
204.24	8.33	0.25
210.23	16.61	0.49
211.59	24.89	0.62
210.63	33.14	0.74
200.44	41.38	0.86
190.17	49.53	1.11
177.48	57.57	1.48
169.33	65.55	1.85
160.85	73.19	2.59
150.93	79.39	3.94
155.61	86.28	5.18
171.36	93.75	6.41
173.21	95.60	7.64
174.21	96.61	8.87
175.91	98.31	10.11
178.26	100.66	11.34
179.78	102.18	12.57
181.22	103.62	13.80
182.58	104.97	15.04
183.85	106.24	16.27
187.61	108.81	17.50
188.43	111.94	18.73
191.80	112.91	19.97
192.36	115.78	21.20
193.23	116.56	22.43
192.74	115.98	23.67
188.56	114.10	24.90
182.08	112.23	26.13
177.90	110.36	27.30
176.03	108.49	28.60

Abernant Sample No. 4

$\bar{p}$	q	%strain
143.44	0	0
138.37	13.36	0.95
132.08	26.69	1.07
134.11	33.33	1.19
133.82	39.94	1.31
126.54	46.49	1.54
120.70	61.80	3.56
109.61	61.80	3.56
111.33	61.04	4.75
105.64	61.07	5.93
108.88	64.22	7.12
107.03	63.48	8.19
105.95	63.50	9.26
106.60	65.26	11.04
106.76	65.42	12.83
107.07	64.62	13.88
107.03	65.70	15.31
107.43	66.09	16.61
105.29	65.15	17.80
106.81	65.48	19.11
111.72	72.69	20.17
124.36	78.24	21.36
129.83	79.02	22.55
134.60	79.09	23.73
139.96	79.76	24.92
143.58	80.99	26.1
145.93	82.14	27.29
156.39	83.22	28.48
165.20	83.92	29.90
161.63	82.74	29.90
153.57	79.46	29.67

Abernant Sample No. 5			Abernant Sample No. 6		
$\bar{p}$	q	%strain	$\bar{p}$	q	%strain
101.46	0	0	101.46	0	0
102.70	8.15	0.24	105.06	8.21	0
106.23	16.28	0.36	113.23	16.39	0.24
109.73	24.40	0.48	102.95	24.52	0.47
110.91	32.49	0.60	100.27	31.06	0.47
114.38	40.56	0.72	96.07	38.37	0.59
111.60	47.00	0.84	93.86	40.77	0.71
107.06	49.37	0.96	92.41	43.93	0.95
105.63	52.54	1.08	92.08	47.01	1.30
101.82	55.64	1.32	85.81	49.95	1.90
100.32	58.65	1.68	91.84	53.59	2.61
101.55	62.28	2.29	91.48	55.45	3.55
101.56	64.59	3.61	91.71	57.89	4.74
101.20	65.34	4.81	95.36	60.26	5.92
104.98	69.12	6.02	94.52	61.63	7.35
104.85	68.99	7.22	95.76	61.68	8.41
106.20	70.34	8.42	95.62	61.54	9.72
106.75	70.90	9.63	94.62	62.85	11.02
108.46	71.44	10.83	96.42	63.37	12.32
111.57	73.32	12.04	94.60	73.76	13.74
112.66	72.02	13.60	96.13	64.01	15.28
115.32	73.49	15.16	95.23	64.21	16.82
114.85	71.82	17.09	96.48	64.27	18.48
113.28	70.25	18.90	96.49	64.37	20.02
114.64	70.41	20.22	90.57	61.01	21.80
114.98	69.56	21.18	88.29	58.91	23.70
112.23	66.81	22.87	91.43	57.44	25.59
108.55	64.33	24.31	93.33	56.94	27.01
103.92	62.09	25.51	86.27	56.80	27.96
97.13	58.88	26.48	85.70	56.14	28.79
92.88	57.02	27.32	85.42	55.46	29.15

Abernant Sample No. 7

$\bar{p}$	q	%strain
52.78	0	0
56.94	9.72	0.12
60.17	12.94	0.24
61.55	16.18	0.24
62.13	18.60	0.24
62.68	21.01	0.36
64.03	24.21	0.47
65.28	28.24	0.47
65.66	31.40	0.71
66.48	34.53	0.95
67.20	37.57	1.42
67.68	39.53	2.49
68.76	41.45	3.56
70.93	43.15	4.98
71.80	44.02	6.40
70.71	44.79	7.94
70.39	45.39	9.72
69.61	44.61	11.26
67.54	44.54	12.80
69.45	44.45	14.34
68.18	43.77	15.65
67.23	43.16	16.83
66.22	42.61	17.90
65.32	42.16	18.73
63.97	41.74	19.56
63.05	39.90	20.62
62.98	39.37	21.69
64.57	40.96	23.47
64.86	40.32	24.65
62.71	39.56	26.08
61.86	38.71	26.55

Abernant Sample No. 8

$\bar{p}$	q	%strain
30.56	0	0
30.06	1.35	0.24
30.90	4.04	0.36
32.66	6.73	0.47
33.25	10.10	0.47
33.49	13.11	0.59
34.05	16.46	0.71
35.64	19.43	0.95
35.67	22.70	1.30
38.39	25.89	1.90
41.46	28.96	2.73
46.28	32.39	4.27
50.55	35.73	5.69
52.82	37.08	7.11
54.15	37.94	8.06
55.86	39.19	9.48
54.10	39.39	10.67
55.94	40.20	11.97
56.87	41.13	13.16
55.85	40.57	14.34
56.72	40.98	15.88
56.62	41.34	17.42
55.51	40.69	18.73
55.54	40.73	20.27
55.73	40.45	21.33
55.06	39.78	22.64
55.38	39.17	23.82
55.17	38.50	25.13
53.19	37.45	26.19
51.67	35.93	27.26
50.16	35.34	28.44

Abernant Sample No. 9

p̄	q	%strain
47.19	0	0
50.05	4.29	0.35
54.74	11.77	0.58
54.54	12.48	0.58
58.44	21.01	0.70
58.88	24.22	0.70
59.16	27.78	0.70
59.90	31.30	0.82
61.56	34.82	0.93
61.09	36.20	1.05
61.55	37.57	1.17
64.13	39.65	1.28
65.49	41.02	1.40
65.94	42.38	1.52
69.94	46.38	1.63
68.43	45.80	1.75
70.94	47.81	1.98
74.01	49.44	2.22
75.58	51.01	2.57
77.43	52.86	3.03
79.81	54.74	3.38
81.37	55.79	3.97
84.26	56.75	4.67
85.01	58.42	5.83
85.95	59.36	7.00
87.18	60.60	8.17
89.79	61.68	9.33
90.93	62.90	10.50
92.51	63.99	12.83
92.76	64.15	14.00
94.23	64.19	15.17
94.74	64.21	16.33
95.03	64.50	17.50
95.21	64.17	18.67
96.30	63.82	19.83
95.01	63.46	21.00
93.98	63.36	22.17
95.29	63.23	23.33
95.37	62.81	24.50
94.94	62.38	25.67
93.58	61.92	26.83
93.09	61.95	28.00

Abernant Sample No. 10

p̄	q	%strain
54.34	0	0
58.93	6.44	0.47
62.38	13.59	0.59
65.74	22.50	0.71
66.35	26.39	0.83
64.75	29.92	0.94
66.43	33.45	1.06
67.74	36.61	1.18
69.00	38.29	1.42
69.28	40.42	1.42
70.18	41.74	1.65
71.67	43.65	2.13
73.26	45.65	2.36
76.76	48.57	3.54
78.97	49.69	4.72
77.27	49.75	5.90
79.24	51.13	7.08
77.07	50.81	8.26
80.39	52.11	9.45
80.90	53.04	10.63
82.37	53.92	11.81
81.75	54.14	12.99
82.33	53.71	14.17
82.88	55.10	15.35
83.43	54.64	16.53
81.10	54.16	17.71
82.58	55.13	18.89
82.57	54.62	20.07
81.76	53.81	21.25
80.22	54.12	22.43
79.40	52.47	24.79
81.31	53.78	25.97
81.88	52.92	27.15
77.91	51.81	28.34
78.07	51.97	27.52
74.51	50.35	30.70

100% Seatearth No. 1				100% Seatearth No. 2		
$\bar{p}$	q	%strain		$\bar{p}$	q	%strain
51.48	0	0		50.05	0	0
52.99	2.44	0		54.37	8.02	0.40
55.72	6.09	0.13		54.51	11.45	0.53
52.79	10.14	0.26		54.61	15.24	0.66
51.58	12.12	0.64		49.09	18.97	1.06
47.85	14.45	1.28		45.03	23.15	2.65
49.82	16.25	2.56		42.85	23.57	3.97
44.95	16.42	3.84		40.16	25.43	5.29
44.51	17.75	5.11		39.77	25.79	6.61
42.34	18.27	6.39		38.05	25.43	7.94
42.00	18.77	7.67		36.46	26.11	9.26
39.79	19.25	8.95		37.20	26.76	10.58
36.83	18.98	10.23		34.96	26.36	11.90
35.22	18.71	11.51		34.80	26.63	13.23
37.88	19.86	12.79		34.82	26.22	14.55
37.17	19.57	14.06		33.39	25.81	15.87
37.38	19.28	15.34		33.12	26.05	17.19
34.82	18.65	16.62		33.33	26.26	18.52
33.35	18.70	17.90		32.60	26.45	19.84
33.56	18.40	19.18		34.74	26.31	21.16
32.86	17.79	20.46		31.73	26.15	22.48
31.97	17.82	21.74		34.73	26.30	23.81
32.10	17.53	23.01		32.28	26.12	25.12
33.04	17.55	24.29		33.74	27.08	26.45
32.31	18.16	25.57		34.36	27.71	27.77
34.23	18.14	26.85		33.31	26.65	29.10
31.69	17.54	28.13		33.38	27.23	30.42
30.23	16.25	28.64		32.87	26.71	31.74
				31.25	24.84	32.54

	100% Seatearth No. 3			50 AB/50SE No. 1	
$\bar{p}$	q	%strain	$\bar{p}$	q	%strain
48.62	0.00	0.00	60.06	0	0
51.16	9.10	0.25	61.91	1.85	0
48.28	13.62	0.49	62.27	2.21	0
48.16	15.77	1.23	65.55	11.04	0.24
38.30	21.13	2.47	64.82	15.44	0.36
30.80	20.86	3.70	59.57	19.44	0.66
31.81	23.13	4.93	53.80	23.34	1.19
28.40	22.83	6.16	51.14	25.22	2.38
28.44	24.64	7.40	46.88	24.91	3.57
30.60	25.70	8.63	45.82	24.60	4.76
28.41	25.70	9.86	45.17	24.29	5.95
28.06	25.68	11.09	45.72	24.67	7.14
28.62	26.66	12.33	44.99	25.71	8.34
30.06	27.93	13.56	44.57	26.04	9.53
29.05	28.19	14.79	46.31	26.69	10.72
29.97	28.09	16.02	47.10	27.31	11.91
28.11	27.99	17.26	47.68	28.22	13.10
31.17	29.12	18.49	48.60	28.47	14.29
33.36	29.29	19.72	50.55	29.32	15.48
31.06	28.84	20.96	52.15	29.83	16.67
30.78	28.98	22.19	53.73	30.31	17.86
33.35	29.11	23.42	51.80	31.07	19.05
29.45	28.07	24.65	55.25	31.49	20.24
31.96	28.73	25.89	57.67	31.89	21.43
31.49	28.26	27.12			
30.00	27.78	28.35			
29.52	27.30	29.58			
24.79	23.75	30.57			

50AB/50SE No. 2

$\bar{p}$	q	%strain
52.91	0	0
55.08	5.87	0.47
52.60	14.99	0.83
47.44	18.58	1.19
38.22	20.88	2.37
36.07	21.33	3.56
37.18	21.77	4.74
36.00	21.85	5.93
36.00	22.60	7.12
36.30	23.66	8.30
36.84	24.03	9.49
37.68	24.70	10.67
38.50	25.35	11.86
37.86	25.97	13.05
38.41	25.93	14.23
39.26	26.19	15.42
40.72	27.06	16.61
41.11	27.28	17.79
40.98	27.48	18.98
38.89	27.67	20.16
38.57	27.26	21.35
38.66	26.85	22.54
38.67	27.28	23.72
40.17	27.68	24.91
40.37	27.79	26.09
40.01	27.35	27.28
39.56	26.90	28.47
38.10	26.45	29.65
37.15	25.50	30.84

75 AB/25SE No. 1

$\bar{p}$	q	%strain
57.70	0	0
61.73	6.38	0.93
64.69	14.89	0.93
67.62	23.37	1.05
69.28	26.88	1.17
69.09	30.39	1.28
68.88	33.88	1.40
72.09	37.93	1.86
74.38	43.00	2.33
81.25	48.35	3.50
82.82	51.18	4.66
84.64	52.92	5.83
86.83	53.59	6.99
87.39	54.57	8.16
87.25	54.85	9.32
88.51	55.10	10.49
88.32	55.33	11.65
89.54	55.54	12.82
89.51	55.51	13.98
88.73	55.57	15.15
89.58	55.41	16.32
88.98	55.23	17.48
88.36	55.03	18.65
89.16	54.82	19.81
88.51	54.59	20.98
89.04	54.62	22.14
87.85	54.35	23.31
88.07	54.06	24.47
87.77	53.76	25.64
87.20	53.70	26.80
87.04	53.62	27.97
87.10	53.77	29.14
86.70	54.38	30.30

75 AB/25 SE No. 2

$\bar{p}$	q	%strain
55.77	0	0
58.80	8.73	0.23
61.64	15.12	0.35
61.77	22.65	0.47
61.39	25.97	0.58
61.90	29.25	0.82
60.68	31.65	1.17
60.07	34.57	2.34
59.71	34.97	3.50
60.94	36.95	4.67
60.24	36.50	5.84
60.32	36.83	7.01
59.88	37.14	8.17
61.26	37.43	9.34
61.03	38.46	10.51
63.94	40.19	11.68
63.58	39.66	12.84
63.24	40.58	14.01
59.70	40.74	15.18
64.73	40.89	16.35
64.75	40.32	17.52
65.72	41.12	18.68
64.96	41.20	19.85
65.20	41.27	21.02
64.76	40.66	22.19
63.95	40.69	23.35
65.99	40.71	24.52
65.14	40.70	25.69
64.28	40.68	26.86
65.01	41.24	28.02
64.69	41.17	29.19
63.43	41.08	30.36

80AB/20SE

$\bar{p}$	q	%strain
50.05	0	0
50.58	4.13	0.12
51.80	8.73	0.24
55.16	16.73	0.35
53.35	26.01	0.94
51.95	25.95	1.18
51.87	29.91	2.36
51.81	30.60	3.54
57.28	34.05	4.72
56.05	35.00	5.90
58.81	35.24	7.08
57.86	35.13	8.26
56.22	35.34	9.43
57.74	35.85	10.61
59.57	36.67	11.79
58.87	36.81	12.97
60.94	36.94	14.15
62.17	37.67	15.33
60.60	37.45	16.51
57.60	37.22	17.69
58.79	36.98	18.87
58.71	37.32	20.05
56.88	37.34	21.23
57.75	36.78	22.41
57.70	36.22	23.59
57.31	36.76	24.77
55.54	35.92	25.95
54.09	34.55	27.13
54.37	33.99	28.30
56.14	32.40	29.48

85AB/15SE

$\bar{p}$	q	%strain
51.48	0	0
55.18	4.62	0.23
61.25	13.47	0.59
62.00	16.99	0.70
64.40	21.24	0.70
66.09	24.78	0.70
67.29	26.91	0.70
67.52	28.99	0.82
67.80	31.12	0.82
68.25	32.49	0.94
68.52	34.61	0.94
69.67	36.69	1.06
69.18	38.05	1.17
69.40	40.12	1.29
69.61	42.18	1.41
69.06	43.48	1.64
72.26	46.18	1.88
73.71	48.05	2.35
76.27	50.52	2.94
78.12	52.28	3.52
78.43	54.36	4.70
78.61	54.37	5.87
82.09	56.34	7.05
82.03	56.61	8.22
84.16	58.15	9.39
84.34	58.67	10.57
84.60	58.84	11.74
85.15	60.23	12.92
85.96	60.03	14.09
86.15	59.21	15.27
85.27	60.18	16.44
84.80	59.63	17.61
84.33	59.07	18.79
82.55	58.21	19.96
83.04	58.20	21.14
81.67	57.34	22.31
81.08	56.74	23.49
80.12	55.87	24.66
79.16	55.00	25.83
77.20	54.13	27.01
77.27	54.28	28.18
74.78	52.39	29.36

100% Shale No. 1

$\bar{p}$	q	%strain
48.62	0	0
52.60	8.19	0.25
52.45	17.80	0.63
47.75	21.42	1.01
44.55	22.84	1.26
36.04	24.01	2.52
34.83	24.06	3.78
31.76	24.10	5.04
30.96	24.13	6.30
31.57	24.15	7.56
31.75	25.18	8.82
31.58	24.83	10.08
31.97	25.14	11.34
31.70	24.79	12.60
29.50	24.43	13.86
29.14	24.07	15.12
30.84	23.34	16.38
30.05	23.97	17.64
28.68	23.61	18.90
28.60	23.53	20.15
28.78	22.87	21.41
26.08	21.35	22.67
24.70	21.57	23.93
25.32	21.77	25.19
23.18	19.63	26.45
26.67	22.12	27.71
26.28	21.23	28.93
27.19	22.13	30.23
25.11	21.99	31.49
27.14	22.58	32.75
26.20	22.65	34.01

100% Shale No. 2

$\bar{p}$	q	%strain
97.24	0	0
103.92	6.68	0.25
106.07	16.33	0.25
104.51	25.94	0.37
100.40	29.23	0.49
95.14	33.22	0.74
91.29	35.35	0.98
87.30	37.84	1.23
71.27	38.45	2.45
68.19	39.40	3.68
66.71	39.60	4.90
65.22	39.79	6.13
63.39	40.65	7.35
66.13	41.47	8.58
68.20	42.26	9.80
67.02	42.35	11.03
67.26	42.42	12.25
66.33	40.32	13.48
64.62	41.87	14.70
66.03	41.27	15.93
65.21	41.28	17.16
64.18	40.67	18.38
65.00	40.06	19.61
61.53	39.54	20.83
61.18	38.26	22.06
58.15	37.66	23.28
56.66	35.93	24.51
52.65	33.69	25.73
51.21	32.59	26.96
48.53	31.51	28.18
49.88	32.02	29.41
51.44	32.15	30.27
53.73	33.02	30.63
53.60	33.81	31.12
53.07	34.20	31.37
54.97	35.09	31.61
56.99	36.11	31.61
57.00	37.13	31.61

APPENDIX IV

RESULTS OF CONTROLLED LOAD TESTS

ON FINE DISCARDS

Peckfield Sample No. 12

$\bar{p}$	q	%strain
47.31	0	0
50.98	5.46	0.28
53.76	10.91	0.28
58.28	16.32	0.56
61.04	21.76	0.56
64.69	27.20	0.56
68.08	31.87	0.84
72.68	37.66	1.68
75.24	40.12	2.24
75.08	41.64	3.37
74.36	41.81	4.49
73.62	41.96	5.61
75.00	42.74	6.73
74.49	42.23	7.85
76.84	43.58	8.97
75.91	43.04	10.10
75.37	42.50	11.22
74.54	42.57	12.34
73.99	42.02	13.46
75.12	42.65	14.58
74.16	42.09	15.70
74.60	41.53	16.83
73.60	41.53	17.95
74.14	40.96	19.07
74.57	40.39	20.19
72.57	39.29	21.31
74.43	39.26	22.44
72.94	38.17	23.56
72.88	37.61	23.56
72.88	37.61	24.68
72.81	36.54	25.80
74.25	35.99	26.92
74.70	35.43	28.04
74.66	34.40	29.17
75.63	33.37	30.29
79.55	31.31	33.65
81.91	28.68	36.46
84.80	26.59	39.26
84.48	24.57	42.07
84.00	23.38	44.87
82.31	21.47	47.68
74.35	19.87	49.92

Peckfield Sample No. 13

$\bar{p}$	q	%strain
100.19	0	0
104.06	7.45	0.56
105.23	12.19	0.56
106.40	16.93	0.56
108.96	21.67	0.56
109.38	25.66	0.84
109.42	31.06	0.84
111.37	36.68	1.12
113.57	40.95	1.40
112.56	46.19	1.68
113.06	50.59	2.24
116.35	50.67	3.36
110.40	50.08	4.47
106.50	50.14	5.59
103.72	49.54	6.71
105.74	51.46	7.83
103.33	50.84	8.95
98.14	50.21	10.07
103.40	50.80	11.18
103.76	50.16	12.30
103.61	49.52	13.42
102.08	48.88	14.54
102.51	48.81	15.66
103.76	48.16	16.78
108.34	48.08	17.90
110.97	47.42	19.01
113.60	46.77	20.13
115.69	45.58	21.25
116.90	44.40	22.37
119.04	43.76	23.49
122.18	43.12	24.61
125.71	41.98	25.72
129.25	40.84	26.84
129.63	40.22	27.96
131.82	38.63	29.08
136.30	37.55	30.20
146.72	34.84	33.55
154.73	32.50	36.35
170.58	30.66	39.15
179.51	29.25	41.94
172.37	27.47	44.74
161.54	23.77	48.65

Peckfield Sample No. 14

$\bar{p}$	q	%strain
202.09	0	C
203.48	1.39	0
211.77	9.69	0.56
215.74	15.91	0.56
217.64	20.06	0.56
223.17	25.60	0.56
222.72	29.66	0.84
225.88	35.18	0.84
228.44	39.90	1.13
229.43	45.40	1.13
230.27	50.76	1.41
230.56	55.56	1.41
232.93	60.19	1.69
233.89	65.66	1.69
234.16	70.45	1.69
231.96	75.02	1.97
231.32	78.89	2.25
229.37	82.48	2.81
214.01	80.67	3.38
212.17	84.38	4.50
206.05	84.70	5.63
211.37	85.63	6.75
215.05	84.60	7.88
215.24	83.57	9.00
215.43	82.53	10.13
211.52	80.88	11.25
211.12	79.25	12.38
211.33	78.23	13.50
208.05	77.21	14.63
208.26	76.19	15.75
210.15	74.60	16.88
206.31	73.02	18.01
206.54	72.02	19.13
206.76	71.01	20.26
208.70	69.46	21.38
208.93	68.47	22.51
214.37	66.94	23.63
217.57	65.43	24.76
223.05	63.94	25.88
226.28	62.46	27.01
228.30	61.00	28.13
228.57	60.04	29.27
231.36	58.12	30.38
246.27	54.38	33.76
250.24	51.19	36.57
265.78	48.07	39.39
260.48	45.04	42.20
253.78	42.85	45.01
213.11	37.02	47.83

Peckfield Sample No. 15

$\bar{p}$	q	%strain
50.09	0	0
53.16	3.96	0.28
57.70	11.18	0.56
61.21	15.08	0.84
66.90	20.27	1.12
71.41	27.46	1.12
76.62	34.46	1.69
81.22	40.84	1.97
87.28	46.41	2.53
92.14	52.55	3.09
96.29	56.70	3.65
98.36	58.27	4.21
101.84	61.26	4.50
101.90	62.78	5.06
105.73	65.14	6.18
106.78	66.20	7.31
108.82	68.23	7.87
110.83	70.74	8.43
112.58	71.99	9.27
117.07	75.48	10.12
116.80	75.71	11.24
118.16	77.07	12.36
117.99	77.80	13.49
116.98	76.79	14.61
115.69	76.89	15.74
119.65	78.07	16.86
117.44	78.64	17.98
117.97	79.17	19.11
115.87	78.07	20.23
114.77	76.97	21.36
115.07	76.38	22.48
121.41	80.83	23.60
124.11	80.63	24.73
122.50	79.92	25.85
120.79	78.71	26.98
119.56	77.97	28.14
117.34	76.75	29.22
116.58	76.00	30.35

Peckfield Sample No. 16.

$\bar{p}$	q	%strain
105.75	0	0
108.18	9.46	0.55
107.58	16.90	0.55
107.82	18.93	0.55
108.76	24.33	0.55
110.06	28.31	0.83
109.55	32.27	1.10
111.35	34.95	1.10
111.81	38.99	1.10
112.60	41.56	1.38
113.72	43.57	1.38
115.73	48.26	1.38
117.37	53.48	1.65
120.93	58.62	1.65
124.20	62.48	2.20
128.43	67.61	2.48
132.21	71.38	2.76
136.03	73.82	3.03
140.66	77.55	3.31
150.01	85.11	4.41
163.57	93.2?	6.06
163.92	92.67	6.61
166.40	91.58	7.72
182.86	107.84	8.82
192.23	111.43	9.92
192.86	110.07	11.02
191.41	109.90	12.13
187.17	106. 6	13.23
191.10	108.31	14.33
193.43	108.64	15.43
198.01	106.65	16.54
196.61	103.57	17.64
198.76	101.63	18.74
200.07	91.16	19.84
205.37	95.90	22.05
212.42	90.61	24.25
220.91	84.98	26.46
241.31	77.34	29.76

Peckfield Sample No. 17

$\bar{p}$	q	%strain
202.09	0	0
201.74	4.17	0.30
203.42	10.36	0.71
211.15	24.86	0.91
210.77	29.00	0.91
214.54	37.29	0.91
213.85	43.37	1.22
215.53	49.56	1.22
217.21	55.76	1.22
214.38	61.95	1.22
211.34	67.94	1.52
208.48	74.11	1.52
207.64	80.04	1.82
206.76	85.93	2.13
203.58	91.78	2.43
195.35	97.29	3.04
201.18	102.72	3.65
192.75	102.08	4.26
198.54	111.37	4.87
196.82	111.91	6.08
194.73	114.34	7.30
192.88	114.75	8.51
195.13	117.00	9.73
195.42	117.28	10.95
196.07	115.68	12.16
196.73	114.08	13.38
199.64	112.48	14.60
198.54	109.12	15.81
201.66	111.01	17.03
202.97	111.09	18.24
200.74	111.12	19.46
205.00	109.44	20.68
202.29	107.77	21.89
203.84	104.41	24.33
200.78	98.70	27.37
213.24	94.56	30.41
219.59	89.04	33.45

Peckfield Sample No. 18

$\bar{p}$	q	%strain
58.44	0	0
60.81	1.37	0.28
63.20	10.91	0.84
64.36	15.63	1.12
65.49	20.33	1.40
65.63	24.94	1.96
66.12	28.90	2.24
69.78	28.56	3.36
69.55	28.23	4.48
67.93	27.90	5.60
66.21	27.57	6.72
62.73	27.87	7.84
63.18	27.54	8.96
60.46	27.20	10.08
60.84	28.08	11.20
61.30	28.33	12.32
63.32	27.97	13.44
62.07	27.60	14.56
59.82	27.24	15.68
62.67	28.60	16.80
62.49	28.21	17.92
62.11	27.83	19.04
61.72	27.44	20.15
61.34	27.06	21.27
60.45	26.67	22.39
59.57	26.29	23.51
60.58	25.90	24.63
61.82	26.54	25.75
62.13	26.64	26.87
64.22	25.74	27.99
63.03	25.34	29.11
61.36	24.46	30.23
62.93	22.82	33.59
58.95	21.43	36.39
57.59	20.06	39.19
54.38	18.74	41.99
51.61	17.08	44.79

Aberrant Sample 2

p̄	q	%strain
90.59	0	0
88.33	0	0
88.33	0	0.11
89.09	5.27	0.34
86.83	5.27	0.34
87.59	10.53	0.45
85.32	10.53	0.45
86.56	14.02	0.56
84.30	14.02	0.56
87.28	15.77	0.56
86.77	17.53	0.56
85.74	21.01	0.68
85.21	22.73	0.79
82.41	24.46	0.9
80.13	24.43	1.01
80.32	28.63	1.13
81.93	29.56	1.35
81.39	31.23	1.58
79.06	31.16	1.8
60.62	32.13	4.06
75.56	31.19	6.88
78.26	30.21	9.81
67.32	29.53	11.83
64.27	28.74	14.2
61.22	27.94	16.57
53.43	26.92	19.61
54.17	27.27	22.65
50.51	25.63	28.35

Aberrant Sample 1

p̄	q	%strain
125.45	0	0
127.02	6.10	0.11
121.73	99.49	0.11
117.93	12.86	0.22
117.96	19.61	0.33
115.03	18.94	0.33
117.48	23.64	0.44
118.15	24.32	0.44
113.61	24.29	0.55
112.03	24.97	0.55
111.77	26.96	0.66
110.83	28.23	0.76
106.28	28.25	0.87
106.04	30.27	0.87
106.71	30.94	0.87
104.42	30.90	0.98
103.71	33.48	1.31

Aberrant Sample 3

p̄	q	%strain
58.44	0	0
58.81	7.51	0.44
60	12.27	0.55
57.99	12.94	0.67
57.99	12.94	0.67
57.34	14.96	0.78
57.57	16.98	0.89
56.21	18.3	1.1
56	18.98	1.11
56	20.27	1.44
54.12	20.18	1.89
54.55	22.76	2.33
53.92	21.84	3.44
52.46	21.57	4.66
50.95	21.24	6.1
52.44	21.42	8.10
48.98	20.72	11.09
48.15	20.18	13.42
45.82	19.64	15.75
45.33	19.04	18.3
43.0	18.39	21.07
42.91	17.70	24.07
41.71	16.79	27.95

Aberrant Sample 6

p̄	q	%strain
153.30	0	0
154.65	3.41	1.45
154.92	8.18	1.47
152.24	12.86	1.47
150.87	17.68	1.76
149.54	23.12	1.76
147.44	27.80	2.05
143.84	33.22	2.05
128.72	38.41	2.64
126.46	38.41	2.64
123.06	41.78	2.64
116.16	41.65	2.93
110.88	45.41	3.52
111.89	45.00	4.4
102.17	44.31	5.87
97.77	46.08	8.80
90.13	43.99	11.74
85.82	42.97	13.79
84.94	42.09	15.55
79.06	40.91	17.60
65.06	41.90	21.12

Abernant Sample 4 cont....

p̄	q	%strain
101.49	34.55	2.07
95.49	34.09	3.38
97.52	33.66	4.59
96.93	35.97	6.99
91.35	34.71	11.79
85.58	33.65	15.94
83.41	32.71	19.65
87.01	33.66	21.49
82.30	30.82	26.75

Abernant Sample 7

p̄	q	%strain
222.29	0	0
222.72	1.98	0
223.63	7.26	0.29
223.78	11.83	0.29
222.95	17.81	0.29
221.35	18.47	0.29
219.79	23.68	0.58
216.02	28.95	0.58
219.88	31.58	0.58
216.77	37.50	0.58
210.18	43.42	0.58
210.55	49.34	0.58
205.03	55.10	0.87
197.60	54.84	0.87
194.47	60.35	0.87
186.87	59.52	1.16
183.08	64.75	1.16
173.56	65.52	1.45
167.24	66.97	1.74
149.27	67.06	3.47
148.44	66.25	3.76
148.24	66.03	4.05
146.33	64.12	4.05
156.45	73.01	4.05
154.64	77.78	5.21
148.36	76.03	7.81
147.59	77.31	10.13
144.04	74.08	12.15
144.57	73.25	14.18
141.8	70.18	16.79
142.78	67.98	19.10
138.8	64	21.99
135.93	61.10	24.89
136.36	56.2	29.51
134.03	49.83	36.18
132.34	46.10	39.94

Abernant Sample 6 cont....

p̄	q	%strain
77.29	38.36	26.11
72.91	36.05	29.63
71.43	33.33	34.03
70.44	31.12	37.55
77.34	27.61	44.59

Abernant Sample 9

p̄	q	%strain
271.77	0	0
261.60	7.89	0.86
247.05	16.94	1.73
248.43	19.55	1.73
242.59	22.74	2.02
246.14	31.83	2.02
236.6	41.58	2.02
230.52	65.87	2.59
212.27	65.68	2.83
207.13	75.11	3.17
191.30	75.08	4.03
175.05	74.63	4.61
163.64	73.23	6.33
153.91	74.64	9.21
141.11	74.36	12.38
131.99	74.26	16.41
129.53	73.04	19.00
129.45	71.73	22.17
124.66	71.65	23.89
125.53	71.28	25.33
120.39	69.64	27.06
122.59	73.69	29.65
115.72	68.89	33.39
113.14	66.51	35.70
113.93	64.01	37.71
111.45	61.72	39.15
107.93	60.16	41.17
107.38	58.69	42.89
108.31	55.10	43.47

Abernant Sample 11

p	q	% strain
55.74	0	0
59.82	6.33	0
58.3	10.55	0
68.38	23.92	0
62.46	22.51	0
71.19	32.27	0.28
78.76	43.13	1.11
81.58	52.73	1.39
83	51.83	1.67
84.71	55.11	1.67
83.33	56.73	1.67
87.66	62.09	1.95
98.35	73.81	1.95
96.08	71.54	2.23
100.21	75.57	2.23
100.68	76.14	2.50
106.62	82.08	2.78
105.95	81.39	2.78
105.25	80.71	2.78
110.04	85.90	2.78
116.70	98.97	3.34
125.37	110.89	3.9
113.82	97.08	4.17
113.27	97.75	4.17
131.45	116.97	4.45
135.5	121.3	5.01
140.03	128.89	5.57
142.72	132.75	6.12
153.60	144.66	6.96
157.70	153.28	8.07

Abernant Sample 12

p	q	% strain
97.56	0	0
109.78	25.76	0.31
105.26	35.92	0.64
104.22	39.29	0.74
104.77	37.59	0.74
107.64	42.71	0.74
109.66	56.02	1.33
114.17	56.02	1.38
110.16	54.26	1.48
119.16	64.30	1.70
116.84	64.23	1.80
127.78	80.52	2.54
124.54	88.21	8.48
120.94	80.10	12.19
120.48	79.65	14.31
116.89	78.31	17.28
117.06	74.80	20.93
121.53	64.15	29.68

Abernant Sample 13

p	q	% strain
73.17	0	0
81.23	23.06	0
84.25	47.20	1.11
94.36	71.88	1.93
102.79	73.34	2.21
95.49	79.78	2.49
100.44	89.25	3.04
107.82	98.08	3.32
113.19	105.51	3.87
115.14	106.20	4.14
131.74	122.58	4.97
132.87	126.45	5.80
130.96	122.03	5.80
140.21	131.28	6.08
144.73	131.28	6.08
158.11	151.43	7.46
160.69	155.04	7.18
159.91	150.98	7.74
181.25	175.58	8.84
181.38	172.45	9.67
187.61	176.42	10.77
195.77	182.31	11.60
200.64	182.67	12.16
206.93	188.96	12.17
221.53	194.54	13.54
203.57	177.80	15.19
234.21	204.76	16.58
233.78	205.56	19.06

Abernant Sample 13 cont.....

p	q	% strain
230.4	203.41	20.44
239.99	203.97	21.27
250.11	203.98	25.69
264.84	194.17	30.11
262.99	181.42	31.77
245.46	157.52	32.05
240.64	152.89	32.05
389.14	153.19	45.86

Aberrant Sample 14

D	σ	% strain
79.92	0	0
70.05	1.41	0.00
81.25	23.90	0.29
71.51	23.19	0.29
70.66	24.60	0.29
76.83	49.9	0.29
69.00	47.79	0.29
64.44	73.58	0.57
57.67	73.58	0.57
50.12	96.41	2.30
39.39	94.71	4.02
28.28	92.63	5.46
21.04	92.16	6.61
11.25	103.13	14.93
00.03	99.17	18.67
81.57	97.63	20.39
76.00	96.78	21.54
74.25	99.54	22.40
69.98	97.53	23.55
69.97	99.73	24.70
66.19	93.26	25.85
66.34	99.43	27.28
63.87	96.97	28.72
62.40	100.01	30.44
56.46	98.39	34.16
53.84	95.82	38.48
58.10	97.89	43.08
49.21	97.77	44.52

Aberrant Sample 15

D	σ	% strain
306.62	0	0
318.53	11.52	1.12
313.05	21	1.12
313.6	27.10	1.12
309.55	33.11	1.4
301.56	26.35	1.4
307.27	39.86	1.4
296.14	27.70	1.4
289.82	50.53	1.63
284.42	75.7	2.24
274.05	74.36	2.24
256.35	73.69	2.24
256.63	90.05	2.52
257.37	100.37	3.64
250.59	95.84	4.20
244.86	94.63	4.76
242.32	94.35	5.04
237.53	94.07	5.32
233.77	93.80	5.60
241.0	105.15	8.0
222.84	102.2	14.28
201.9	95.64	19.32
188.50	88.82	24.64
174.19	81.08	30.80
164.92	69.29	39.21
165.20	57.80	47.61

Aberrant Sample 16

D	σ	% strain
4.53	0	0
4.54	16.79	0.28
8.36	31.89	0.28
3.76	31.80	0.55
5.16	53.27	1.10
8.01	51.60	1.10
5.60	54.93	1.10
0.75	56.60	1.10
1.05	75.93	1.93
5.35	75.72	2.21
5.60	86.59	2.49
8.01	91.65	2.76
5.34	98.09	3.59
5.45	96.81	4.14
5.75	101.35	4.42
6.66	110.03	5.52
1.27	114.92	7.73
5.07	113.20	9.11

Aberrant Sample 16 cont....

D	σ	% strain
191.48	119.38	10.22
189.53	118.66	11.37
193.55	123.71	13.53
188.56	119.76	16.29
184.72	118.37	18.23
190.59	121.78	19.61
187.72	113.81	24.03
193.6	89.85	35.45
239.44	67.48	48.60

REFERENCES

Akroyd, T.   1957   _Laboratory testing in soil engineering_, Soil Mechanics Ltd.

Allen, D.W.   1973   _The Effect of Coal Content on Two Colliery Spoils of extreme Rank._   M.Sc. Thesis, Advanced Course in Engineering Geology, University od Durham.

Bishop, A.W.   1973   The stability of tips and spoil heaps, _Q.J.Eng.Geol._, _v.6_, pp 335-376.

Bishop, A.W. and Henkel, D.J.   1962   _The measurements of soil properties in the triaxial test._   2nd Edition, 281 pp, Edward Arnold, London.

Bishop, A.W., Hutchinson, J.N., Penman, A.D.M. and Evans, H.E.   1969   Geotechnical investigation into the causes and circumstances of the disaster of 21st October,1966. A selection of Technical Reports submitted to the Aberfan Tribunal, Item 1, pp 1-80, Welsh Office, HMSO, London.

British Standards Institution   1967   Methods for Sampling and Testing of Mineral Aggregates, Sands and Fillers, B.S.I. BS812: 1967, pp 71-74.

British Standards Institution   1975   Soils for Civil Engineering Purposes, B.S.1377: 1975.

Casagrande, A   1976   Liquefaction and cyclic deformation of sands – a critical review.   Harvard Soil Mechanics Series No.88, Cambridge, Massachusetts.

Castro, G.   1969   _Liquefaction of sand deposits._   Ph.D. thesis, Harvard University.

Cobb, A.E.   1977   _Stability and Degradation of Colliery Shale Embankments and properties of Tailings Lagoon Deposits._   Ph.D.Thesis Durham University.

Dorby, R. and Alvarez, L.   1967   Seismic Failures in Chilean Tailings
                Dams, J. Soil Mech. and Found. Engrg Div., A.S.C.E.,
                v.93, No. SM6 pp 237-260.

Finey, J.T , 1973 .   see Mckechnie Thomson & Rodin , 1973

Hird, C.C. and Humphreys,J.D. (In press)   An experimental scheme for the
                disposal of Micaceous Residues from the China Clay Industry
                                                        Q.J.E.G.

Hutchinson,J.N.   1967.   Discussion 214-215 Proc. Geotechnical Conf.,Oslo,2.293pp.

Keeling, P.S.   1962   Some experiments on the low-temperature removal of
                carbonaceous material from clays.   Clay Min. Bull.Min.Soc.,
                London, V.5, p.155.

Ladd, R.S.   1977   Specimen preparation and cyclic stability of soils, J.Geotechn
                Eng. Div., ASCE, v.103, GT6, pp 535-547.

Lambe, W.T.   1967   The Stress Path Method.   J.Soil Mech. and Found.Engrg,
                ASCE, SM6, pp 309-331.

Lawrence, J.A.   1972   Some properties of South Wales Discards, Colliery
                Guardian, v.220, No. 6, pp 270-278.

McKechnie Thomson G.& Rodin, S.   1972   Colliery spoil tips - after Aberfan.
                Inst. of Civ. Engrs, Paper 7522, London.

McKechnie Thomson, G. and Rodin, S.   1973   Colliery spoil tips - after
                Aberfan - Discussion sections cited Taylor, R.K. *
                                            Finey,   J.T. * .

Mullis, J.P., Chan, C.K. and Seed, H.B.   1975   The effects of method of sample
                preparation on the cyclic stress-strain behaviour of
                sands.   Report No. EERC 76-18, Earthquake Engrg Research
                Centre, University of California, Berkeley,Calif.

Nägelschmidt, G. and Hicks, D.   1943   The mica of certain Coal Measure shales
                in South Wales.   Mineralogy Mag.22,pp 92-99.

National Coal Board   1970   Technical Handbook - Spoil Heaps and Lagoons, 2nd
                Draft, National Coal Board, London.

National Coal Board   1972   Review of research on properties of spoil tip
                materials, Headquarters Research Report, Wimpey
                Laboratories Ltd., Hayes, Middlesex.

Oda, M.   1972   Initial Fabrics and their relations to Mechanical Properties
of Granular Material: Soil and Foundations, Japanese
Soc. of Soil Mech. and Found.Engrg. v.12,No.1,
pp 17-36.

Seed, H.B., Kerji Mori and Chan, C.K.   1977   Influence of Seismic History
on Liquefaction of Sands, J.Geotech. Eng.Div.,
ASCE, v.103,GT4 pp 257-270.

Shergold, F.A. and Hosking, J.R.   1963   Investigation of Test Procedures
for Argillaceous and Gritty Rocks in Relation to
Breakdown under traffic.   Rds. and Rd.Construction.,
41, (492), 376/8.

Shorten, J.M.P. (In preparation, 1977)   The liquefaction potential of
pulverised fuel ash from Gale Common, South
Yorkshire, M.Sc. Advanced Course Dissertation,
University of Durham.

Taylor, R.K. and Spears, D.A.   1970   The breakdown of British Coal Measures
Rocks, Int.J. Rock Mech.Un. Sci., v.7, pp 481-501.

Taylor, R.K. *   1974   Influence of coal content on the peak shear strength of
colliery shales, Geotechnique, v.24, no. 4, pp 683-688.

Taylor, R.K. and Cobb, A.E.   1977   Mineralogical and Geotechnical Controls on
the Storage and Use of British Coal-mine Wastes, 9th
Int. Conf. for Soil Mech. and Found. Engrg, Tokyo, 1977.

Terzaghi, K. and Peck, R.B.   1948   Soil Mechanics in Engineering Practice, 1st
Edition, Wiley & Sons, New York.

Youd, L.T.   1973   Liquefaction, flow and associated ground failure, Geological
Survey circular 688.

*   see also Mckechnie Thomson & Rodin (1973)